13 Disinfection

Terminology for Disinfection

Term	Definition
Absorbance	Amount of light of a specified wavelength absorbed by the constituents in water.
Biodosimetry	Determination of the dose of a disinfectant to inactivate a specific biological test organism.
Breakpoint chlorination	Process in which chlorine is added to react with all oxidizable substances in water so that if additional chlorine is added it will remain as free chlorine (see below, $HOCl + OCl^-$).
Combined chlorine residual	Concentration of chlorine species resulting from the reaction of chlorine and ammonia, specifically the sum of monochloramine (NH_2Cl), dichloramine ($NHCl_2$), and trichloramine (NCl_3), expressed as mg/L as Cl_2.
Ct	Product of chlorine residual expressed in mg/L and contact time expressed in min. The term *Ct* is used to assess the effectiveness of the disinfection process for regulatory purposes.
Disinfection	Partial destruction and inactivation of disease-causing organisms from exposure to chemical agents (e.g., chlorine) or physical processes (e.g., UV irradiation).

Term	Definition
Decay rate	Rate at which the concentration of a disinfectant decreases over time.
Disinfection by-products (DBPs)	Undesirable products of reactions between disinfecants and other species in the feed water. DBPs of concern are those that are carcinogenic or have other negative health effects.
Dose–response curve	Relationship between the degree of microorganism inactivation and the dose of a disinfectant.
Free chlorine residual	Sum of the hypochlorous acid (HOCl) and hypochlorite ion (OCl^-) in solution, expressed as mg/L as Cl_2.
Inactivation	Rendering microorganisms incapable of reproducing and thus limiting their ability to cause disease.
Pathogens	Microorganisms capable of causing disease.
Photoreactivation and dark repair	Methods used by microorganisms to repair the damage caused by exposure to UV irradiation.
Reactivation	Process by which organisms repair the damage caused by exposure to a disinfectant.
Sterilization	Total destruction of disease-causing and other organisms.
Transmittance	Ability of water to transmit light. Transmittance is related to absorbance.
Total chlorine residual	Sum of the concentrations of free and combined chlorine.
UV light	Portion of the electromagnetic spectrum between 100 and 400 nm.

The threat of microbiological contaminants in drinking water is eliminated by three complementary strategies: (1) preventing their access to the water source, (2) employing water treatment to reduce their concentration in the water, and (3) maximizing the integrity of the distribution system for finished water. Early in the history of public drinking water systems, the emphasis was almost entirely on gaining access to a protected source. In recent years, greater emphasis has been directed toward providing effective water treatment to reduce microbiological contaminants. Today, there is increasing emphasis on employing both source protection and treatment to ensure that safe water is produced and on improving distribution system integrity to ensure that contamination does not occur during transport from the treatment plant to the consumer's tap.

In the water treatment process, *reducing* microbiological contaminants is accomplished by two basic strategies, *removing* them from the water or *inactivating* them. Inactivated microorganisms, although still present in the water, are no longer able to cause disease in the consumer. Processes that

use inactivation as their strategy are traditionally referred to as disinfection, the focus of this chapter.

In water works practice, the term *disinfection* is used to refer to two activities: (1) primary disinfection—the inactivation of microorganisms in the water—and (2) secondary disinfection—maintaining a disinfectant residual in the treated-water distribution system. The characteristics that make a disinfectant the best choice for each of these purposes are not the same.

Primary disinfection is discussed in this chapter, along with the role disinfection plays in protecting the public, the strengths and weaknesses of inactivation versus removal, the kinetics of the disinfection process, and some specific details about the design of disinfection facilities. Disinfection by-products are discussed in Chap. 19.

13-1 Historical Perspective

Beginning a decade before the work of Dr. John Snow (1849 and 1853, see Chap. 3) and continuing for five decades after, two principal means were employed to control waterborne disease: (1) using water supplies not exposed to fecal contamination and (2) filtration through sand. At first, slow sand filtration was the dominant water treatment process; however, it was not always effective. The first efforts in rapid sand filtration were even less effective. Eventually George W. Fuller (1897) demonstrated that it is essential that complete coagulation precede the filtration step. Even with proper coagulation, however, filtration alone was not consistently successful in reducing the microorganisms to safe levels (Johnson, 1911; Whipple, 1906).

In 1881, not long before Fuller did his work on coagulation and filtration, Koch, the German scientist who demonstrated the role bacteria play in waterborne disease, also demonstrated that chlorine could inactivate pathogenic bacteria. The first continuous use of chlorination for disinfection of drinking water occurred in Middelkerke, Belgium, in 1902. The first continuous application to drinking water in the United States was at the Boonton Reservoir for the water works of Jersey City, New Jersey, in late 1908. In these first applications, disinfection was accomplished by feeding solid calcium hypochlorite. Soon after, liquid chlorine gas became available, making large-scale continuous chlorination more feasible. The first water treatment facility to use liquid chlorine gas on a permanent basis was in Philadelphia in 1913. Most of these early installations were used to address serious contamination or to avoid filtration, but in the three decades following the installation in Philadelphia, the practice of chlorination was expanded rapidly to include most surface water supplies, even those that were filtered. By 1941, 85 percent of the drinking water supplies in the United States were chlorinated (U.S. PHS, 1943). Also, by the 1940s, disinfection with chlorine had become a world water treatment standard and, even today, many water supplies are treated with chlorination alone.

The presence of a free chlorine residual in water at the tap was generally taken as a guarantee of microbiological safety by health officials and the public. Disinfection thus became established as the most important water treatment process. A more detailed discussion of the use of chlorine can be found in Baker (1948) and White (1999).

From the beginning, the use of chlorine has been contentious with many of its opponents arguing for the use of protected supplies in place of disinfection (Drown, 1893/1894). Equally important, a significant portion of the population has always had an aversion to the use of chlorine, complaining about its impact on the water's aesthetic qualities and wishing to avoid exposure to a chemical with such toxic properties, even at low concentrations. Largely for this second reason, ozone became the preferred primary disinfectant in much of mainland Europe in the late 1960s and 1970s.

In the mid-1970s, events took place that stimulated a reevaluation of disinfection practice. In Holland and the United States, researchers demonstrated that free chlorine reacts with natural organic matter (NOM) in water to produce chlorinated organics, specifically the trihalomethanes (THMs) (Bellar and Lichtenberg, 1974; Rook, 1974). Not long thereafter, limits were set on the allowable THM concentrations in potable water (U.S. EPA, 1979; WHO, 1994). Since then, more by-products have been identified resulting from chlorination and the use of other disinfectants (Bull et al., 1990). Limits have also been established for many of these by-products (U.S. EPA, 1998). It is likely that chemical by-products are formed any time an oxidant is employed in water treatment and that some of these by-products will be regulated in the future (Trussell, 1992, 1993).

During the last two decades of the twentieth century, events occurred that have also resulted in the questioning of the effectiveness of chlorination in controlling waterborne disease. In the 1980s, the protozoa *Giardia lamblia* was identified as an important waterborne pathogen. Because *G. lamblia* is more resistant to chlorine than other targets of disinfection, more stringent standards for reduction of pathogens were established (U.S. EPA, 1989). More recently, another protozoa, *Cryptosporidium parvum,* has also been identified as an important source of waterborne disease and is even more resistant to chlorine than *G. lamblia*. In fact, chlorination is ineffective for *C. parvum*.

The discovery of chlorination by-products and chlorine-resistant organisms is causing a reevaluation of the use of chlorine as the primary disinfectant and a reevaluation of the role of inactivation itself in the control of pathogens. For example, because methods are not available to determine if *C. parvum* oocysts found in water supplies will cause disease if ingested by a consumer, the Drinking Water Inspectorate in the United Kingdom recognizes only *removal*, not *inactivation*, as a viable strategy for addressing the control of this pathogen (U.K. Department of the Environment, 1999a,b).

New treatment processes have also come to the fore that show promise for the removal or inactivation of chlorine-resistant organisms and others as well. Membrane filtration processes, developed originally in the mid-1950s and later employed for sterilizing laboratory solutions, juices, and eventually brewed beverages, have now reached a stage in their development where they are commercially viable at large scale. Membranes are capable of removing pathogens much more effectively than traditional physical treatment processes such as coagulation and granular media filtration. In fact, the removals that have been demonstrated using membranes are on the same order of magnitude of inactivation of bacteria customarily achieved by chlorine (Jacangelo et al., 1989). Disinfection with UV light is also effective for inactivating *Giardia* (Stolarik et al., 2001) and *Cryptosporidium* (Craik et al., 2001). While chlorine remains the dominant drinking water disinfectant and disinfection (inactivation) remains the cornerstone of water treatment, this situation may change in the future.

13-2 Methods of Disinfection Commonly Used in Water Treatment

Five disinfection agents are commonly used in drinking water treatment today: (1) free chlorine, (2) combined chlorine (chlorine combined with ammonia, also known as chloramines), (3) chlorine dioxide, (4) ozone, and (5) UV light. The first four are chemical oxidants, whereas UV light involves the use of electromagnetic radiation. Of the five, by far the most common in the United States is free chlorine. As shown on Fig. 13-1, surveys of disinfectant use by the American Water Works Association Disinfection Systems Committee in 1978, 1989, 1998, and 2007 found that nearly all water utilities in the United States use free chlorine, although the method of application has been changing over time (AWWA, 2008). In 1978, 91 percent of utilities used chlorine gas to apply free chlorine to the water and 7 percent used sodium hypochlorite (i.e., bleach). By 2007, however, only 63 percent of utilities were using chlorine gas and nearly 40 percent were using either bulk liquid or onsite generation of sodium hypochlorite. The transition from chlorine gas to hypochlorite is primarily because of safety and security reasons because chlorine gas is highly toxic.

As shown on Fig. 13-1, the number of utilities using chloramines for disinfection has increased to 30 percent by 2007. Its use, however, is often limited to residual maintenance, and typically a different disinfectant is used for primary disinfection when chloramine is used.

Ozone is the strongest of the four oxidants and its use has increased from less than 1 percent of utilities in 1989 to 9 percent in 2007. The increasing use is in part because of its stronger disinfecting properties and in part because it controls taste and odor compounds, specifically geosmin

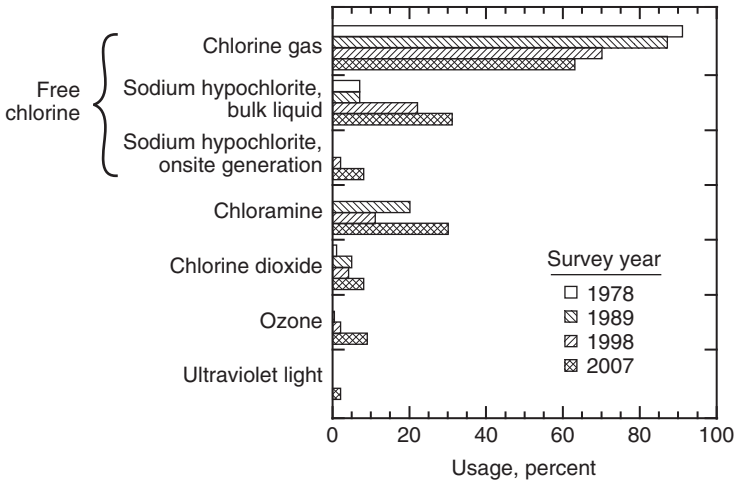

Figure 13-1
Disinfectant use in municipal drinking water treatment in the United States. (Adapted from AWWA 2008.)

and methyl isoborneol. UV light is not frequently used for disinfecting in drinking water applications, with only 2 percent of utilities reporting to use it in 2007. Its use may increase in the future, however, because of its lack of by-product generation and its effectiveness against protozoa. Information on each of these common disinfectants is summarized in Table 13-1.

Historically, chlorine was added to the raw water at a treatment plant and disinfection occurred during contact over the residence time of the entire plant. This practice has become obsolete and disinfection is now best applied as a separate unit process. The chemical disinfectants are most often applied in baffled, serpentine contact chambers or long pipelines when these are available. Both types of contactors can be designed to be highly efficient, closely approaching ideal plug flow. Additionally, ozone can be introduced in over–under baffled contactors. Over–under baffled contactors, however, have bigger problems with short circuiting, so pipeline and serpentine basin contactors have become more common for ozone disinfection. Design of contactors for chemical disinfectants is discussed in Sec. 13-8 in this chapter.

Ultraviolet light disinfection is often applied in proprietary reactors. Short circuiting is a special concern for UV reactors, particularly the proprietary reactors because their contact times are so short. Proprietary pressure vessels are particularly common where medium-pressure UV lamps are used because the high intensity of the UV lamps enables the delivery of a high UV dosage in a small space. Standards to address these issues exist in Europe (DVGW, 1997) and are being developed in the United States (NWRI, 2003; U.S. EPA, 2006).

Table 13-1
Characteristics of five most common disinfectants

Issue	Disinfectant				
	Free Chlorine	**Combined Chlorine**	**Chlorine Dioxide**	**Ozone**	**Ultraviolet Light**
Effectiveness in disinfection					
Bacteria	Excellent	Good	Excellent	Excellent	Good
Viruses	Excellent	Fair	Excellent	Excellent	Fair
Protozoa	Fair to poor	Poor	Good	Good	Excellent
Endospores	Good to poor	Poor	Fair	Excellent	Fair
Regulatory limit on residuals	4 mg/L	4 mg/L	0.8 mg/L	—	—
Formation of chemical by-products					
Regulated by-products	Forms 4 THMs[a] and 5 HAAs[b]	Traces of THMs and HAAs	Chlorite	Bromate	None
By-products that may be regulated in future	Several	Cyanogen halides, NDMA[c]	Chlorate	Biodegradable organic carbon	None known
Typical application					

Dose, mg/L (kg/ML)	1–6	2–6	0.2–1.5	1–5	20–100 mJ/cm^2
Dose, lb/MG	8–50	17–50	2–13	8–42	—
Chemical source	Delivered: as liquid gas in tank cars, 1 tonne and 68-kg (150-lb) cylinders, or as liquid bleach. Onsite generation from salt and water using electrolysis. Calcium hypochlorite powder is used for very small applications.	Same sources for chlorine. Ammonia is delivered as aqua ammonia solution, liquid gas in cylinders, or solid ammonium sulfate. Chlorine and ammonia are mixed in treatment process.	ClO_2 is manufactured with an onsite generator from chlorine and chlorite. Same sources for chlorine. Chlorite as powder or stabilized liquid solution.	Manufactured onsite using a corona discharge in dry air or pure oxygen. Oxygen is usually delivered as a liquid. Oxygen can also be manufactured onsite.	Uses low-pressure or low-pressure, high-intensity UV (254-nm) or medium-pressure UV (several wavelengths) lamps in the contactor itself.

[a]THMs = trihalomethanes.
[b]HAAs = haloacetic acids.
[c]NDMA = N: nitrosodimethy lamine.

13-3 Disinfection Kinetics

For chemical disinfectants, the specific mechanisms of microorganism inactivation are not well understood. Inactivation depends on the properties of each microorganism, the disinfectant, and the water. As will be shown later, the reaction rates that have been observed can vary by as much as six orders of magnitude from one organism to the next, even for one disinfectant. Even for disinfection reactions where the reaction mechanism is well understood, for example, UV light, reaction rates vary by one and one-half orders of magnitude.

Nevertheless, there is one simple kinetic model that is widely used, and there is enough commonality in the behavior of all these reactions to allow the development of some phenomenological laws that are useful in modeling all of these reactions. As these disinfection processes are physiochemical processes, they are also subject to the rules of analysis discussed in Chaps. 6 and 7. In the following discussion, the form of disinfection data resulting from laboratory experiments is examined by considering the shape of classical disinfection kinetic plots. Following this discussion, useful phenomenological kinetic models are discussed along with the merits of each.

Classical Disinfection Kinetics—Chick–Watson

Near the beginning of the twentieth century, Dr. Harriet Chick, a research assistant at the Lister Institute of Preventive Medicine in Chelsea, England, proposed that disinfection could be modeled as a first-order reaction with respect to the concentration of the organisms. Chick demonstrated her concept by plotting the concentration of viable organisms versus time on a semilog graph for disinfection data for a broad variety of disinfectants and organisms (Chick, 1908). Chick worked with disinfectants such as phenol, mercuric chloride, and silver nitrate and organisms such as *Salmonella typhi, Salmonella paratyphi, Escherischia coli, Staphylococcus aureus, Yersinia pestis,* and *Bacillus anthracis*. Over the subsequent years ''Chick's law'' has been shown to be broadly applicable to disinfection data. Chick's law takes the form

$$r = -k_c N \tag{13-1}$$

where r = reaction rate for the decrease in viable organisms with time, org/L·min
k_c = Chick's law rate constant, min^{-1}
N = concentration of organisms, org/L

Application of Chick's concept met with immediate success, and that success has continued through the years and across all the disciplines interested in disinfection.

While Chick's law has broad applicability, one important effect not addressed in the model is the effect of the concentration of the disinfectant. Frequently, different concentrations of disinfectant will lead to different

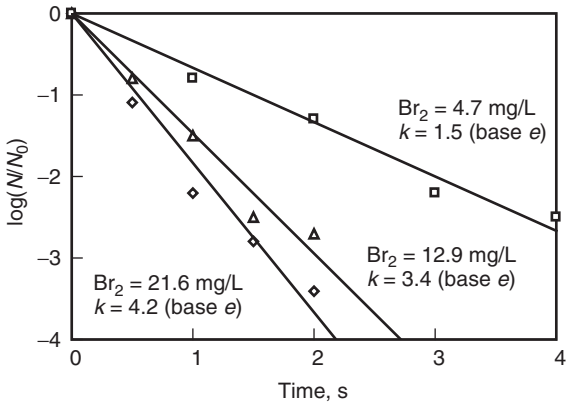

Figure 13-2
Inactivation of poliovirus type I with three concentrations of bromine in a batch reactor. (Adapted from Floyd et al., 1978.)

rates in the decrease in viable organisms, as illustrated on Fig. 13-2. Note that there is a different slope for each concentration of bromine and, using Eq. 13-1, the reaction has a different rate constant for each concentration. Thus, while Chick's first-order concept is consistent with the data, a better means for accounting for disinfectant concentration is necessary.

In the same year that Chick proposed her model, Herbert Watson proposed that the time needed to reach a specific level of disinfection was related to the disinfectant concentration by the equation (Watson, 1908)

$$C^n t = \text{constant} \tag{13-2}$$

where C = concentration of disinfectant, mg/L
n = empirical constant related to concentration, unitless
t = time required to achieve a constant percentage of inactivation (e.g., 99%)
constant = value for given percentage of inactivation, dimensionless

Watson demonstrated the concept by plotting data showing equal inactivation on a plot of $\log(C)$ versus $\log(t)$. The slope of the log–log plot, n, is often called the coefficient of dilution, which reflects the effect of diluting the disinfectant (Morris, 1975). Such plots are still used today, and an example is shown on Fig. 13-3. As a matter of convention, Watson plots are generally constructed with data corresponding to a removal of 99 percent. In such plots, the dilution coefficient is generally found to be approximately 1, and given the inaccuracies involved in collecting disinfection data, there is little evidence for a dilution coefficient other than unity. A dilution coefficient equal to 1 suggests that disinfection concentration and time are of equal importance for inactivating microorganisms.

With the knowledge that disinfection concentration and time are of equal importance, Chick's law and the Watson equation can be combined

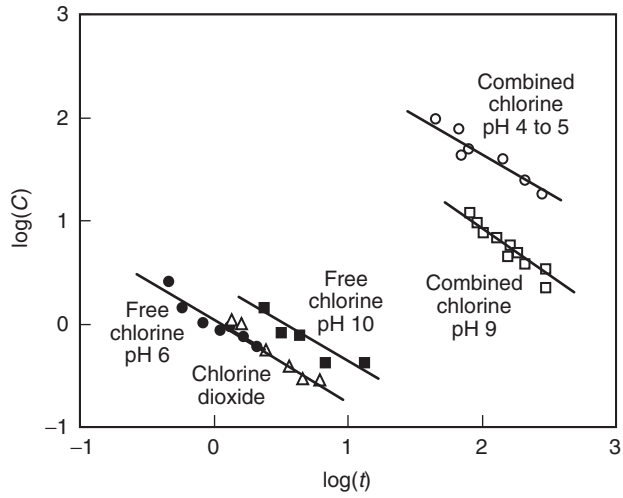

Figure 13-3
Watson plot of requirements for 99 percent inactivation of poliovirus type I. (Adapted from Scarpino et al., 1977.)

and are often referred to as the ''Chick–Watson model'' (Haas and Karra, 1984):

$$r = -\Lambda_{CW}\, CN \tag{13-3}$$

where Λ_{CW} = coefficient of specific lethality (disinfection rate constant), L/mg·min
C = concentration of disinfectant, mg/L

Most laboratory disinfection studies are conducted using completely mixed batch reactors (CMBR). Using concepts presented in Chap. 6, a mass balance on a batch reactor can be written and integrated, leading to

$$\ln\left(\frac{N}{N_0}\right) = -\Lambda_{CW} Ct \tag{13-4}$$

where N_0 = concentration of organisms at time = 0, org/L
t = time, min

It is important to note that even though laboratory disinfection studies typically use batch reactors, the rate equation (Eq. 13-3) can be applied to other reactors using the concepts presented in Chap. 6.

When Chick did her work, she plotted the organism concentration directly against time on a semilog graph [$\log(N)$ vs. t]. Now that Eq. 13-4 has received broad recognition, it is more common to plot the log or natural log of the survival ratio, where $S = N/N_0$, versus time [$\ln(N/N_0)$ or $\log(N/N_0)$ vs. t]. In disinfection studies, however, it is typically difficult to get an accurate measurement of the initial concentration of organisms, N_0, even with several replicates of the tests. As a result, a line fit through the data may not pass through zero

[i.e., $\ln(N/N_0)_{t=0} \neq 0$]. Although it is not consistent with the definition of N_0 [at $t = 0, \ln(N/N_0) \equiv 0$], it is often best to find the coefficient of specific lethality without forcing the regression line to pass through zero.

Equation 13-4 was derived using calculus so the term on the left is a natural logarithm (i.e., base e). However, disinfection effectiveness is typically expressed using the log removal value (LRV), which uses base 10 logarithms as described in Sec. 4-5. Thus, it is necessary to convert between natural and base 10 logarithms when evaluating disinfection data. The use of Eq. 13-4 to determine the coefficient of specific lethality for a disinfection reaction is demonstrated in Example 13-1.

Example 13-1 Application of the Chick–Watson model

Plot the data shown on Fig. 13-2, as given below, according to Eq. 13-4. Determine the coefficient of specific lethality and the coefficient of determination (r^2). The data for the inactivation of poliovirus type I with bromine (Floyd et al., 1978) are provided in the following table:

C, mg/L	Time, s	$\log(N/N_0)$	C, mg/L	Time, s	$\log(N/N_0)$
21.6	0	0	12.9	1.5	−2.5
21.6	0.5	−1.1	12.9	2	−2.7
21.6	1	−2.2	4.7	1	−0.8
21.6	1.5	−2.8	4.7	2	−1.3
21.6	2	−3.4	4.7	3	−2.2
12.9	0.5	−0.8	4.7	4	−2.5
12.9	1	−1.5			

Solution

1. Determine the values of Ct and $\ln(N/N_0)$ for each organism survival value.
   a. Ct is calculated simply by multiplying C by t.
   b. To convert from base 10 to base e logarithms, recall the logarithmic identity $\log_b(x) = \log_a(x)/\log_a(b)$, thus:

$$\ln(N/N_0) = \frac{\log(N/N_0)}{\log(e)} = 2.303 \log\left(\frac{N}{N_0}\right)$$

c. The required data table is shown below:

Time, s	C, mg/L	Ct, mg · s/L	ln(N/N0)	Time, s	C, mg/L	Ct, mg · s/L	ln(N/N0)
0.5	21.6	10.8	−2.53	1.5	12.9	19.4	−5.76
1	21.6	21.6	−5.07	2	12.9	25.8	−6.22
1.5	21.6	32.4	−6.45	1	4.7	4.7	−1.84
2	21.6	43.2	−7.83	2	4.7	9.4	−2.99
0.5	12.9	6.5	−1.84	3	4.7	14.1	−5.07
1	12.9	12.9	−3.45	4	4.7	18.8	−5.76

2. Prepare a plot of $\ln(N/N_0)$ as a function of Ct and fit a linear trendline through the data. Select trendline options to display the equation and r^2 value.
3. The required plot is shown below.

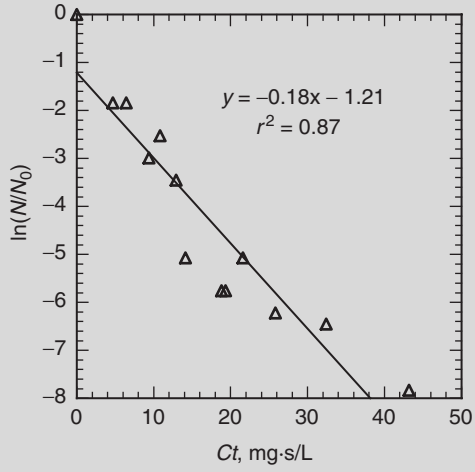

4. The slope of the line in the above plot corresponds to the coefficient of specific lethality, Λ_{CW}. From the plot $\Lambda_{CW} = 0.18$ and $r^2 = 0.87$.

Disinfection data do not always conform to Chick's linear semilog plot. Two anomalies, accelerating rate and decelerating rate, as illustrated on Fig. 13-4, sometimes occur. Reasons often cited in the literature for these particular curve shapes and the circumstances (organism, disinfectant, and magnitude of disinfection) under which each type of curve is sometimes found are also given. Contemporary kinetic models that describe these alternate forms of disinfection data are described in the next section.

Shape of semilog plot of disinfection data	Reasons for shape	Examples
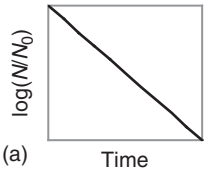 (a)	**Pseudo-first order** The most common form of disinfection data. 1. Data fit Chick's law.	**Free chlorine**: *E. coli,* poliovirus **Ozone**: Poliovirus*, E. coli, G. Lamblia,* and *C. parvum* **UV**: *C. parvum*, MS2 (<4 log), and *G. lamblia* (<3 log)
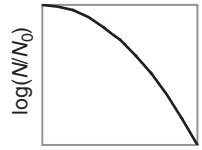 (b)	**Accelerating rate** Often observed at low disinfectant doses. Possible reasons include: 1. Disinfectant must react with more than one critical site in organism (Rahn, 1973; et al., 1975). 2. Disinfectant must take time to diffuse to critical site (Collins and Selleck, 1971). 3. Natural heterogeniety in resistance among organisms (Kim et al., 2002a).	**Combined chlorine**: Most organisms at low inactivation **Any disinfectant**: Suspension of aggregated virus particles of multicellular organisms **Chlorine dioxide**: *C. parvum*, endospores
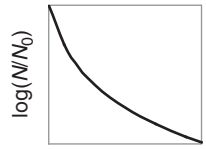 (c)	**Decelerating rate** Often observed after several logs of inactivations. Possible reasons include: 1. Decrease in germicidal properties of the disinfecting agent with time (Gard, 1957; Collins and Selleck, 1971). 2. Resistance to the disinfectant increases with increasing exposure (Gard, 1957; Collins and Selleck, 1971). 3. Natural heterogeniety in resistance among organisms (Hess, 1953). 4. Interference of particles with disinfection (Severin, 1980; Qualls et al, 1983; Parker and Darby, 1995). 5. Organisms are in clumps that test as one unit but must be inactivated individually (Hunt and Mariñas, 1997).	**Combined chlorine**: Most any organism at high removals **UV**: Total coliform in secondary effluent, *G. lamblia* above 3 log removal

Figure 13-4
Graphical forms of disinfection data.

Contemporary Kinetic Models

As discussed earlier, only a limited understanding of the specific mechanisms for the various disinfection reactions is now available. Substantially different kinetics mechanisms may control the rate of inactivation of different microorganisms with the same disinfectant or the same microorganisms with different disinfectants. There is extensive literature on disinfection modeling; two of these models are presented in the following discussion because they are useful in modeling many common disinfection reactions. The models discussed below may be used to model disinfection data for reactions with accelerating and/or decelerating rates on a semilog plot (Figs. 13-4b,c).

RENNECKER–MARIÑAS MODEL (ACCELERATING RATE)

Some organisms do not exhibit significant inactivation until a certain Ct value has been exceeded. This inactivation response is observed, for example, when chemical disinfectants are applied to oocysts and endospores. The Mariñas group at the University of Illinois has recently addressed this situation by proposing the use of a lag coefficient, b for Eq. 13-4 (Kim et al., 1999; Rennecker et al., 1997, 2001). The Rennecker–Mariñas model can be summarized as follows:

$$\ln\left(\frac{N}{N_0}\right) = \begin{cases} 0 & \text{for } Ct < b \quad (13\text{-}5) \\ -\Lambda_{CW}(Ct - b) & \text{for } Ct \geq b \quad (13\text{-}6) \end{cases}$$

where b = lag coefficient, mg · min/L

The lag coefficient b is the maximum value of Ct at which $\ln(N/N_0) = \ln(S_o) = 0$ (i.e., no inactivation has occurred). When b is zero, Eq. 13-6 corresponds to Eq. 13-4. It should be noted that the presentation of the mathematics used in the analysis of Eqs. 13-5 and 13-6 is consistent with but not identical to the approach used by Rennecker et al. (1997). The Rennecker–Mariñas model is demonstrated in Example 13-2.

Example 13-2 Application of the Rennecker–Mariñas model

Apply the Rennecker–Mariñas model to evaluate the coefficient of specific lethality and the lag coefficient for the inactivation of *C. parvum* using chlorine dioxide (ClO_2) based on the data given below. As shown in the data table, inactivation was measured at three concentrations of ClO_2 and at several time intervals. In analyzing the data, do not assume that it was possible to measure N_0 accurately (i.e., $N/N_0 \neq 0$ for $Ct < b$; instead, require N/N_0 = constant for $Ct < b$). Analyze the data by developing a spreadsheet solution and use the Solver function in Excel to determine the model parameters. Also calculate the coefficient of determination (r^2). Data for the inactivation of *C. parvum* by ClO_2 (Corona-Vasquez et al., 2002) are provided in the following table:

C, mg/L	t, min	$\log(N/N_0)$	C, mg/L	t, min	$\log(N/N_0)$
0.96	0.0	−0.21	0.48	122.0	−1.08
0.96	15.5	−0.25	0.48	152.0	−1.68
0.96	30.8	−0.38	4.64	0.0	−0.15
0.96	46.1	−0.55	4.64	2.1	0.02

C, mg/L	t, min	$\log(N/N_0)$	C, mg/L	t, min	$\log(N/N_0)$
0.96	61.2	−1.04	4.64	4.2	−0.11
0.96	76.2	−1.66	4.64	6.2	−0.19
0.96	91.1	−2.03	4.64	8.2	−0.29
0.48	0.0	−0.17	4.64	10.0	−0.56
0.48	32.0	−0.12	4.64	12.0	−0.79
0.48	61.6	−0.31	4.64	13.9	−1.19
0.48	92.0	−0.60	4.64	15.8	−1.47

Solution

Construct a spreadsheet, as shown below, for analysis of the data and determination of the model parameters. Because the Solver function will be used, some of the calculations will need to be automated using advanced features of Excel, including the IF function, as described below.

1. Compute the value of Ct for each experiment and enter the corresponding inactivation value into the spreadsheet.
2. The measured log survival ratios are entered into the column labeled Data in the table below.
3. The value of the model parameters can be determined using an IF statement of the form "IF $[Ct < b, \log(S_o), \log(S_o) + \text{slope}(b - Ct)]$."
4. Solver is used to minimize the sum of the [Data−model]^2 column by varying b, slope, and $\log(S_o)$. The results are displayed in the following table and figure:

Spreadsheet setup for model evaluation

Ct, mg · min/L	$\log(N/N_o)$ Data	$\log(N/N_o)$ Model	[Data-Model]^2	[Data-Data$_{avg}$]^2
0.0	−0.21	−0.2	0.001	0.216
14.9	−0.25	−0.2	0.004	0.182
29.6	−0.38	−0.2	0.036	0.089
44.3	−0.55	−0.5	0.001	0.015
58.8	−1.04	−1.0	0.000	0.138
73.2	−1.66	−1.6	0.010	0.972
87.5	−2.03	−2.1	0.001	1.852
0.0	−0.17	−0.2	0.000	0.259
15.4	−0.12	−0.2	0.005	0.310
29.6	−0.31	−0.2	0.016	0.130
44.2	−0.60	−0.5	0.007	0.005
58.6	−1.08	−1.0	0.002	0.167

(*continued*)

(*continued*)

Ct, mg · min/L	log(N/N_o) Data	log(N/N_o) Model	[Data-Model]^2	[Data-Data$_{avg}$]^2
73.0	−1.68	−1.6	0.017	1.016
0.0	−0.15	−0.2	0.001	0.277
9.7	0.02	−0.2	0.043	0.483
19.3	−0.11	−0.2	0.006	0.319
28.8	−0.19	−0.2	0.000	0.230
38.2	−0.29	−0.3	0.000	0.147
46.6	−0.56	−0.6	0.002	0.012
55.6	−0.79	−0.9	0.020	0.013
64.6	−1.19	−1.3	0.003	0.271
73.5	−1.47	−1.6	0.009	0.642
Average:	−0.67	Sum:	0.184	7.745

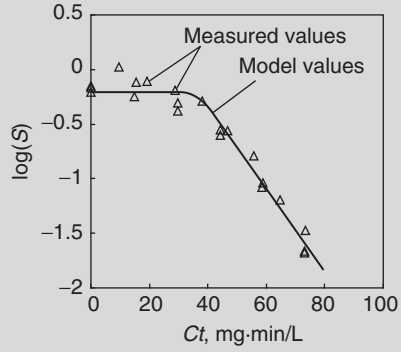

5. Solver minimizes the value of the sum of the [Data−model]^2 when the following values are used:

$$b = 34.9 \text{ mg} \cdot \text{min/L}$$

$$\text{Slope} = 0.036$$

$$\log(N/N_0) = -0.19$$

6. Since the data was plotted on a log (base 10) scale, the coefficient of specific lethality is calculated by dividing the slope by log(*e*):

$$\Lambda_{CW} = (\text{slope base } e) \,/\, \log(e) = 0.036\,(2.303) = 0.083 \text{ L/mg} \cdot \text{min}$$

7. The coefficient of determination (r^2) is calculated using the data in the spreadsheet as follows:

$$r^2 = 1 - \frac{\sum [\text{Data} - \text{model}]^2}{\sum [\text{Data} - \text{data}_{ave}]^2} = 1 - \frac{0.184}{7.745} = 0.98$$

COLLINS–SELLECK MODEL (DECELERATING RATE)

The Collins–Selleck model was developed specifically to address the inactivation of coliform organisms in domestic wastewater using free and combined chlorine (Collins and Selleck, 1971; Selleck and Saunier, 1978; Selleck, et al., 1970), but it has proven valuable for modeling the behavior of a number of other disinfection alternatives as well. The Collins–Selleck model is particularly useful when a declining rate of disinfection is observed (convex curve on Fig. 13-4c). The form of the Collins–Selleck model first published in the literature did not include a lag effect (Selleck et al., 1970). Although the final formulation was published shortly after that (Collins and Selleck, 1971), it did not appear in the peer-reviewed literature until sometime later (Selleck and Saunier 1978), and there was some discussion about its form even at that time (Haas, 1979; Selleck et al., 1980). Collins and Selleck began with a simple formulation that describes a declining rate of inactivation with time as proposed by Gard (1957) and adapted it to the lag in inactivation often observed in real systems. For batch reactors, the model has the form

$$\ln\left(\frac{N}{N_0}\right) = \begin{cases} 0 & \text{for } Ct < b \qquad (13\text{-}7) \\ -\Lambda_{CS}[\ln(Ct) - \ln(b)] & \text{for } Ct \geq b \qquad (13\text{-}8) \end{cases}$$

where Λ_{CS} = Collins–Selleck coefficient of specific lethality, unitless
b = lag coefficient, mg · min/L

An anomaly in the Collins–Selleck model is that the initial conditions are undefined because $\ln(Ct)$ at $t = 0$ is indeterminate. Nevertheless, there is a close parallel between the Collins–Selleck and Rennecker–Mariñas models. They have a similar form, but in the Rennecker–Mariñas model, the observed data are fit with a straight line when log survival is plotted versus Ct, whereas in the Collins–Selleck model, the data can be fit with a straight line when log survival is plotted versus $\log(Ct)$. Each model has only two parameters, Λ_{CW} or Λ_{CS} and b. Based on a large number of tests, it has been found that most disinfection data can be fit to one of these two models.

Example 13-3 Comparison of Chick–Watson and Collins–Selleck models

The Collins–Selleck model is particularly useful for modeling a declining rate of disinfection such as observed in the disinfection of coliform in wastewater above a *Ct* value of approximately 100 mg · min/L. Data from Selleck and Saunier (1978) for the disinfection of total coliform in wastewater with chloramines are presented below. Fit the Chick–Watson model to the data for *Ct* values less than 100 mg · min/L and construct a plot of the

results. Also plot the remainder of the data for *Ct* values greater than 100 mg · min/L on the same plot. Prepare a separate plot to fit the data using the Collins–Selleck model.

Ct, mg · min/L	$\log(N/N_0)$	*Ct*, mg · min/L	$\log(N/N_0)$	*Ct*, mg · min/L	$\log(N/N_0)$
5	−0.79	48	−3.21	244	−5.39
6	−0.61	54	−3.14	244	−5.96
6	−1.36	58	−3.57	291	−5.39
10	−1.79	64	−3.86	300	−5.54
15	−1.18	106	−4.64	319	−5.64
19	−1.86	130	−4.68	390	−5.68
26	−2.21	130	−5.16	417	−6
39	−3.14	175	−4.89	476	−5.74
				602	−5.75

Solution

1. Application of the Chick–Watson model:
   a. The 12 data points with *Ct* values less than 100 mg · min/L are put in an Excel spreadsheet and $\log(N/N_0)$ is plotted as a function of *Ct*.
   b. Use the trendline function to fit a line through the data. Select options to fit the line through the origin and to display the equation. As shown in the plot, the slope of the linear trendline (base 10) is 0.067 L/mg · min. Converting to base *e* by dividing by log(*e*), the following value is obtained:

$$\Lambda_{CW}\,(\text{base } e) = 0.067(2.303) = 0.15\ \text{L/mg} \cdot \text{min}$$

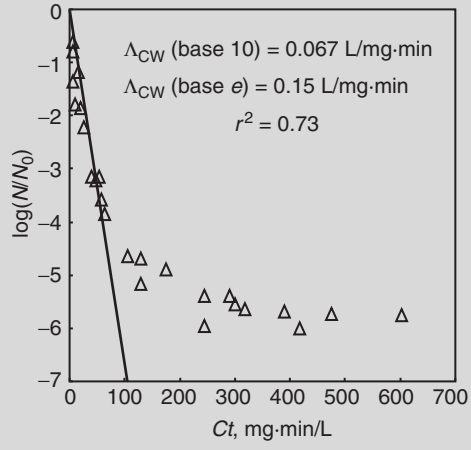

2. Application of the Collins–Selleck model:
   a. All 25 data points are put in an Excel spreadsheet and $\log(N/N_0)$ is plotted as a function of $\log(Ct)$.
   b. The linear trendline is used to determine the slope of the best-fit line.
   c. The slope of the trendline that corresponds to Λ_{CS} (base 10) is equal to 2.76. The value of the intercept b (base 10) is 1.32 mg · min/L. The corresponding base e values are the same. These results are displayed below:

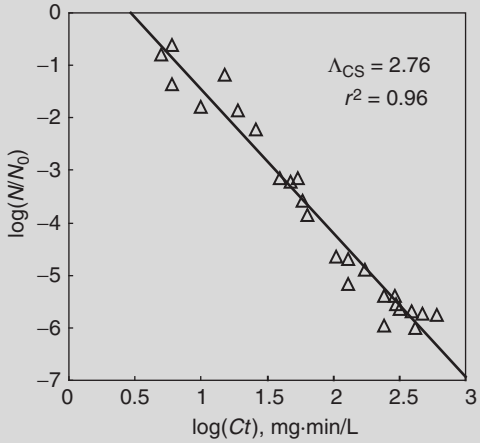

Comment

As shown in this example, the Collins–Selleck model was used effectively to model declining rate disinfection. Based on numerous studies, it has been found that the Collins–Selleck model can be used for a variety of organism–disinfectant combinations where both a declining rate of disinfection and a lag in disinfection are important.

Comparison of Disinfection Models

Some important characteristics of the disinfection models presented in this section are summarized in Table 13-2. The Chick–Watson model (Eq. 13-4) is not shown because it is a special case of the Rennecker–Mariñas model when $b = 0$. A selection of kinetic constants gathered from the literature are reported in Table 13-3. Constants are offered for the disinfection of total coliform from wastewater because this has long been a target organism in effluent reuse. Constants are presented for *E. coli* and poliovirus because these organisms have long been the targets of classical disinfection regulations. Constants are presented for *Giardia* and *Cryptosporidium* because the difficulty in inactivating these organisms is having profound effects on

Table 13-2
Comparison of disinfection models

Disinfection Model	Form of Data	Plots as Straight Line On	Number of Coefficients	Comment
Chick[a]: $\ln\left(\frac{N}{N_0}\right) = -k_c t$ where k_c = Chick's law rate constant, time^{-1}	Pseudo–first order	Semilog graph: $\log(N/N_o)$ vs. t	1	Widely used in microbiology. Approximates a lot of disinfection data.
Rennecker–Mariñas: For $Ct < b$ $\ln\left(\frac{N}{N_0}\right) = 0$ For $Ct > b$ $\ln\left(\frac{N}{N_0}\right) = -\Lambda_{CW}(Ct - b)$ where Λ_{CW} = coefficient of specific lethality, 1/(mg · min/L) b = lag coefficient, mg · min/L	Pseudo–first order with lag	Semilog graph: $\log(N/N_o)$ vs. Ct	2	Equation is consistent with "Ct" concept. Can approximate most disinfection data. Performs poorly only if the disinfection reaction truly shows an accelerating rate from the start or if a decelerating rate of reaction is observed. When $b = 0$, this equation simplifies to the Chick–Watson equation.
Collins–Selleck: For $Ct < b$ $\ln\left(\frac{N}{N_0}\right) = 0$ For $Ct > b$ $\ln\left(\frac{N}{N_0}\right) = -\Lambda_{CS}[\ln(Ct) - \ln(b)]$ where Λ_{CS} = log-based coefficient of specific lethality b = lag coefficient, mg · min/L	Decelerating rate with lag	Log–log graph: $\log(N/N_o)$ vs. $\log(Ct)$	2	Equation is also consistent with "Ct" concept. Can approximate most disinfection data. Performs poorly if only the accelerating phase is of interest or if several logs of first-order behavior are observed.

[a]The Chick–Watson model is not shown because it is a special case of the Rennecker–Mariñas model when $b = 0$.

Table 13-3
Selected kinetic parameters (base *e*) based on data in the literature[a]

Organism	Disinfectant	Chick–Watson and Rennecker–Mariñas Λ_{CW}, L/mg·min or m^2/J	*b*, mg·min/L or J/m^2	Collins–Selleck Λ_{CS}	Source of constant or data used to develop constant
E. coli	Cl_2, pH 8.5, $T = 2–5°C$	3.75	0.2	—	Butterfield et al. (1943)
	NH_2Cl	0.0375	10	—	Butterfield and Wattie (1946)
	NH_2Cl	0.0327	—	—	Butterfield and Wattie (1946)
	ClO_2	3.3	0.33	—	Scarpino et al. (1977)
	O_3	8330	—	—	Hunt and Mariñas (1999)
	UV	0.83	—	—	Harris et al. (1987)
Total coliform (wastewater or wastewater seed)	HOCl	—	0.005	1.2	Selleck and Saunier (1978)
	OCl^-	—	0.1	1.9	Selleck and Saunier (1978)
	NH_2Cl	—	3.0	2.8	Selleck and Saunier (1978)
	ClO_2	—	0.9	2.2	Roberts et al. (1980)
	UV	—	4	26	Tchobanoglous et al. (2003)
Poliovirus	HOCl	0.2	—	—	Floyd and Sharp (1979)
	NH_2Cl	—	—	—	—
	ClO_2	0.47	28	—	Scarpino et al. (1977)
	O_3	0.85	—	—	Katzenelson et al. (1974)
	UV	3	—	—	Cooper et al. 2001 (sewage)
MS-2	Cl_2	3.4	—	—	Haas et al. (1996)
	NH_2Cl	0.005	—	—	Cooper et al. (2001) (buffer)
	ClO_2	—	—	—	—
	O_3	—	—	—	—
	UV	0.96	—	—	Oppenheimer et al. (2001)

(*continued*)

Table 13-3 *(Continued)*

Organism	Disinfectant	Chick–Watson and Rennecker–Mariñas Λ_{CW}, L/mg·min or m^2/J	*b*, mg·min/L or J/m^2	Collins–Selleck Λ_{CS}	Source of constant or data used to develop constant
Giardia	Cl_2, pH 7	—	68	3.8	Haas and Heller (1990)
	NH_2Cl	—	300	5	JMM (1991) (*G. muris*)
	ClO_2	0.21	—	—	Wallis et al. (1989)
	O_3	—	0.02	1.77	JMM (1991) (*G. muris*)
	O_3	1.9	—	—	Wallis et al. (1989)
	UV	38	—	—	Oppenheimer et al. (2001) (*G. muris*)
C. parvum	Cl_2, pH 6	0.0013	375	—	Driedger et al. (2000)
	NH_2Cl	0.00077	5500	—	Rennecker et al. (2001)
	ClO_2	0.083	35	—	Corona-Vasquez et al. (2002)
	O_3	1.7	0.22	—	Driedger et al. (2001)
	O_3	0.83	—	—	Oppenheimer et al. (2000)
	UV	25	—	—	Oppenheimer et al. (2001)
B. subtilis	Cl_2, pH 6	0.0006	—	—	Brazis et al. (1958) (*B. anthracis*)
	NH_2Cl	0.00054	4560	—	Larson and Mariñas (2003)
	ClO_2	0.13	—	—	Radziminski et al. (2002)
	O_3	2.12	4.91	—	Larson and Mariñas (2003)
	UV	0.004	170	—	Knudson (1986) (*B. anthracis*)

[a]Unless otherwise noted all kinetic parameters are given for 25°C.

water treatment regulations. Constants are presented for *Bacillus subtilis* because its behavior in disinfection is thought to be similar to *B. anthracis*, a possible organism that may be used by terrorists.

Declining Concentration of Chemical Disinfectant

Chick's experiments were conducted with constant disinfectant concentrations because excess disinfectant was present. In the laboratory, researchers generally attempt to maintain a constant disinfectant concentration so that disinfection rates can be measured with maximum precision. Given the complexities that exist in the microbiological world that can influence the outcome of such experiments, it is important to minimize variations in chemistry and physical conditions. A constant residual of combined chlorine can usually be achieved in full-scale contactors as well. With free chlorine and chlorine dioxide, a constant residual concentration can be maintained for short contact times. For these same disinfectants at longer contact times or for ozone at any contact time, once must account for residual decay.

Accounting for varying disinfection concentration can be addressed by dividing the problem into two parts: (1) modeling the decay of the disinfectant and (2) integrating that work into the model of the disinfection reaction itself. For all the common oxidizing disinfectants (chlorine, combined chlorine, chlorine dioxide, and ozone), it is often assumed that disinfectant decay can be modeled as first order, that is,

$$r_d = -k_d C \tag{13-9}$$

where r_d = reaction rate for the decline in disinfectant concentration with time, mg/L·s or mol/L·s
k_d = first-order decay rate, s^{-1}
C = disinfectant concentration, mg/L or mol/L

The decay of these disinfectants is often characterized by two phases, an early phase of rapid decay followed by a later phase with slower decay. When two-phase decay occurs, a second-order model with a fast reaction step and a slow reaction step has been used successfully (Kim et al., 2002a; Lev and Regli, 1992), but this model is rather difficult to use because it cannot be solved analytically. Another alternative is the parallel first-order decay model proposed by Haas and Karra (1984b), in which it is assumed that decay may proceed through two mechanisms, each first order but involving a different component of the chlorine residual:

$$r_d = -xk_{d1} C - (1 - x) k_{d2} C \tag{13-10}$$

where x = fraction of disinfectant decaying by the first mechanism, unitless
C = concentration of disinfectant, mg/L or mol/L
k_{d1}, k_{d2} = decay coefficient for two different mechanisms, s^{-1}

The first component, with an initial concentration of xC_0, is subject to first-order decay with a faster rate constant, k_{d1}, and the second component,

with an initial concentration of $(1 - x)\,C_0$, is subject to first-order decay with a slower rate constant, k_{d2}. As noted above, the value of x, by definition, is between 0 and 1. When $x = 0$, the parallel first-order model becomes the simple first-order model; the same is true when $x = 1$.

Finding an analytical solution in which the decay reaction and the disinfection reaction are integrated together adds to the complexity of the mathematics used to describe the disinfection process. Where analytical solutions are not available, it is possible to use computer models to simulate the two processes in parallel. Haas and Joffe (1994) have developed an analytical solution for the Chick–Watson model.

Influence of Temperature on Disinfection Kinetics

The effect of temperature on the rate of a chemical reaction is described by the Arrhenius equation, as discussed in Chap. 5, and is used here to describe the influence of temperature on the pseudo-first-order disinfection rate constant:

$$\ln(k_r) = \ln(A) + \left(-\frac{E_a}{R}\right)\left(\frac{1}{T}\right) \tag{5-85}$$

where k_r = appropriate reaction rate constant, k_c, Λ_{CW}, Λ_{CS}, or k_d.
E_a = activation energy, J/mol
R = universal gas constant, 8.314 J/(mol · K)
T = reaction temperature, K (273 + °C)
A = collision frequency parameter

Once the rate is known at one temperature, the rate at another temperature can be determined if the activation energy E_a is known. In the disinfection literature, an empirical approach used is to specify θ in the following equation:

$$\frac{k_{r,T_1}}{k_{r,T_2}} = \theta^{T_1 - T_2} \tag{13-11}$$

where k_{r,T_1} = reaction rate constant at temperature 1
k_{r,T_2} = reaction rate constant at temperature 2
θ = empirical constant, dimensionless
T_1 = temperature corresponding to known rate constant k_{r,T_1}, K (273 + °C)
T_2 = temperature corresponding to known rate constant k_{r,T_2},K (273 + °C)

Combining Eqs. 5-85 and 13-11 and solving for θ, the following expression is obtained:

$$\theta = e^{E_a/RT_1T_2} \tag{13-12}$$

Because the product $T_1\,T_2$ is somewhat insensitive to changes in temperature, it is reasonable to assume θ is constant in empirical approach. Values of E_a from the literature are summarized in Table 13-4.

Table 13-4
Activation energies for a variety of disinfection reactions

Microorganism	Disinfectant	E_a, kJ/mol	$K_{25°C}/K_{5°C}$	Reference
C. parvum	HOCl	71.9		Rennecker et al. (2001)
C. parvum	HOCl	64.7		Corona-Vasquez et al. (2002)
		72[a]	6.4	
C. parvum	ClO_2	67.5		Corona-Vasquez et al. (2002)
C. parvum	ClO_2	86.3		Ruffell et al. (2000)
		77[a]	8.0	
C. parvum	NH_2Cl	75.6		Driedger et al. (2001)
C. parvum	NH_2Cl	78.7		Rennecker et al. (2001)
C. parvum	NH_2Cl	59.2[b]		Corona-Vasquez et al. (2002)
		77[a]	8.0	
C. parvum	O_3	102		Oppenheimer et al. (2001)
C. Parvum	O_3	75.7		Driedger et al. (2001)
C. Parvum	O_3	81.2		Rennecker et al. (1999)
C. Parvum	O_3	47.6		Finch et al. (2001)
		76[a]	7.8	
C. muris	O_3	92.8	12	Kim et al. (2002b)
E. coli	O_3	37.1	2.7	Hunt and Mariñas (1997)
G. lamblia	O_3	39.2	2.9	Wickramanyake et al. (1984b)
G. muris	O_3	70	6.6	Wickramanyake et al. (1984a)
N. gruberi	O_3	31.4	2.3	Wickramanyake et al. (1984a)
B. subtilis	O_3	46.8	3.6	Larson and Mariñas (2003)
B. subtilis	NH_2Cl	79.6	8.7	Larson and Mariñas (2003)

[a]Recommended value.
[b]Old oocysts.

Approaches to Relating Disinfection Kinetics to Disinfection Effectiveness

The true, detailed kinetics of most chemical disinfectants are exceedingly complex, and they are influenced by the chemistry of the disinfectant as well as the nature of the susceptibility in the organism. Moreover, measuring disinfection effectiveness is difficult to do with great precision, partly because of the complexity of the chemical conditions but also due to the imprecise nature of most microbiological measurements. As a result, it is probably best to employ the simplest approach possible to describe the results of disinfection experiments. In order of increasing complexity, the following alternatives might be considered:

1. *Ct tables.* Numerical *Ct* (concentration × time) values are established to achieve a given degree of inactivation of a specific organism using a defined disinfectant under controlled conditions. This approach is

consistent with all the models presented in this section. Furthermore, the U.S. EPA uses this approach in regulating disinfection of drinking water. When required, different tables can be offered for a range of concentrations, as the U.S. EPA did for the inactivation of *G. lamblia* with free chlorine.

2. *Semilog plots of survival versus Ct values.* The use of semilog plots of log survival as a function of *Ct* is consistent with the Chick–Watson model and the Rennecker–Mariñas model. In this approach, it is assumed that the log survival values will plot as a linear function of time or the product *Ct* on a semilog plot and only one or two constants, Λ_{CW} and *b*, are required for application of the model. This approach is often successful when a modest degree of disinfection is required, a reduction of approximately 3 log inactivation, for example.
3. *Log-log plots of survival versus Ct values.* The use of log–log plots is consistent with the Collins–Selleck model. This approach is useful for situations where a lag time is present (complex organisms, slow disinfectants, etc.) or where a declining rate of disinfection with time is observed. This approach is also useful when disinfection requirements are substantial, for example, 4 log reduction or more. In the Collins–Selleck model, it is assumed that the log survival will plot as a linear function against $\log(Ct)$ and that two constants, Λ_{CS} and *b*, are required for application of the model.

Generally, as disinfection models become more complex, the precision with which they can be used to describe the results of a given disinfection experiment improves. However, comparing the constants of the simpler models provides better perspective on the performance of different disinfectants and on the resistance of different organisms. The ability to compare results is one of the reasons that Chick's law and the Chick–Watson equation continue to be popular.

The *Ct* Approach to Disinfection

In each of the approaches discussed in the previous section, disinfection effectiveness was related to the product *Ct*. In fact, the product *Ct* has long been used as a basis for disinfection requirements. It is equally practical when the Collins–Selleck and Rennecker–Mariñas models are used. The *Ct* product required for achieving a given level of disinfection for a specific microorganism under defined conditions is a useful way of comparing alternate disinfectants and for comparing the resistance of a variety of pathogens. Indeed, the product *Ct* can be thought of as the dose of disinfectant.

The dose concept, analogous to *Ct*, is also applicable when UV light is used for disinfection. The product of the UV light intensity (mW/cm^2) and the time of exposure is used to compute the dose ($mW/cm^2 \times s = mJ/cm^2$). This product is often referred to as *It* (intensity × time). Modeling disinfection with UV light using *It* in place of *Ct* in Eq. 13-4 has been

successful. There is probably greater justification for this equation for UV light because the mechanism of inactivation is not so much a function of light intensity but a function of exposure of the organism to a quantity of potentially damaging photons.

The *Ct* concept also allows for the development of a broad overview of the relative effectiveness of different disinfectants and the resistance of different organisms. The *Ct* required to produce a 99 percent (2 log) inactivation of several microorganisms using the five disinfection techniques most often used in water treatment is illustrated on Fig. 13-5. Because of the difference in the behavior from one organism and one disinfectant combination to the next, *Ct* and *It* products range over seven orders of magnitude. For example, the *Ct* product required to inactivate *C. parvum* must be three orders of magnitude higher with combined chlorine than with ozone. Comparing

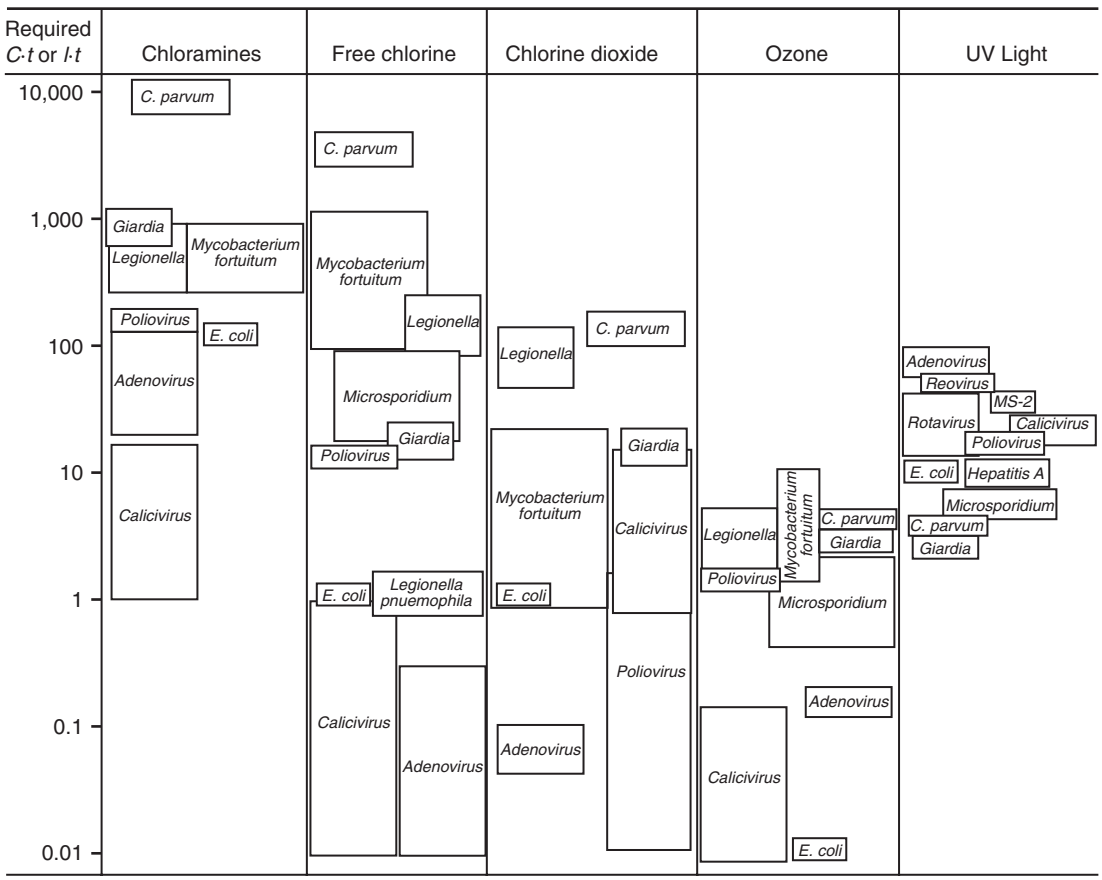

Figure 13-5
Overview of disinfection requirements for 99 percent inactivation. (Adapted from Jacangelo et al., 1997.)

UV disinfection to disinfection with chemical oxidants, little similarity exists between the *It* values and *Ct* values for a single organism. While the required UV doses vary over a range of two orders of magnitude, their variation is much less than that for other disinfectants. The reduced variation may be a result of the fact that UV disinfection of all microorganisms results from a similar protein dimerization mechanism.

The U.S. EPA began the practice of specifying *Ct* products that must be met as a way of regulating the control of pathogens in water treatment with the promulgation of the Surface Water Treatment Rule (U.S. EPA, 1989). Tables of *Ct* and *It* values required to meet the primary disinfection requirements are available in the *Surface Water Treatment Rule Guidance Manual* (U.S. EPA, 1991) available on the EPA website.

A limitation of the *Ct* approach is that the microorganisms in a real disinfection contactor are exposed to a distribution of contact times according to the contactor's residence time distribution (RTD), rather than all microorganisms being exposed to the disinfectant for the same amount of time. The RTD has a significant impact on disinfection effectiveness, as discussed in detail in the next section.

13-4 Disinfection Kinetics in Nonideal Flow-Through Reactors

The disinfection kinetics described in Sec. 13-3 were based on studies conducted in completely mixed batch reactors (CMBRs). While the insight obtained from batch reactors is useful, full-scale continuous-flow systems exhibit more complex nonideal behavior. Of particular importance is the impact of dispersion on the progress of the reaction.

Three approaches to modeling the performance of real (nonideal) reactors are introduced in Chap. 6: (1) the tanks-in-series (TIS) model, (2) the dispersed-flow model (DFM), and (3) the segregated-flow model (SFM). The TIS model simulates the effects of dispersion on the RTD curve by an analogy between a real reactor and a series of completely mixed flow reactors (CMFRs). The parameter that describes dispersion in the TIS model is the number of reactors in series, n. A high value of n corresponds to low dispersion.

The DFM simulates the effects of dispersion on the RTD by including mass transport by axial dispersion in addition to advection into the mass balance of a plug flow reactor (PFR) In the DFM, dispersion is described using the Peclet number (Pe) or the dispersion number ($d, \mathrm{Pe} = 1/\mathrm{d}$). A high value of Pe or a low value of d corresponds to low dispersion.

The SFM, presented in Sec. 6-9, simulates the effects of nonideal mixing by an analogy between a real reactor and a series of parallel PFRs having detention times that, in sum, match the RTD of the real reactor. While the TIS model and the DFM incorporate assumptions about the nature of the RTD curve, an RTD curve must be provided to use the SFM.

In the TIS model, it is assumed that all the reactants are mixed completely throughout each reactor at all times. In the DFM, it is assumed that all

reactants are mixed completely in the lateral direction but axial transport occurs by advection and dispersion. When dispersion is low, the TIS and DFM models produce similar results. In the SFM, it is assumed that the reactants are never completely blended in the reactor; rather the target reactant travels through the reactor in small cells or discrete elements that react with the bulk solution.

Application of the SFM Model to Disinfection

Disinfection processes are an ideal application of the SFM because microorganisms actually do travel through the reactor as particles, separate from the fluid, but react with disinfectants in their environment as they pass through (Trussell and Chao, 1977). If disinfection conditions are uniform throughout the reactor (e.g., the reactant residual or the intensity of inactivating irradiance is uniform throughout), the inactivation of each individual microorganism is the same as it would be in a batch reactor after the same residence time. The RTD of a conservative tracer can reasonably be used to describe the RTD of the microorganisms themselves. Thus, the disinfection process can be modeled by the SFM (see Sec. 6-9):

$$\frac{N}{N_0} = \sum_{i=1}^{n} R(\theta_i)E(\theta_i)\ \Delta\theta_i \tag{6-123}$$

where
N = number of microorganisms in the effluent from the real reactor, org/mL
N_0 = number of microorganisms in the influent to the real reactor, org/mL
$R(\theta_i) = N_i/N_0$ = inactivation of microorganisms achieved in CMBR (or PFR) after reaction time equal to θ_i
θ_i = normalized time (time divided by mean residence time, $t_i/\bar{t}$), dimensionless
$E(\theta_i)$ = exit age distribution at time θ_i (see Chap. 6)
$\Delta\theta_i$ = differential normalized time step
i = time step in RTD
n = total number of time steps in RTD

Selleck first introduced the approach outlined above to modeling in the early 1970s (Selleck et al., 1970). Trussell and Chao (1977) then employed this approach to demonstrate the influence of dispersion on chlorine contactor performance. Both authors worked on disinfection of coliform bacteria using combined chlorine and, in both studies, the disinfectant residual was assumed to be constant and uniform throughout the reactor. Scheible (1987) introduced a similar approach to the modeling of UV disinfection in the U.S. EPA disinfection design manual (U.S. EPA, 1986). The approach is appropriate for UV disinfection if it is assumed that turbulent flow exists, no short circuiting occurs, and each organism takes a path through the contactor such that its average exposure to UV light is equal to the average intensity of UV light in the reactor.

The promulgation of the U.S. EPA's Surface Water Treatment Rule substantially increased disinfection requirements for drinking water in the United States (U.S. EPA, 1989) and, as a result, has stimulated further interest in methods of refining the rule's approach to specifying disinfection. Lawler and Singer (1993) reintroduced the concept again and later Haas demonstrated its application (Haas et al., 1995). Subsequently, the SFM concept was incorporated in the *integrated disinfection design framework*, an effort to further optimize the design and operation of water disinfection systems (Bellamy et al., 1998; Ducoste et al., 2001). An example of the application of the SFM to disinfection is demonstrated in Example 13-4.

Example 13-4 Application of SFM to estimate disinfection efficiency

Use the disinfection data from Example 13-2 to determine the hydraulic detention time of a contactor designed for the inactivation of *C. parvum* using chlorine dioxide. The contact chamber is to be designed with a hydraulic detention time to provide a $C\tau$ value equal to the Ct value that achieves 4 log inactivation in the batch tests. The target chlorine dioxide residual in the full-scale contactor is 0.8 mg/L.

After the full-size contactor was built, tracer tests were conducted to evaluate the hydraulic characteristics of the contactor. Using the procedures outlined in Chap. 6, the tracer curve has been analyzed to produce the exit age distribution. The mean residence time was found to be 178 min and the results of the tracer study are given in the following table:

θ_i	$E(\theta_i)$	θ_i	$E(\theta_i)$	θ_i	$E(\theta_i)$
0.15	0	0.91	1.995	1.67	0.128
0.31	0	1.06	1.541	1.82	0.067
0.46	0.017	1.21	0.928	1.98	0.046
0.61	0.279	1.36	0.446	2.13	0.036
0.76	0.895	1.52	0.251	2.28	0.015

Use the tracer study data and contactor design information: (a) plot the exit age distribution $E(\theta_i)$ versus θ_i; (b) use the SFM to estimate the level of inactivation, $\log(N/N_0)$, that will actually occur in the full-scale reactor with dispersion.

Solution

1. Determine the hydraulic detention time for the full-scale contact chamber using the batch data.

a. The values for the disinfection parameters found in Example 13-2 were $\Lambda_{CW} = 0.083$ L/mg·min and $b = 34.9$ mg·min/L. Thus, inactivation as expressed by the Rennecker–Mariñas model is

$$\ln\left(\frac{N}{N_0}\right) = \begin{cases} 0 & \text{for } Ct < 34.9 \\ -0.083(Ct - 34.9) & \text{for } Ct \geq 34.9 \end{cases} \quad (1)$$

b. Find the value of Ct that corresponds to 4 log inactivation. For 4 log inactivation, $\log(N_0/N) = 4$, so $N/N_0 = 10^{-4} = 0.0001$. Rearranging Eq. 1 to solve for Ct yields

$$\ln(0.0001) = -0.083 \text{ L/mg} \cdot \text{min}\,(Ct - 34.9 \text{ mg} \cdot \text{min/L})$$

$$Ct = \frac{-\ln(0.0001)}{0.083 \text{ L/mg} \cdot \text{min}} + 34.9 \text{ mg} \cdot \text{min/L} = 145.5 \text{ mg} \cdot \text{min/L}$$

c. Find the hydraulic detention time that provides a Ct value of 146 mg · min/L when the chlorine dioxide residual is 0.8 mg/L:

$$\tau = t = \frac{Ct}{C} = \frac{145.5 \text{ mg} \cdot \text{min/L}}{0.8 \text{ mg/L}} = 182 \text{ min}$$

2. Plot the exit age distribution using the data provided in the problem statement. The exit age distribution is plotted below:

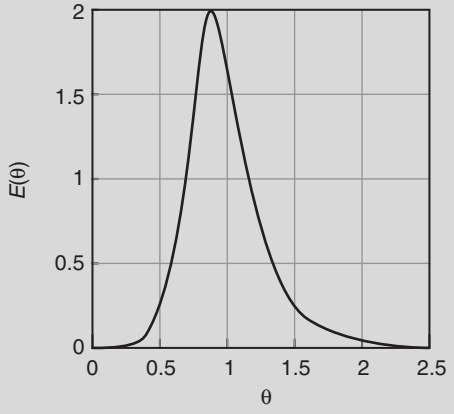

3. Determine the degree of inactivation achieved with the contactor using the SFM. Using the data given in the problem statement, a spreadsheet is developed using the principles of the SFM shown in Chap. 6. The resulting spreadsheet is shown below. As an example, calculations for the fifth row of the spreadsheet are as follows:
   a. Columns 1 and 2 contain values of θ_i and $E(\theta_i)$ given in the problem statement.

b. Column 3 ($\Delta\theta_i$):

$$\Delta\theta_i = \theta_i - \theta_{i-1} = 0.61 - 0.46 = 0.15$$

c. Column 4 [$R(\theta_i)$] is developed using an IF statement because the value changes depending on whether Ct_i is less or greater than b:
If $Ct_i < b$, then $N_i/N_0 = e^0 = 1$.
If $Ct \geq b$, then $N_i/N_0 = \exp\left[-\Lambda_{CW}\left(Ct_i - b\right)\right]$, where $t_i = \theta_i \bar{t}$.

$$\frac{N_0}{N_i} = \exp\left\{-0.083\ \text{L/mg} \cdot \min\left[(0.8\ \text{mg/L})\,(0.61)\,(178\ \text{min})\right.\right.$$
$$\left.\left. -34.5\ \text{mg} \cdot \text{min/L}\right]\right\} = 0.013$$

d. Column 5 [$R(\theta_i)E(\theta_i)\Delta\theta_i$]:

$$R\,(\theta_i)\,E\,(\theta_i)\,\Delta\theta_i = (0.0130)\,(0.279)\,(0.15) = 5.42 \times 10^{-4}$$

θ_i	$E(\theta_i)$	$\Delta\theta_i$	$R(\theta_i)$	$R(\theta_i)E(\theta_i)\Delta\theta_i$
0				
0.15	0	0.15	1	0
0.31	0	0.16	0.449	0
0.46	0.017	0.15	0.0763	1.95×10^{-4}
0.61	0.279	0.15	0.0130	5.42×10^{-4}
0.76	0.895	0.15	2.20×10^{-3}	2.95×10^{-4}
0.91	1.995	0.15	3.74×10^{-4}	1.12×10^{-4}
1.06	1.541	0.15	6.35×10^{-5}	1.47×10^{-5}
1.21	0.928	0.15	1.08×10^{-5}	1.50×10^{-6}
1.36	0.446	0.15	1.83×10^{-6}	1.22×10^{-7}
1.52	0.251	0.16	2.76×10^{-7}	1.11×10^{-8}
1.67	0.128	0.15	4.69×10^{-8}	9.01×10^{-10}
1.82	0.067	0.15	7.97×10^{-9}	8.01×10^{-11}
1.98	0.046	0.16	1.20×10^{-9}	8.85×10^{-12}
2.13	0.036	0.15	2.04×10^{-10}	1.10×10^{-12}
2.28	0.015	0.15	3.47×10^{-11}	7.81×10^{-14}
				$\Sigma = 0.00116$

e. The degree of inactivation is the sum of column 5 [$R(\theta_i)E(\theta_i)\Delta\theta_i$]. Thus, $N/N_0 = 0.00116$ and the log removal value (LRV) is

$$LRV = \log\left(\frac{N}{N_0}\right) = -\log(0.00116) = 2.94$$

Comment

Due to dispersion, the full-scale contactor achieves less than 3 log of inactivation when the hydraulic residence time was set equal to the time necessary to achieve 4 log of inactivation in laboratory batch tests (see Sec. 4-5 for additional discussion of expressing removal in terms of log removal) Clearly, a different approach must be used to determine the hydraulic residence time of a full-scale reactor when dispersion is important.

When Dispersion Is Important in Disinfection

Minimizing dispersion and short circuiting in disinfection contactors is widely accepted. The U.S. EPA limits the credit for disinfection contact time to the time it takes for the first 10 percent of a tracer to pass through a disinfection contactor (t_{10}), that is, the value of t in Ct is t_{10} instead of τ. California requires the minimum time to the peak concentration on the tracer curve (t_{modal}) to be 90 min and a minimum length-to-width ratio of 40 : 1 for baffled chlorine contactors in its regulations for reclaiming wastewater for nonrestricted reuse (Cal DHS, 1999).

As a general rule, reducing dispersion is more important when disinfection goals are substantial. For example, dispersion is more important in the design of a contactor that must achieve 4 log of inactivation than in the design of a contactor that must achieve 1 log of reduction. This effect is true regardless of the organism under consideration or its specific reaction kinetics.

A thought experiment can be used to illustrate this effect. Assume a disinfection process is designed to achieve a 4 log reduction of a particular virus and a 1 log reduction of a certain protozoa. Further assume the reactor operates as designed and achieves exactly those objectives. A small bypass pipe is installed and 1 percent of the flow coming into the reactor is diverted so that it flows around the reactor and blends, without disinfection, with the treated water from the reactor. The result of the experiment is illustrated on Fig. 13-6. As illustrated, the small diversion has almost no impact on the removal of protozoa (only 9 percent increase in effluent concentration) but severely compromises the removal of the virus, exposing the consumer to virus levels over 100 times higher than the goal that was being sought.

Using the reactor dispersion models presented in Chap. 6, it is possible to compare the performance of a real reactor with dispersion with an ideal plug flow reactor. A model may be prepared to estimate the amount of dispersion that could be allowed without compromising plug flow performance more than 5 percent (in other words, without reducing the log removal more than 5 percent). As shown on Fig. 13-7, which was developed for a first-order reaction and with a removal goal that spans several orders of magnitude, the requirements for controlling dispersion are modest when the required removal is modest. As the removal requirements increase to 3 log or more,

Prior to modifications:

Influent:	
Protozoa A	1 org/10,000 L
Virus B	1 org/10 L
Goal for both	1 org/100,000 L

→ Patented, guaranteed, virus and Cyst killer. Achieves 1 log removal for protozoa A and 4 logs removal for virus B →

Effluent:	
Protozoa A	1 org/100,000 L
Virus B	1 org/100,000 L
Success!	

After modifications:

Influent:	
Protozoa A	1 org/10,000 L
Virus B	1 org/10 L
Goal for both	1 org/100,000 L

→ Patented, guaranteed, virus and Cyst killer. Achieves 1 log removal for protozoa A and 4 logs removal for virus B →

Effluent:	
Protozoa A	1.1 org/100,000 L
Virus B	101 org/100,000 L
Fails Virus B	

Bypass for 1% of flow

Calculations:

Effluent protozoa A = (1)(0.99) + (10)(0.01) = 1.09/100,000 L
Log removal = 0.96, somewhat below goal

Effluent virus B = (1)(0.99) + (10,000)(0.01) = 101/100,000 L
Log removal = 2.0, far below goal

Figure 13-6
Thought experiment: Dispersion and short circuiting are more important when removal goals are high.

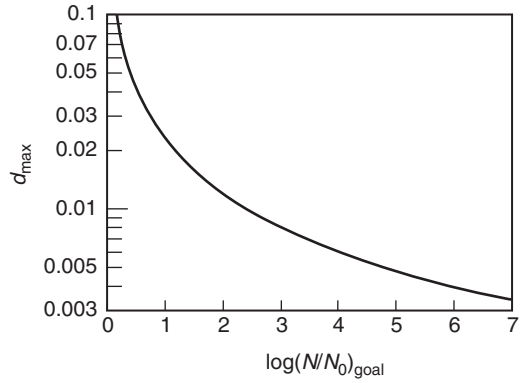

Figure 13-7
Allowable dispersion for contactor versus inactivation goals. At d_{max}, performance is short of goal by 5 percent.

it becomes difficult to prevent the dispersion from being greater than the allowable amount. Removals higher than 3 log generally can only be accomplished by constructing reactors with a significantly greater hydraulic detention time (and greater *Ct* value) than predicted by removal measured in a batch reactor. For instance, the reactor in Example 13-4 could meet 4 log inactivation requirements if the mean residence time were 30 percent greater than the time predicted by the batch tests.

Assessing Dispersion with the t_{10} Concept

A number of indices have been used to assess performance of full-scale disinfection contactors. Some of the more common indices are the dispersion number d, t_{10}/τ, t_{10}/t_{90}, and t_{modal}. A reasonable simulation of the original RTD of a reactor can be produced using the dispersion number and the DFM for a closed system (see Chap. 6). The RTD curve generated by the DFM for a given dispersion number can be used as a substitute for actual tracer data to estimate reactor performance using the SFM (Trussell and Chao, 1977) as demonstrated in Example 13-4. As a result, the dispersion number is perhaps the best measure of the suitability of a reactor for accomplishing disinfection. Nevertheless, regulators tend to prefer parameters such as t_{10} (US EPA, 1986) or t_{modal} (Cal DHS, 1999) as these values are easier to determine and more readily understood by operating personnel. Because of the U.S. EPA's regulations, t_{10} deserves special attention where water treatment is concerned.

To assess whether using the t_{10} value provides the same level of protection as controlling dispersion, Fig. 13-8 was constructed using Eq. 6-123 and a reaction that would achieve 4 log of removal in a plug flow reactor. The performance estimated by the SFM for the reactor with dispersion (middle curve) is compared to the performance credit that would be allowed for the reactor based on the batch equation and the product Ct_{10} (bottom curve). The inactivations estimated by the SFM and by the product Ct_{10} both improve as dispersion is reduced. From the presentation on Fig. 13-8 it can be concluded that the U.S. EPA's t_{10} approach is effective, but conservative.

The design of disinfection contact chambers that exhibit low dispersion is presented later in this chapter, after sections that describe each of the chemical disinfectants.

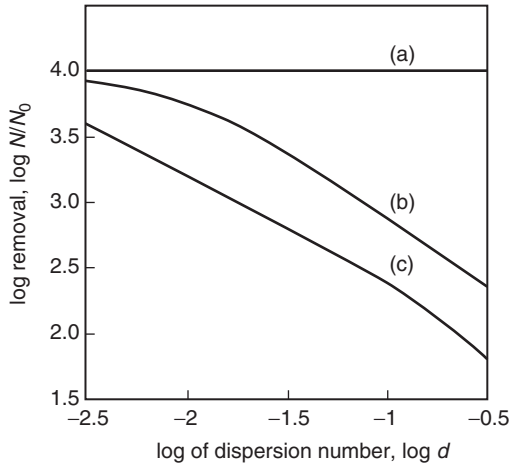

Figure 13-8
Reactor disinfection performance predictions: (a) ideal plug flow; (b) segregated-flow model (SFM) with dispersion, derived from residence time distribution (RTD) curve produced using closed-system dispersion flow model (DFM); and (c) predicted using t_{10} values derived from $E(\theta)$ curves based on closed-system DFM.

13-5 Disinfection with Free and Combined Chlorine

Until approximately World War II, free and combined chlorine (chlorine combined with ammonia, also known as chloramines) were both commonly used and viewed as effective disinfectants. In 1943, the U.S. PHS demonstrated that free chlorine exhibits more rapid kinetics in the disinfection of several bacteria (Wattie and Butterfield, 1944). As a result, the use of combined chlorine declined between 1943 and the mid-1970s. In the mid-1970s, it became widely recognized that free chlorine formed chemical by-products (Bellar and Lichtenberg, 1974; Rook, 1974) and that combined chlorine did so to a much lesser degree (Stevens and Symons, 1977). Since that realization, the use of combined chlorine has increased, particularly the addition of ammonia to convert a free-chlorine residual to a combined chlorine residual once primary disinfection has been accomplished. By 2004, about one in four utilities in the United States were using combined chlorine (U.S. EPA, 2004).

Chemistry of Free Chlorine

When chlorine gas is injected into water, it dissolves according to Henry's law and then rapidly reacts with the water to form hydrochloric acid and hypochlorous acid:

$$Cl_2(g) + H_2O \rightarrow HCl + HOCl \tag{13-13}$$

Hydrochloric acid is a strong acid that dissociates completely, causing a reduction in alkalinity and pH:

$$HCl \rightarrow H^+ + Cl^- \tag{13-14}$$

Hypochlorous acid is a weak acid and the extent of dissociation depends on pH (see Chap. 5 for discussion of weak acids):

$$HOCl \rightleftarrows H^+ + OCl^- \tag{13-15}$$

$$K_a = \frac{[H^+][OCl^-]}{[HOCl]} \tag{13-16}$$

The pK_a for HOCl is 7.6 at 20°C; hypochlorous acid (HOCl) is the predominant form below this pH value and hypochlorite ion (OCl^-) is the predominant form above it. The distribution between HOCl and OCl^- is illustrated on Fig. 13-9 as a function of pH and temperature. Hypochlorous acid (HOCl) exhibits faster disinfection kinetics than does hypochlorite ion (OCl^-) (see Table 13-3). Consequently, a pH of 7 or less is desirable where disinfection alone is concerned. As can be seen from Fig. 13-9, temperature has a small effect, warmer waters causing hypochlorous acid to dissociate at somewhat lower pH.

Chlorine is relatively stable in pure water but reacts slowly with the organic matter naturally present in drinking waters and rapidly with sunlight. Where sunlight is concerned, photons react with hypochlorite ion to produce

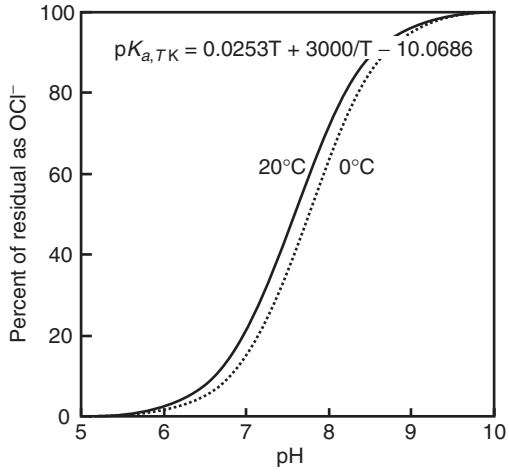

Figure 13-9
Effect of temperature and pH on fraction of free chlorine present as hypochlorous acid. (Adapted from Morris, 1966.)

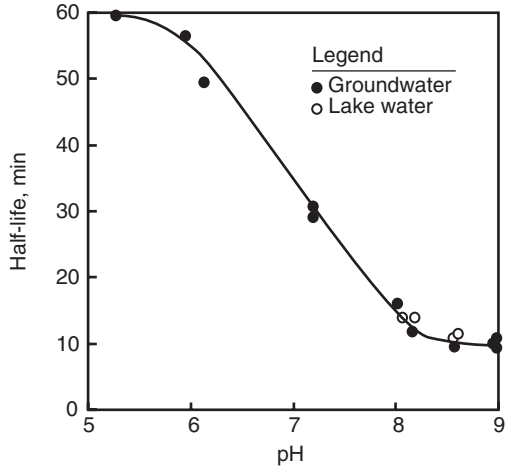

Figure 13-10
Half-life of free chlorine residual in sunlight.

oxygen, chlorite ion, and chloride ion (Buxton and Subhani, 1971). The sensitivity of the reaction rate to pH, a consequence of the fact that the photolytic reaction is with hypochlorite ion and not hypochlorous acid, is illustrated on Fig. 13-10, constructed using the data of Nowell and Hoigné (1992a,b).

Although significant research has investigated the decay of chlorine residuals in the presence of natural organic matter, no universal relationships have evolved. Rather, the decay of free chlorine is often best modeled with the simple first-order reaction depicted in Eq. 13-9. Sometimes the process is modeled as two reactions operating in parallel, a fast reaction with rapidly reducible substances and a slower first-order reaction (Eq. 13-10). Studying data from multiple sources, Powell et al. (2000)

concluded that the activation energy for the chlorine decay reaction is on the order of 62 kJ/mol. Modeling chlorine decay as a first-order reaction is illustrated in Example 13-5.

Example 13-5 Evaluating chlorine residual decay data

One milligram of chlorine was added to 1 L of water. The water was stored in the dark at a constant temperature of 10°C and the chlorine residual was measured periodically. The results of the chlorine decay experiment are given below. Assuming a simple first-order decay reaction, estimate the constant for first-order decay, k_d, of chlorine. Assuming that the activation energy E_a, is 62 kJ/mol, what would k_d be at 25°C? What would the residual have been at the end of the same decay test at 25°C?

Time, h	Concentration, mg/L
0	0.97
1	0.80
2	0.69
3	0.63
5	0.54
8	0.45
9	0.39
12	0.30

Solution

1. Determine the first-order decay rate constant for 10°C.
   a. To find the rate, $\ln(C/C_0)$ is plotted as a function of time and a linear best fit is forced through zero as shown below:

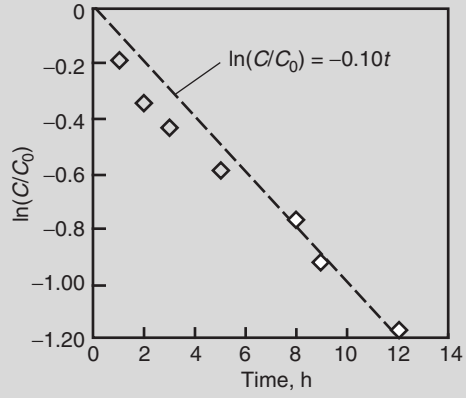

b. From the plot, k_d at 10°C is estimated to be approximately 0.10 h^{-1}.

c. Determine the value of k_d at 25°C. The value of k_d at 25°C can be computed using Eq. 5-85 (see Chap. 5):

$$\ln(k) = \ln(A) + \left(-\frac{E_a}{R}\right) \times \left(\frac{1}{T}\right)$$

The Arrhenius factor A needed for computing the k_d at 25°C is determined using the k_d value for 10°C:

$$\ln(A) = \ln(0.10) + \frac{62{,}000 \text{ J/mol}}{(8.314 \text{J/mol} \cdot \text{ K})(273 + 10) \text{ K}}$$

$$\ln(A) = 24.05$$

The k_d at 25°C is given below:

$$\ln(k_d) = 24.05 - \frac{62{,}000 \text{ J/mol}}{(8.314 \text{J/mol} \cdot \text{K})(273 + 25) \text{ K}} = -0.976$$

$$k_d = e^{-0.976} = 0.377$$

2. Determine the residual concentration of chlorine:

$$C_{t=12} = C_{t=0}\, e^{-0.377t} = C_{t=0}\, e^{(-0.377)(12)}$$

$$= (0.97)(0.0109) = 0.0106 \text{ mg/L}$$

Chemistry of Combined Chlorine

When ammonia is present in water, chlorine reacts to form species that combine chlorine and ammonia, known as chloramines. In general, chlorine reacts successively with ammonia to form the three chloramine species as more chlorine is added.

$$NH_3 + HOCl \rightarrow NH_2Cl + H_2O \quad \text{(monochloramine formation)} \quad (13\text{-}17)$$

$$NH_2Cl + HOCl \rightarrow NHCl_2 + H_2O \quad \text{(dichloramine formation)} \quad (13\text{-}18)$$

$$NHCl_2 + HOCl \rightarrow NCl_3 + H_2O \quad \text{(trichloramine formation)} \quad (13\text{-}19)$$

The sum of these three reaction products is called combined chlorine. The total chlorine residual is the sum of the combined residual and any free-chlorine residual. A summary of these definitions is provided below:

$$\text{Free chlorine} = HOCl + OCl^- \quad (13\text{-}20)$$

$$\text{Combined chlorine} = NH_2Cl + NHCl_2 + NCl_3 \quad (13\text{-}21)$$

$$\text{Total chlorine} = \text{free chlorine} + \text{combined chlorine} \quad (13\text{-}22)$$

All chlorine species are expressed as milligrams per liter as Cl_2 and the ammonia concentration is expressed as mg/L as nitrogen (i.e., mg/L NH_3 − N). When small amounts of chlorine are added to water, the reactions

are much like the simple model above. However, as the amount of chlorine added increases, the reactions become more complex. These reactions and their behavior are partially illustrated by the three zones on Fig. 13-11. At first, as depicted in zone A, the total chlorine residual increases by approximately the amount of chlorine added until the molar ratio of chlorine to ammonia approaches 1 (a weight ratio of 5.07 as Cl_2 to $NH_3 - N$), assuming no other species that consume chlorine are present.

Beyond a molar ratio of 1, the addition of more chlorine decreases, rather than increases, the total chlorine residual (zone B) because the chlorine is oxidizing some of the chloramine species. Eventually, essentially all of the chloramines species are oxidized. The point at which the

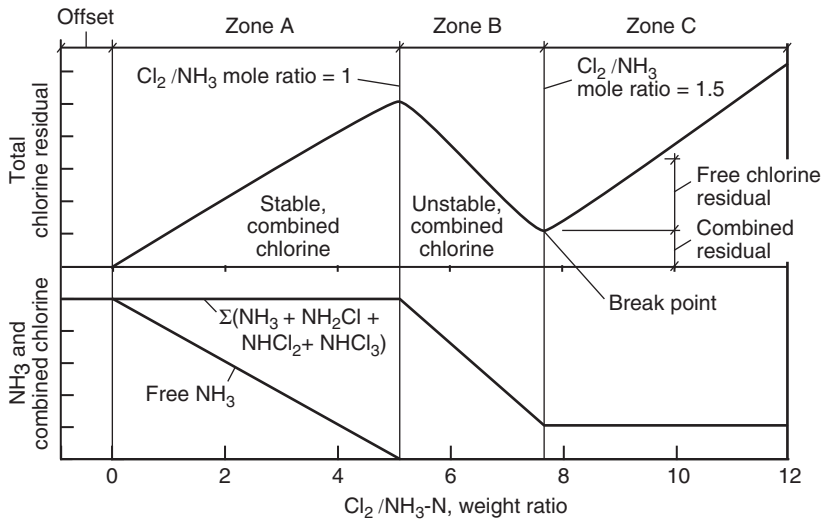

Parameter	Offset	Zone A	Zone B	Zone C
Time to metastable equilibrium	Fraction of a second	Seconds to a few minutes	10 to 60 min	10 to 60 min
Composition of metastable residual.	Reduction of readily oxidizable substances such as Fe(II), Mn(II), and H_2S.	Mostly monochloramine, some dichloramine and traces of trichloramine at neutral or acid pH or at high Cl_2 /NH_3 ratios.	A mixture of monochloramine and dichloramine, some free chlorine and traces of trichloramine at low pH.	Mostly free chlorine, trichloramine can be significant (aesthetically, but not as fraction of residual) at neutral pH, but especially in acid region.

Figure 13-11
Overview of chlorine break-point stoichiometry.

oxidation of chloramine species is complete is called the break point and is the beginning of zone C. The exact locations of maximum residual and breakpoint (minimum residual) are influenced by the presence of dissolved organic matter, organic nitrogen, and reduced substances [e.g., S^{2-}, Fe(II), Mn(II)]. The presence of any of these will shift all three zones to the right. The degree to which they shift the point of maximum residual depends on how easily they are oxidized. The shift in the breakpoint corresponds to their stoichiometric chlorine demand. After the breakpoint is reached, the free-chlorine residual increases in proportion to the amount of additional chlorine added. Prior to concerns about disinfection by-products, ''break-point'' chlorination was often used as a simple means of ammonia removal.

In zone A, monochloramine forms rapidly and with little interference. Nevertheless, the species present in zone A are influenced by pH. At low pH values, dichloramine can form via the following reactions:

$$NH_2Cl + H^+ \rightleftarrows NH_3Cl^+ \tag{13-23}$$

$$NH_3Cl^+ + NH_2Cl \rightleftarrows NHCl_2 + NH_4{}^+ \tag{13-24}$$

Monochloramine is the only chloramine present in zone A at pH 8, but significant amounts of dichloramine can be present at pH 6 (Palin, 1975). In zone B, which is richer in chlorine, some dichloramine will be present even at pH 8 (Palin, 1975). In zone B, hypochlorous acid can oxidize ammonia to nitrogen gas and nitrate ion, resulting in the complete loss of chlorine residual. Between these, the conversion to nitrogen gas is the dominant reaction commonly observed (Saunier and Selleck, 1979):

$$3HOCl + 2NH_3 \rightarrow N_2(g) + 3H_2O + 3HCl \quad \text{(ammonia to nitrogen gas)} \tag{13-25}$$

$$4HOCl + NH_3 \rightarrow H^+ + NO_3{}^- + H_2O + 4HCl \quad \text{(ammonia to nitrate ion)} \tag{13-26}$$

Although break-point chlorine can be described with equilibrium reactions, the behavior of the $Cl_2 - NH_3$ system is actually quite dynamic, and the break-point curve shown on Fig. 13-11 should be considered more of a metastable than an equilibrium state. As a result, laboratory studies to construct a breakpoint curve require precise timing to be reproducible, especially for Cl_2/NH_3 mole ratios above 1. Above this ratio the reaction proceeds rapidly until the metastable state is reached. Anywhere along the curve, the rate at which the reaction progresses is strongly influenced by the pH (Fig. 13-12), particularly in the vicinity of the break point itself. Near the break point, the reaction is at its maximum rate at a pH between 7 and 8. The rate decreases rapidly at pH values outside that range. Facilities engineered to accomplish ammonia removal via the break-point reaction should be designed to accommodate the time for this reaction. Even in the optimum range, the reaction time can be significant.

Example 13-6 Estimating break-point chlorine requirements

Ammonia is added to pure water in the laboratory to reach a concentration of 1 mg N/L. Estimate the chlorine dose needed to reach break point for the following conditions: (1) all the ammonia is converted to nitrogen gas and (2) all the ammonia is converted to nitrate ion. When using breakpoint chlorination to remove ammonia, which reaction requires less chlorine?

Solution

1. Determine the chlorine dose needed to convert ammonia to nitrogen gas. From Eq. 13-25, 3 mol of HOCl is needed for every 2 mol of NH_3:

$$\text{Weight ratio} = (1.5 \text{ mol/mol})\frac{71 \text{ g } Cl_2}{14 \text{ g N}} = 7.61 \text{ mg } Cl_2/\text{mg N}$$

$$\text{Required dose} = 7.61 \text{ mg } Cl_2/\text{mg N} \times 1 \text{ mg N/L} = 7.61 \text{ mg } Cl_2/\text{L}$$

2. Determine the chlorine dose to convert ammonia to nitrate. From Eq. 13-26, 4 moles of HOCl is needed for each mole of NH_3:

$$\text{Weight ratio} = (4 \text{ mol/mol})\frac{71 \text{ g } Cl_2}{14 \text{ g N}} = 20.2$$

$$\text{Required dose} = 20.2 \text{ mg } Cl_2/\text{mg N} \times 1 \text{ mg N/L} = 20.2 \text{ mg } Cl_2/\text{L}$$

3. The reaction to nitrogen gas uses less chlorine.

Forms of Chlorine (Liquid, Gas, Hypochlorite, etc.)

The forms of chlorine most often used in the treatment of drinking water are chlorine gas and sodium hypochlorite solution. Calcium hypochlorite powder is also used in some smaller systems. In the United States, chlorine gas can be purchased in 68-kg (150-lb) cylinders, in 908-kg (1-ton) cylinders (in Europe 1000-kg cylinders are used), by tank truck, or in railroad tank cars of between 14.5 and 49.9 metric tons in capacity (16 and 55 American tons). Generally the cost of chlorine is lower when it is shipped in larger volumes, the cost delivered in 1-ton cylinders being approximately half the cost delivered in 68-kg cylinders but nearly twice that when delivered by rail. As a result, some very large utilities purchase liquid chlorine by rail and repackage it for use at various sites.

Liquid Chlorine

The elements of a chlorination facility address each of the following:

1. Storage of liquid chlorine gas
2. Conduits for the transport of liquid chlorine
3. Evaporation of liquid chlorine

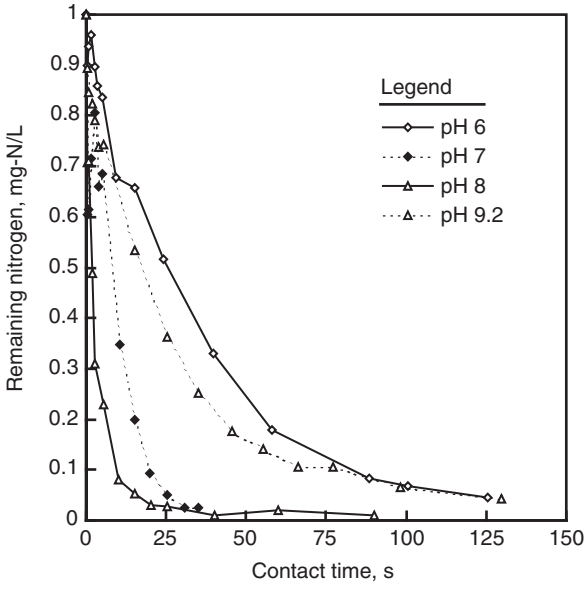

Figure 13-12
Effect of pH on break-point chlorination. (Data from Saunier and Selleck, 1979, Temp. 15 to 18.5°C, $[NH_3]_0 = 1$ mg/L, and $[Cl_2/NH_3]_0 \sim 10$.)

4. Conduits for the transport of chlorine gas under pressure
5. Regulation of the chlorine feed rate
6. Conduits for the transport of chlorine gas under vacuum
7. Chlorine-to-water mass transfer
8. Mixing of chlorine water with the process flow
9. The chlorine contact facility
10. Chlorine sampling and analysis
11. Chlorination control system

In small systems many of these elements are found in one device and other elements, such as the control system, are very rudimentary. In large chlorination systems, each of these elements can sometimes present a separate, specific design challenge. Each of these elements requires different materials and different design considerations apply to each.

DESIGN ISSUES WITH LIQUID CHLORINE

The details of the design of systems for handling the delivery, storage, and dosing of liquid chlorine are beyond the scope of this book. An overview of a variety of the more important issues is provided in Table 13-5. Chlorine is truly a hazardous material so it is important that care be taken in the design of these facilities. White's (1999) handbook is an excellent source for design details.

Table 13-5
Overview of key design issues for chlorination systems

Item	Description
Delivery	In cylinders 68 kg (150 lb) and 908 kg (1 ton); in tank trucks 13,600–18,200 kg (15–20 tons); and in rail cars 14,500–49,900 kg (16–55 tons).
Storage	In cylinders; in tank trucks; in rail cars or in custom tanks.
Conduits for liquid chlorine	Schedule 80 stainless steel (SS), schedule 80 carbon steel, or cast iron (DO NOT USE PVC). Should be seamlessly welded. Use cast-iron valves. Use pipe sizes recommended by White (1999) to avoid "flashing."
Evaporation of liquid	Can use vapor pressure of container to feed up to 19 kg/d (40 lb/d) with 68-kg cylinder and up to 150 kg/d (330 lb/d) with 908-kg cylinders. Multiple cylinders are often used with automatic switchover. At feed rates above 680 kg/d (1.5 tons/d) a separate evaporator is recommended to convert liquid chlorine to chlorine gas.
Conduits for chlorine gas under pressure	Use schedule 80 SS, schedule 80 carbon steel-or cast iron (DO NOT USE PVC). Should be seamlessly welded. Use cast-iron valves.
Regulation of chlorine gas feed rate	Accomplished by the chlorinator. Most chlorinators include four principal elements: (a) a pressure-reducing valve, (b) a rotometer, (c) a control valve, and (d) a vacuum regulator.
Conduits for transport of chlorine gas under vacuum	Often constructed of schedule 80 PVC or reinforced fiberglass pipe. Piping should be carefully sized to maintain pressure drop below 50–60 mm Hg (see White, 1999).
Chlorine-to-water mass transfer	Chlorine is highly soluble and reacts vigorously with water to form hypochlorous and hydrochloric acids. Chlorine-to-water mass transfer is normally accomplished via chlorine injector, a venturi-type device. The maximum solution strength downstream of the injector is approximately 3.5 g/L. The injector is also used to create the vacuum in the system.
Blending of chlorine water into process flow	Under normal conditions, blending must be accomplished before the chlorine residual monitoring point. With normal turbulent flow in a conduit, this requires travel down the conduit an axial distance of 40–200 times the hydraulic radius. Blending can be expedited with devices normally used for rapid mixing or via flow structures that dissipate energy (e.g., a hydraulic jump or a fall over a sharp-crested weir). When ammonia is present, it is important that chlorine be rapidly blended with the bulk flow. If not, both chlorine and ammonia are lost in localized breakpoint reactions and disinfection is compromised. In this case rapid mixing is required.
Chlorine contact facility	Historically, the contact time in existing facilities (e.g., sedimentation basins, clearwells) has been used. Modern treatment plants use specially designed chlorine contact tanks. The most efficient designs, from the standpoint of dispersion, are long, straight pipelines and carefully designed, serpentine contact chambers. Most contact chambers are of concrete.
Chlorine sampling and analysis	Reliable equipment for the sampling and analysis of free and total chlorine has been available for some time. Several devices are available on the market.
Chlorination control system	Historically control systems were manual, feed-forward, feedback, and compound loop in design. Today control systems and methods of sampling and analysis have improved so complex control is possible.

Control of Gas Chlorination

Four methods have traditionally been used for controlling the feed rate of chlorine gas when it is used for residual control in drinking water systems. Each is displayed on Fig. 13-13: (1) manual control, (2) feed-forward control, (3) residual feedback control, and (4) compound loop control. Through the middle of the twentieth century, manual control was the most common. Significant operator attention was required to ensure that a suitable residual was reliably provided, especially when the flow rate through the plant was adjusted. By the mid-1950s flow measurement and chlorine metering techniques improved until feed-forward control systems began to appear. This important advance allowed automatic adjustment for flow but still required the operator to adjust for any changes in the water quality (chlorine demand) or any drifts in monitoring and feed rates.

By the mid-1960s direct residual control began to appear. In principle, the feedback method of control is more robust than feed-forward control, but residual measurement did not approach suitable levels of reliability and precision for two more decades. As a result, compound loop control evolved as a compromise. With this method, changes in flow could be

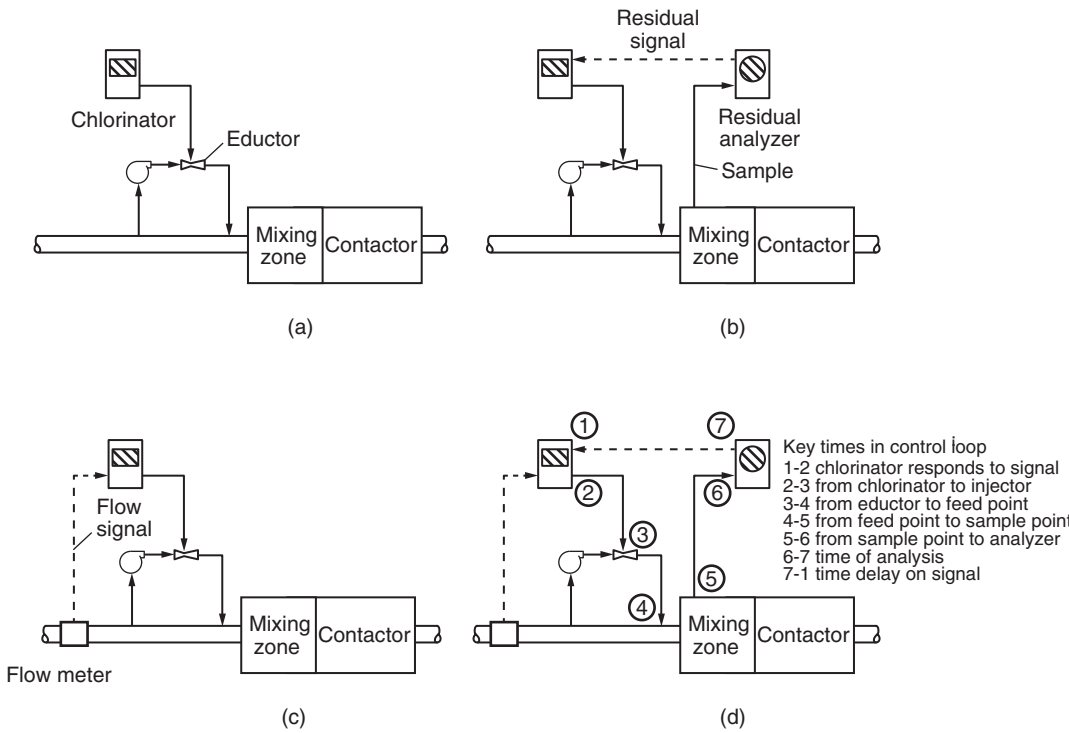

Figure 13-13
Control of chlorine gas feed rate: (a) manual control, (b) feedback or residual control, (c) feed forward control, and (d) compound loop control.

accommodated via the flow signal and an additional control increment could be added via residual control for minor water quality changes. Properly maintained, compound loop control was the first system to provide reliable, continuous residual control.

During the last decade of the twentieth century, computerized supervisory control systems had evolved to the point where these same inputs (flow and residual) could be combined with other measurements to provide improved reliability. None of these control systems, however, is an adequate substitute for vigilant attention from the operator.

Residual control system

The sequence of events in the residual control system must be carefully designed and controlled. All the elements shown and labeled in the diagram as ''compound loop control'' on Fig. 13-13 must be considered in designing the system and envisioning its method of control. The time between the instant when a change in chloride feed rate is made and when the change in residual is detected by the control system has a significant effect on the effectiveness of the control system. The instructions of the supervisory control and data acquisition (SCADA) system must be designed with a full understanding of the effect of timing delays in each element of the system.

The time required for the chlorinator to completely respond to an instruction from the SCADA system is normally not too significant. The time required for the change in feed rate established by the chlorinator to be recognized at the eductor must be considered. This time to change feed rates is normally not too long either, but it can be too long when the chlorinator is located a long way from the injector and when the chlorine feed rate is very low. White (1999) suggests that this time be estimated by assuming that the change in pressure will travel in a wave about three times as fast as the gas flow in the line.

Next, the time for the water in the chlorine water line to travel from the eductor to the application point must be considered. This time is a function of the distance between the eductor and the application point and the flow rate (velocity) in the chlorine water line. Again, designs with long distances between the eductor and the application point can cause trouble for control. Ideally the chlorine is stored near the application point so that both the time in the vacuum line and the time in the chlorine line are minimized. When nearby storage is not possible, it is usually best to lengthen the vacuum line, not the chlorine water line, as a signal ordinarily travels much faster down a vacuum line.

Sampling point

Another important constraint is the time between the chlorine application point and sampling point. There is an inherent design conflict in the distance between these locations. Putting these points too close together

can result in poor blending before the treated water reaches the sampling point. When this happens, the control system constantly ''searches'' for control but can never quite find it. Putting them too far apart can result in too much delay between when a change in dose is made and when it is detected by the control system. To avoid control problems, the residual for sample control must be taken after mixing is satisfactory. Depending on the method of chlorine introduction and the criteria used for mixing, the distance downstream to accomplish satisfactory blending is between 40 and 200 times the hydraulic radius of the water conduit. Problems associated with this distance are aggravated in larger applications because of the larger conduit diameters that are used.

The time required for the sample to travel from the sample point to the analyzer is also important. Sample travel time can be a significant complication if the analyzer is located in some central location far from the sampling site. The time for the analyzer to assay the sample (normally between 15 and 20 s) can also be important in some applications. In designing such a control system, it is important to analyze all these times and the sequence in which they operate at both high- and low-flow conditions, both early and late in the life of the design, to ensure that problems do not occur after the installation is complete.

Example 13-7 Establishing time between chlorine application and residual control sampling

Consider two treatment plants A and B. In plant A the filtered water line is 305 mm (12 in.) in diameter. In plant B, the filtered water line is 3050 mm (120 in.) in diameter. Both pipelines are designed for a velocity of 1.5 m/s (5 ft/s). Assume that both have equivalent mixing at the point of chlorine injection and that the flow in both pipelines will be suitably blended for sampling at a point 50 pipe diameters downstream (100 hydraulic radii).

Estimate how far down the pipeline the sample point must be and how long it will take for the water to travel from the point of chlorine injection to the sampling point in each case.

Solution

1. Estimate the travel time from application point to sampling point (4 to 5 on Fig 13-13d):
   a. For plant A, pipe diameter is 305 mm, 50 pipe diameters equal 15 m, and at a velocity of 1.5 m/s the travel time is ~10 s.
   b. For plant B, pipe diameter is 3050 mm, 50 pipe diameters equal 150 m, and at a velocity of 1.5 m/s the travel time is ~100 s.

Sodium Hypochlorite

When chlorine was first used for disinfection, it was often applied in the form of hypochlorite. Sodium hypochlorite (NaOCl), or liquid bleach, came into use near the beginning of the Great Depression in the late 1920s. Later, chlorination using liquid chlorine became predominant because of its lower cost, but now hypochlorite is again becoming more common because of the hazardousness of liquid chlorine.

Sodium hypochlorite is the most widely used form of hypochlorite today. It is widely used not only in disinfection of water but also for a myriad of other household and industrial uses. Calcium hypochlorite [$Ca(OCl)_2$] is used by some small utilities.

Whereas chlorine gas is prepared by an electrolytic process that breaks sodium chloride solution into chlorine gas and sodium hydroxide, ironically, sodium hypochlorite is generally prepared by mixing sodium hydroxide and chlorine gas together:

$$2NaOH + Cl_2 \rightarrow NaOCl + NaCl + H_2O \qquad (13\text{-}27)$$

On a weight basis, 1.128 kg of NaOH reacts with 1 kg of chlorine to produce 1.05 kg of NaOCl and 0.83 kg of NaCl. The process is complicated by the fact that the reaction generates a significant amount of heat. It is common practice to add an excess of NaOH because, as will be shown, hypochlorite is more stable at higher pH values. As a result, the density of one hypochlorite solution is not necessarily the same as another, even if both have the same strength (percent Cl_2). This density difference occurs because the final density depends on the amount of excess NaOH added during manufacture. Liquid bleach usually has a pH between 11 and 13. Hypochlorite can also be manufactured via onsite generation; this process is becoming more common.

STABILITY OF HYPOCHLORITE

Under some conditions, the strength of hypochlorite can decline significantly in just a few days. In fact, stability is one of the major issues that must be addressed in both designing and operating a hypochlorite facility. A utility should not consider using hypochlorite unless it is prepared to dedicate time and energy to a regular program of monitoring and controlling its decay. Of considerable significance is the fact that, when hypochlorite does decay, chlorate ion is one of the principal by-products of the reaction. The stability of hypochlorite is affected by the strength of the solution, the storage temperature, the pH, and the contamination of heavy metals, which can catalyze its decay. Light is also a problem. As a general rule, the rate of decay is accelerated by (1) higher concentration, (2) higher temperature, (3) lower pH, (4) exposure to sunlight, and (5) the presence of certain heavy metals, notably copper and nickel.

Under basic conditions, the decomposition of hypochlorite ion to chlorate ion follows a disproportionation reaction, which exhibits second-order

reaction kinetics and the following overall stoichiometry (Gordon et al., 1995a,b):

$$OCl^- + OCl^- \rightarrow ClO_2^- + Cl^- \quad (13\text{-}28)$$

$$OCl^- + ClO_2^- \rightarrow ClO_3^- + Cl^- \quad (13\text{-}29)$$

$$3OCl^- \rightarrow ClO_3^- + 2Cl^- \quad (13\text{-}30)$$

The second reaction, as given by Eq. 13-29, is the faster of the two. As a result, the first reaction is the rate-limiting step in the consumption of hypochlorite ion. Bleach also decays via a slow reaction that forms oxygen and an acid-forming reaction that also forms chlorate ion, as shown in the following reactions:

$$OCl^- + OCl^- \rightarrow O_2 + 2Cl^- \quad (13\text{-}31)$$

$$2HOCl + OCl^- \rightarrow ClO_3^- + 2H^+ + 2Cl^- \quad (13\text{-}32)$$

Gordon and colleagues (1995a,b) have shown that copper and nickel catalyze oxygen formation (see Eq. 13-31) and research at the Swiss Federal Institute for Environmental Science and Technology (EAWAG) has shown that a similar reaction occurs via proteolysis (Nowell and Hoigné, 1992a,b). The relationships between the three principal reactions that result in hypochlorite decay are displayed on Fig. 13-14.

The pH at which a sodium hypochlorite solution is stored has important impacts on its rate of decay, as shown on Fig. 13-15a (Gordon et al. 1995a,b). The rate of decay is low at pH 11 and above but increases rapidly below pH 10. Some evidence suggests that a decay minimum occurs between pH 12 and 13. As liquid bleach is normally delivered at pH 12 or above, low-pH decay is normally not a problem with the undiluted product. Often

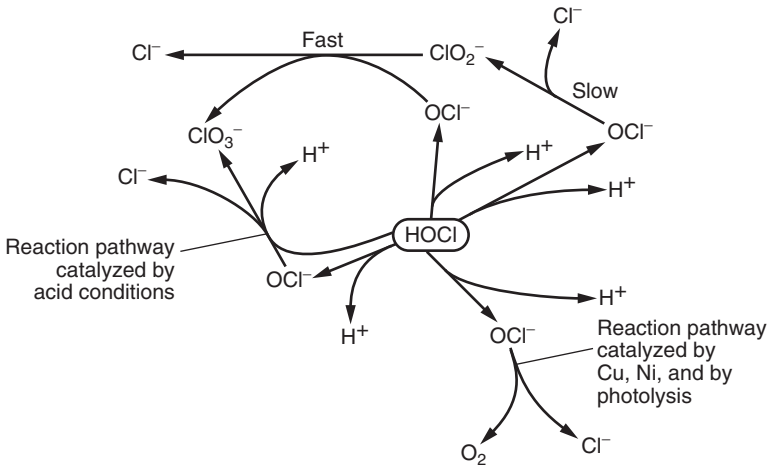

Figure 13-14
Decay reactions of hypochlorite.

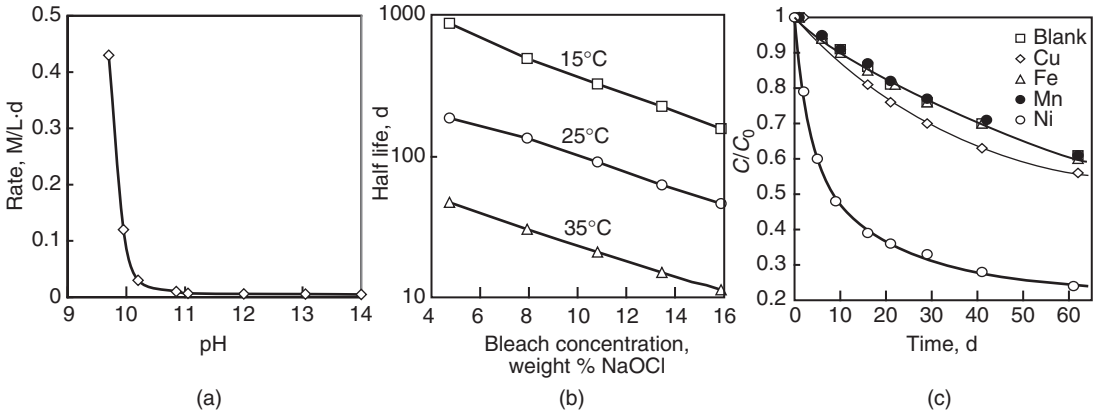

Figure 13-15
Factors that influence decay of sodium hypochlorite: (a) effect of pH on rate of decay of hypochlorite; (b) effect of temperature and concentration on decay of hypochlorite; and (c) effect of trace metals on rate of decay of hypochlorite. (Data from Gordon et al., 1993, 1995a,b.)

it is delivered with enough excess hydroxide to allow a 50 percent dilution without increasing the rate of decay. Nevertheless, pH monitoring and control are important in a hypochlorite management program.

As mentioned earlier, the rate of the dominant decay reaction in liquid bleach (Eq. 13-30) is a second-order reaction (Gordon et al., 1995a,b). As a result, a stronger bleach solution will decay faster. This effect can be illustrated by the solution of the second-order rate equation for a completely mixed batch reactor:

$$\frac{C}{C_0} = \frac{1}{1 - k_d C_0 t} \tag{13-33}$$

where C = bleach concentration after time t, mol/L
C_0 = bleach concentration at time 0, mol/L
k_d = second-order decay coefficient, L/mol · s
t = time, s

The effects of bleach strength and temperature are illustrated on Fig. 13-15b. Based on the data in this figure, diluting bleach delivered at a concentration of 15 percent to a concentration of 7.5 percent will increase its half-life from about 50 to about 140 days (at 25°C). If the 7.5 percent bleach is also stored at 15°C instead of 25°C, the combined effect of dilution and temperature control will increase its half-life to more than 500 days.

Finally, since the work of Lister (1952, 1956), bleach technologists have understood that certain metals can catalyze the decomposition of bleach. In the mid-1950s rhodium, iridium, cobalt, copper, manganese, iron, and nickel were issues. Today the principal concerns are copper and nickel, and manganese has also been shown to exacerbate the destructive effect of nickel. Gordon et al. (1995a,b) conducted tests to examine the effect

of a concentration of 1 mg/L of copper, iron, manganese, and nickel, individually, on the decay of a 13.5 percent bleach. These are illustrated on Fig. 13-15c. The authors recommended that copper and nickel be kept below 0.1 mg/L. Bleaches are also filtered in an attempt to reduce metals contamination, but, with one exception, additional filtering of modern commercial bleaches showed only small improvements (Gordon et al., 1995a,b). It appears that many modern bleaches are produced in such a condition that additional filtering is of little benefit.

FORMATION OF CHLORITE AND CHLORATE ION

In 1992, the U.S. EPA discovered that hypochlorite solutions containing significant concentrations of chlorate ion were responsible for introducing chlorate ions into drinking water (Bolyard et al., 1992). Of special significance in this regard is the fact that the principal bleach decay reaction results in the production of chlorite (ClO_2^-) and chlorate (ClO_3^-) ions (see Eqs. 13-28 and 13-29). Chlorite is regulated by the U.S. EPA. Chlorate is regulated in some jurisdictions; for example, the State of California has set an action limit of 0.8 mg/L (Cal DHS, 2002). As a result, it seems prudent to limit the production of chlorate as well.

As noted earlier, the disassociation of chlorite to chlorate and chloride (Eq. 13-29) is much faster than the disproportionation of hypochlorite ion to chlorite and chloride (Eq. 13-28), and this minimizes the formation of chlorite ion. As a result, it is estimated that chlorite normally stays below 0.5 percent of the hypochlorite concentration (Gordon et al., 1997). Thus, a chlorine dose of 1 mg/L delivers less than 0.005 mg/L of chlorite ion into solution (Gordon et al., 1997), considerably less than the MCL of 0.8 mg/L. Thus, even though chlorite generally does not pose a problem in hypochlorite solutions; the same is not true for chlorate.

If hypochlorite decomposition were only the result of Eq. 13-30, the chlorate generated would be about 33 percent of the hypochlorite decomposed (molar basis). But other pathways for hypochlorite decay (decomposition catalyzed by light and metals) normally produces oxygen and not chlorate (Eq. 13-31). Gordon et al. (1995b) examined chlorate production in 12 tests with commercial bleaches and found that the actual production of chlorate was slightly less, about 31 percent (Fig. 13-16a). As a rule of thumb, it is conservative to assume that one-third of the bleach lost to decomposition ends up as chlorate ion.

Two surveys were also conducted to evaluate the contribution of chlorate ion to water systems using sodium hypochlorite for disinfection (Bolyard et al., 1993; Gordon et al., 1993). Both authors looked at the ratio of chlorate ion and hypochlorite ion in the bleaches being used as well as the concentration of chlorate ion in the drinking water system itself. A probability plot of the chlorate/hypochlorite ratio in the bleaches from both surveys is presented on Fig. 13-16b. In both cases, the median was slightly less than 0.1 mol[ClO_3^-]/mol[OCl^-]. On the other hand, levels greater than

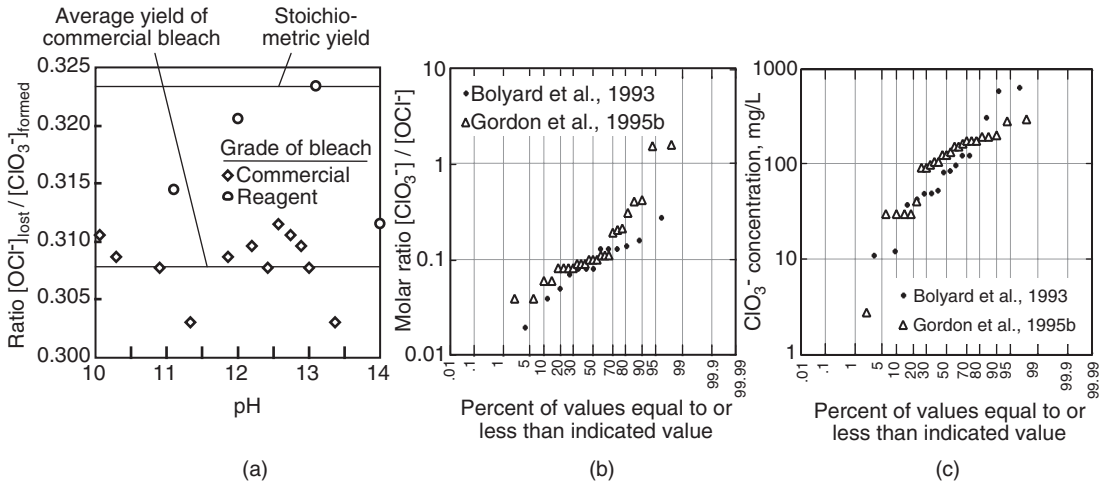

Figure 13-16
Formation of and impacts of chlorate in hypochlorite feedstock: (a) chlorate formation during decomposition of reagent and commercial hypochlorite; (b) surveys of chlorate content in bleach; and (c) surveys of chlorate content in systems using bleach. (Data from Bolyard et al., 1993; Gordon et al., 1993, 1995a,b, 1997.)

1 mol $[ClO_3^-]$/mol$[OCl^-]$ and as low as 0.02 mol $[ClO_3^-]$/mol$[OCl^-]$ were observed, indicating that bleach manufacturing and storages practice can result in substantial differences. At a ratio of 0.1, a chlorine dose of 3 mg/L would cause chlorate concentrations of approximately 0.1 mg/L. Thus the chlorate that is found in bleach under typical conditions of use should not be a significant issue. Many of the considerations that affect the stability of bleach are also important in limiting its chlorate content. Nevertheless, surveys of chlorate in systems using hypochlorite did sometimes show the presence of significant chlorate (Fig. 13-16c), suggesting that utilities using hypochlorite should occasionally monitor for chlorate and consider modifying their practice if significant amounts are observed.

STORAGE AND FEEDING OF SODIUM HYPOCHLORITE

Experience with materials for the construction of large hypochlorite tanks has not been uniformly good. Early projects in Chicago had unsatisfactory experience with filament-wound fiberglass tanks and with underground concrete tanks with fiberglass lining. These tanks were replaced with hand lay-up fabricated fiberglass tanks using a vinyl resin binder and with plastic, continuous-weld, full-weight carbon steel tanks lined with a fiberglass-reinforced polyester material at a thickness of 0.9 mm (35 mil). The latter gave acceptable performance (White, 1999). Properly fabricated fiberglass tanks or steel tanks with a rubber or polyvinyl chloride (PVC) lining give satisfactory service as well.

Hypochlorite is an extremely aggressive chemical, and no equipment used to store or feed it can be expected to last indefinitely. Some particularly robust diaphragm and solenoid metering pumps have been successfully used, and this is the approach found in most plants (White, 1999). In very large plants (>380 ML/d or 100 mgd), White recommends metering the chemical by gravity from the storage tank through a Teflon-lined magnetic flowmeter and rate-modulating valve to the point of application.

Hypochlorite can be transported in schedule 80 PVC piping; except where exposed to sunlight, chlorinated polyvinyl chloride (CPVC) should be used. Ball valves and plug valves made of steel lined with PVC or propylene should be avoided. In general, precautions should also be taken for the potential for precipitation of calcium carbonate whenever the hypochlorite is mixed with carrying water or at the application point with the water being treated.

The high specific gravity of hypochlorite solution must be overcome to accomplish effective mixing at the point of application. This can be accomplished by using a diffuser and carrying water (be cautious about the potential formation of $CaCO_3$) or by the use of a pumped jet mixer like that often used for coagulants. Mixing can also be accomplished by introducing the hypochlorite at a point of significant turbulence.

Ammonia

Ammonia can be supplied for water treatment applications in three forms: as a pure liquid (anhydrous ammonia), dissolved in water (aqueous ammonia), or as a dry ammonium salt, usually ammonium sulfate. Ammonia is not expensive, but the relative cost of these alternative forms of ammonia varies from one location and one application to another. For reasons of convenience, aqua ammonia is the form most commonly used. Exposure to high concentrations of ammonia vapor can be fatal. At concentrations of several hundred parts per million by volume (ppm_v), it causes throat and eye irritation, and at higher concentrations it can cause convulsions or even rapid asphyxia. While not addressed in this discussion, appropriate precautions should be taken both in design and operation of ammonia facilities.

STORAGE AND FEEDING OF ANHYDROUS AMMONIA

At normal temperatures and pressures, anhydrous ammonia (>99 percent NH_3) is a gas. However, it can be easily liquefied and is commonly stored and transported in liquid form in pressurized containers of the same size and same design as those used for chlorine (they are usually a different color). At atmospheric pressure, liquid anhydrous ammonia has a density of 680 kg/m^3 (42.6 lb/ft^3 or 5.7 lb/gal), approximately two-thirds that of water. Anhydrous ammonia containers comply with International Code Council (ICC) regulations, which require a minimum working pressure of 1760 kPa (256 psig) with safety valves set to release at that pressure. Valves and fittings used for anhydrous ammonia are normally rated at 2070 kPa

(300 psig). In the United States, bulk shipments of anhydrous ammonia are normally made in 23- and 73-metric-ton (25- and 80-U.S.-ton) rail tank cars, in 18-tonne (20-U.S.-ton) tank trailers, and cylinders the same size and design as those used to deliver 908 and 68 kg of liquid chlorine. It is common for vendors to provide storage tanks. Permanent (stationary) storage tanks for anhydrous ammonia can also be custom fabricated to any desired size. Such tanks must meet the same pressure restrictions as the shipping containers and are usually made of carbon steel. No copper, bronze, or brass fittings should be used because ammonia attacks copper-based alloys. Storage tanks should be sheltered from the sun to prevent excessive pressure buildup. The vapor pressure of anhydrous ammonia at 10°C is slightly more than 611 kPa (89 psig). At 30°C it nearly doubles to 1183 kPa (172 psig). The formula below may be used to estimate the vapor pressure at temperatures between 0 and 40°C:

$$P_{v,\mathrm{NH_3}} = 434.9 + 13.96T + 0.3645T^2 \qquad (13\text{-}34)$$

where $P_{v,\mathrm{NH_3}}$ = vapor pressure of anhydrous ammonia, kPa
T = temperature, °C

Anhydrous ammonia can be fed by two methods: direct feed and solution feed. In direct gas feed, the ammonia gas is directly introduced into the water to be treated. Unless the plant is very small, this method often suffers from poor distribution at the application point because of the low flow rate of ammonia gas. The solution feed method is analogous to the technology used to feed chlorine, except the vapor pressure of ammonia is higher. Precipitation of $CaCO_3$ is often a problem in the vicinity of the application point.

Direct gas feed

Direct gas ammonia feeders are commercially available and differ only with respect to minor material changes from chlorinators in that they include an ammonia pressure-regulating valve, pressure gauges, a pressure relief valve, rotameters, and a control valve with back-pressure regulator, all in a modular cabinet. The ammoniator meters gaseous ammonia into the process stream under positive pressure. The high pressure in the storage tank is normally reduced to approximately 276 kPa (40 psi) using the pressure regulator. At this reduced pressure the ammonia flows through the rotameter where the gas flow can be read directly in mass/time units (In the United States the units are usually pounds per hour or pounds per day). Finally, the gas flows through the back-pressure valve, which maintains a constant back pressure on the system. This pressure is limited to a range of 101 to 122 kPa (15 to 18 psig). The back-pressue valve is used to keep the feed rate constant with changes in the pressure at the application site. Ammoniators should be housed separately from chlorination equipment. A direct-feed ammonia application is illustrated on Fig. 13-17a. For completeness, an evaporator is

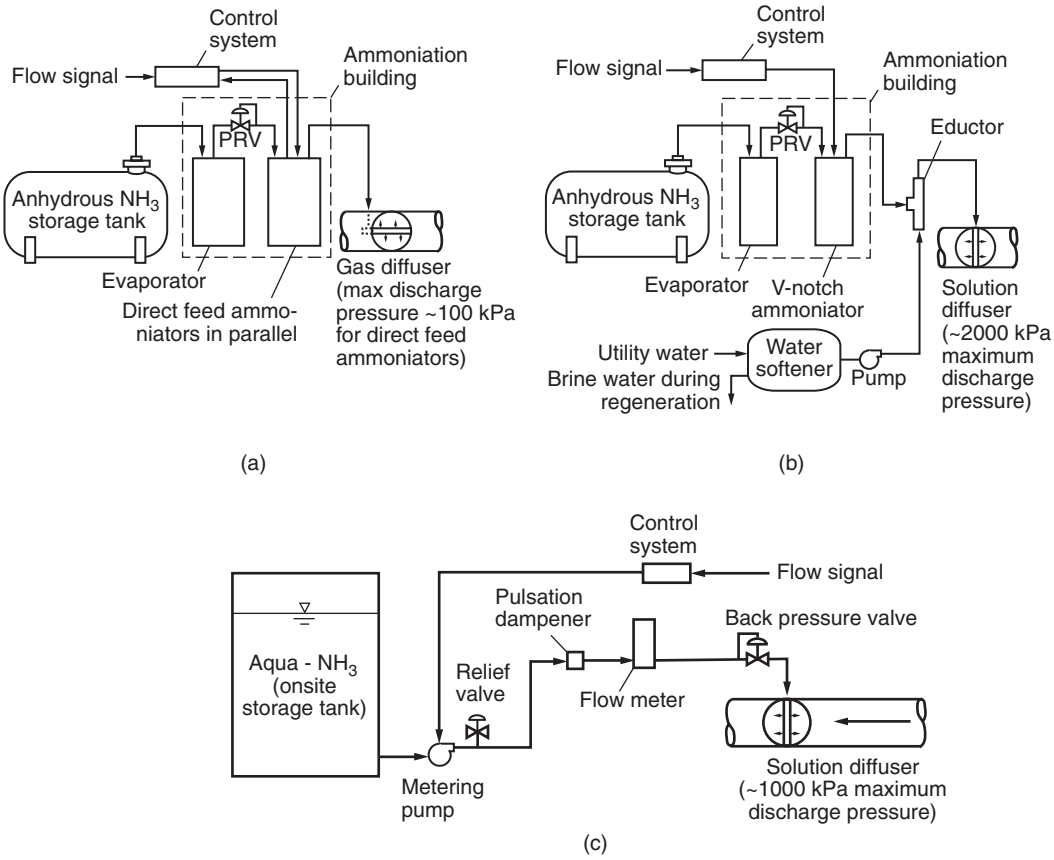

Figure 13-17
Schematics of alternate ammonia feed systems: (a) direct feed of anhydrous ammonia; (b) solution feed of anhydrous ammonia; and (c) aqua ammonia feed system.

shown, although these are not always required. If ammonia feed rates are high enough, the anhydrous liquid would be withdrawn from the bottom of the storage tank and converted to gas in the evaporator prior to entering the ammoniator. The largest direct-feed ammoniators have a maximum feed capacity (determined by the rotameter rating) of 455 kg/d (1000 lb/d).

Solution feed of anhydrous ammonia

The design of these systems closely parallels the design of modern gas chlorination systems. An ammoniator and a gas diffuser are often used to feed the anhydrous ammonia solution (see Fig. 13-17a). A solution-feed ammoniator (see Fig. 13-17b) is typically recommended when higher feed rates or greater discharge pressures prohibit the use of direct-feed ammoniators. (It is important to remember that direct-feed ammoniators

are limited by their back-pressure valve to a pressure of approximately 100 kPa.) An important difference between ammoniation and chlorination systems is that the utility water for a solution ammoniation system must be softened to prevent the deposition of $CaCO_3$ in the system.

STORAGE AND FEEDING OF AQUA AMMONIA

Ammonia is very soluble in water. As an example, 1 volume of water will dissolve 1150 volumes of anhydrous ammonia at a temperature of 0°C and atmospheric pressure. As a consequence, ammonia is commercially available as an aqueous solution of between 20 and 30 percent strength ''aqua ammonia.'' It is usually dissolved in deionized or softened water and stored in low-pressure tanks. The vapor pressure of 30 percent aqua ammonia at 37.8°C (100°F), a temperature common in many parts of the world, is greater than 1 atm. To prevent off-gassing of ammonia in these locations, a slightly pressurized tank should be used. In contrast, the vapor pressure of 20 percent aqua ammonia is less than 1 atm, permitting storage in a nonpressure tank with a minimum of off-gassing. Aqua ammonia is not commonly shipped long distances; hence the largest transport vessel in the United States is a 28,300-L (7500-gal) tank trailer. There seems to be less standardization for onsite aqua ammonia storage tanks, probably because low-pressure tanks are acceptable. Steel and fiberglass tanks are both used in water treatment applications.

Depending on the concentration of aqua ammonia, excessive temperatures can cause ammonia gas to come out of solution. Off-gassing should be considered in design, and a slightly pressurized storage tank with a relief valve vented to a water trap or ammonia scrubber may be necessary to keep vapors from escaping to the atmosphere.

Aqua ammonia can sometimes be fed directly to the process stream using a metering pump. Suitable metering pumps are commercially available. Progressive cavity pumps have also been successfully used. The storage tank is a permanent onsite facility and should have enough storage for at least 10 days of maximum usage. The tank should have a liquid-level monitor to allow monitoring of the inventory in the tank. The flow metering pump should be located in the proximity of the tank and below its hydraulic grade to minimize chances of ammonia vaporization in the piping. If necessary, the metering pumps can be sheltered in a building; however, the pumps themselves do not necessarily require shelter as do the anhydrous ammonia feed equipment mentioned earlier. An aqua ammonia feed system is illustrated on Fig. 13-17c.

STORAGE AND FEEDING OF AMMONIUM SULFATE

The most common salt of ammonia used in water treatment is ammonium sulfate, $(NH_4)_2SO_4$. This form of ammonia has the advantage that it does not raise the pH as much as the others do. As a result, it is easier to combine it with dilution water to obtain proper mixing. Mixing can be an important

consideration when adding ammonia to water containing free chlorine to arrest the formation of DBPs.

MIXING

Adding chlorine to water that already has ammonia in it can result in undesirable reactions while mixing takes place. To prevent free ammonia and thus minimize nitrification, it is common for water systems today to add ammonia at a total dose that is at the peak of the breakpoint curve (a 1:1 molar ratio). By definition, the ratio of chlorine to ammonia in the entire mixing zone is on the left side of the breakpoint curve. This condition necessitates that the mixing be rapid relative to the time for the irreversible oxidation of ammonia. That is,

$$t_{mix} \ll t_{rx} \tag{13-35}$$

where t_{mix} = time required to obtain mixing to microscale, s
t_{rx} = half-life of breakpoint reaction, s

Although this circumstance is easily described in a qualitative way, it is quite difficult to characterize quantitatively because t_{rx} is a function of not only the pH but also the local Cl_2/NH_3 ratio (affected by the degree of mixing). When ammonia is added to a chlorinated water to arrest the formation of disinfection by-products, very good mixing is required to ensure that chemicals are efficiently used (see Chap. 6).

MANAGING COMBINED CHLORINE (CHLORAMINE) RESIDUALS

Maintaining a combined chlorine residual involves some considerations that are not important when a free-chlorine residual is used. Chloramines have the advantage that their odor threshold is lower (Krasner and Barrett, 1984), that they are more effective in controlling microbial growth on pipe surfaces (Le Chevallier et al., 1988), and that they are generally much more stable (Trussell and Kreft, 1984). It should be noted that combined chlorine residuals are subject to destruction by biological nitrification, especially if temperatures are warm and if ammonia is used in excess. Also there is recent evidence that the use of combined chlorine can result in the formation of low levels of NDMA, a suspected human carcinogen (Najm and Trussell, 2000, 2001). Some of the conditions that aggravate NDMA formation, namely a high chlorine-to-ammonia ratio, are the same things that discourage nitrification.

13-6 Disinfection with Chlorine Dioxide

When the regulation of the chlorination by-products began, chlorine dioxide (along with ozone) was a fairly high-profile disinfection alternative (U.S. EPA, 1979). Chlorine dioxide is widely used in continental Europe,

particularly Germany, Switzerland, and France, and produces almost no identifiable organic by-products, except low levels of a few aldehydes and ketones (Bull et al., 1990). Chlorine dioxide was known to produce two inorganic by-products, chlorite and chlorate ion. As a result, most applications of chlorine dioxide were on low-TOC waters that did not require a high dose to overcome oxidant demand. Late in the 1980s, concern about the toxicity of chlorite ion and chlorine dioxide itself reached a peak. Also, based on field experience, it was found that the use of chlorine dioxide was sometimes responsible for a very undesirable ''cat urine'' odor (Hoehn et al., 1990). As a precautionary measure, the State of California banned the use of chlorine dioxide for the disinfection of drinking water and several other states followed.

Eventually, when the disinfectant by-product rule was promulgated (U.S. EPA, 1998), an MCL of 0.8 mg/L was set for chlorite ion and a maximum disinfectant residual limit (MDRL) of 1 mg/L was set for chlorine dioxide. No MCL was placed on chlorate ion, but utilities were encouraged to be cautious about the production of chlorate and, again as a precautionary measure, the State of California has set an action level of 0.8 mg/L. Methods for reducing the concentration of chlorite ion downstream of the use of chlorine dioxide have been demonstrated (Griese et al., 1991; Iatrou and Knocke, 1992), and it has been established that the cat urine odor only occurs when chlorite ion is exposed to a free chlorine residual. As a result, it appears that chlorine dioxide may indeed play an important role in DBP control, particularly in systems using combined chlorine for residual maintenance and looking for a small boost in primary disinfection.

Generation of Chlorine Dioxide

The principal reactions that occur in most chlorine dioxide generators have been known for a long time. In industry, large-scale chlorine dioxide generators use chlorate as a feedstock, but for potable water applications chlorine dioxide is usually generated onsite using a 25 percent sodium chlorite solution. Although a sodium chlorite feedstock is a common starting point, a number of different approaches are used to convert the chlorite to chlorine dioxide. These include reactions with gaseous chlorine (Cl_2), aqueous chlorine (HOCl), or acid (usually hydrochloric acid, HCl). The reactions are

$$2NaClO_2 + Cl_{2(g)} \rightarrow 2ClO_{2(g)} + 2Na^+ + 2Cl^- \quad (13\text{-}36)$$

$$2NaClO_2 + HOCl \rightarrow 2ClO_{2(g)} + 2Na^+ + Cl^- + OH^- \quad (13\text{-}37)$$

$$5NaClO_2 + 4HCl \rightarrow 4ClO_{2(g)} + 5Na^+ + 5Cl^- + 2H_2O \quad (13\text{-}38)$$

The stoichiometry of Eq. 13-36 requires 0.5 kg of chlorine and 1.34 kg of sodium chlorite to produce 1 kg of chlorine dioxide. Several of the alternative approaches used for the generation of chlorine dioxide are summarized in Table 13-6.

Table 13-6
Chlorine dioxide generation alternatives

Generator Type	Main Reactions, Reactants, By-products, Key Reactions, and Chemistry Notes	Special Attributes
Acid–chlorite: (direct acid system)	$5NaClO_2 + 4HCl \rightarrow 4ClO_2(g) + 5NaCl + 2H_2O$ ❑ Low pH ❑ ClO_3^- also possible ❑ Slow reaction rates	Chemical feed pump interlocks required; production limit ~10–15 kg/d (25–30 lb/d); maximum yield is ~80% of stoichiometric yield.
Aqueous chlorine–chlorite: (Cl_2 gas ejectors with chemical pumps for liquids or booster pump for ejector water)	$Cl_2 + H_2O \rightarrow HOCl + HCl$ $HOCl + 2NaClO_2 \rightarrow ClO_2(g) + NaCl + NaOH$ ❑ Low pH ❑ ClO_3^- also possible ❑ Relatively slow reaction rates ❑ Excess Cl_2 or acid to neutralize NaOH	Production rates limited to ~450 kg/d (1000 lb/d); high conversion but yield only 80–92%; more corrosive effluent due to low pH (~2.8–3.5); three chemical systems pump HCl, hypochlorite, chlorite, and dilution water to reaction chamber
Recycled aqueous chlorine–chlorite: (saturated Cl_2 solution via a recycling loop prior to mixing with chlorite solution)	$2HOCl + 2NaClO_2 \rightarrow 2ClO_2 + Cl_2 + 2NaOH$ ❑ Excess Cl_2 or HCl needed due to NaOH formed ❑ Concentration of ~3 g/L required for maximum efficiency	Production rate limited to ~450 kg/d (1000 lb/d); yield of 92–98% with ~10% excess Cl_2 reported; highly corrosive to pumps; drawdown; calibration needed; maturation tank required after mixing
Gaseous chlorine–chlorite: (gaseous Cl_2 and 25% solution of sodium chlorite; pulled by ejector into the reaction column)	$Cl_2(g) + 2NaClO_2 \rightarrow 2ClO_2(g) + 2NaCl$ ❑ Neutral pH ❑ Rapid reaction ❑ Potential scaling in reactor under vacuum due to hardness of feedstock	Production rates 2300–55,000 kg/d (5000–120,000 lb/d); ejector based, with no pumps; motive water is dilution water; near-neutral pH effluent; no excess Cl_2; turndown rated at 5–10X with yield of 95–99%; less than 2% excess Cl_2; highly calibrated flowmeters with minimum line pressure ~275 kPa (40 psig) needed

Source: Adapted in part from U.S. EPA (1999).

The differences between Eqs. 13-36, 13-37, and 13-38 help to explain how generators can differ even though the same feedstock chemicals are used and why some should be pH controlled and others are less dependent on pH. In most generators, more than one reaction may be taking place.

Chlorine dioxide generators are relatively simple mixing chambers. The reactors are frequently filled with media (Teflon chips, ceramic, or Raschig rings) to generate hydraulic turbulence for mixing. A sample petcock valve on the discharge side of the generator is desirable to allow for monitoring of the generation process. An excellent source for additional information on chlorine dioxide generation may be found in Masschelein (1992).

Sodium Chlorite

Sodium chlorite is used as a solution, normally with a concentration of approximately 25 percent sodium chlorite or less. It is commercially available as a 25 or 38 percent solution. The major safety concern for solutions of sodium chlorite is the unintentional and uncontrollable release of high levels of chlorine dioxide gas. Levels that approach an explosive mix can sometimes occur if the sodium chlorite is exposed to acid.

Another concern to be addressed with sodium chlorite is crystallization. Like most salts, sodium chlorite solutions are prone to crystallization at low temperatures and/or higher concentrations. When crystallization occurs, it may obstruct flow in pipelines, valves, and other equipment.

Sodium chlorite is not stable as a powder. If dried, it is a fire hazard and can ignite when in contact with combustible materials. A sodium chlorite explosion may occur if too much water and inappropriate firefighting techniques are used to quench such a fire. Burning sodium chlorite will quickly generate enough heat to turn water to steam. At high temperatures, the breakdown products of sodium chlorite include oxygen. As a result, highly trained firefighters are required to extinguish closed containers or dry material that has been ignited.

Stratification in holding tanks for sodium chlorite solutions may also occur and, when it does, will adversely influence the chlorine dioxide yield in the generator. As stratification develops, the sodium chlorite solution being fed gradually changes from low to high density as the generator operates. In stratified tanks, excess chlorite will be fed to the generator as the bottom of the tank will have denser material, and this material will have more chlorite than required. Similarly, the bulk tank will later yield chlorite that is too dilute. Although infrequent, such stratification is not readily apparent and may likely remain unnoticed by an operator unless the generator performance is evaluated frequently. Operators should be aware of the possibility of stratification and crystallization during delivery conditions.

13-7 Disinfection with Ozone

Ozone is the strongest of the chemical disinfectants and its use is becoming increasingly common. Ozone (O_3) is an allotrope of oxygen with three oxygen atoms. The word *ozone* comes from the Greek word *ozein*, which means ''to smell.'' In air, ozone has a pungent odor that is noticeable to

most persons at levels above 0.1 ppm_v. Ozone is generated at the treatment plant site as a gas and is then injected into water.

Once dissolved in water, ozone begins a process of decay that results in the formation of the hydroxyl radical (HO·). Ozone reacts in two ways with contaminants and microbes: (1) by direct oxidation and (2) through the action of hydroxyl radicals generated during its decomposition. The consensus is that action of ozone as a disinfectant is primarily dependent on its direct reactions; hence it is the residual of the ozone itself that is important.

Ozone Demand and Ozone Decay

The ozone demand is the ozone dose that must be added before any ozone residual is measured in the water. It corresponds to the amount of ozone consumed during rapid reactions with readily degradable compounds. Ozone decay is the rate at which the residual ozone concentration decreases over time when the ozone dose is greater than the ozone demand. The overall rate of ozone decay in water is generally consistent with first-order kinetics. Like chlorine, it can be modeled successfully using a parallel first-order decay model, as shown in Eq.13-9. Although simple reactions serve as good phenomenological models for ozone decay, it is unlikely that they correctly characterize the actual mechanism of decay. From work done in this area (Grasso and Weber, 1989; Gurol and Singer, 1982; Hermanowicz et al., 1999; Staehelin and Hoigné, 1982, 1985; Tomiyasu et al., 1985), it appears more likely that ozone decay consists of a large number of *n*th-order reactions operating in parallel that, in sum, appear to be simple first order.

An introduction to ozone decay based on the models developed by Staehelin and Hoigné (1982, 1985) is provided on Fig. 13-18. The cyclic nature of the ozone decay process in pure water is illustrated on Fig. 13-18a. The process must be initiated by a reaction between ozone and the hydroxide ion to form superoxide radicals (O_2^-) and peroxide ions (HO_2^-), a slow process. As a result, decay is accelerated at higher pH. Once completed, the decay reactions enter a cyclic process represented in the figure by a circle. The cyclic reactions are promoted by ozone itself. If the concentration of ozone is increased, the cycle is accelerated.

In natural waters, other ''initiators'' besides hydroxide ion can be present as shown on Fig. 13-18b. Prominent among them are the ferrous ion and hydrogen peroxide. In natural waters certain natural organic materials have also been shown to promote the cycle, accelerating decay. Finally, the continuation of the cycle depends on the action of the hydroxyl radical on the ozone residual. As a result, scavengers that react with the hydroxyl radical, removing it from the process, also slow the rate of decay. The carbonate and bicarbonate ions are important examples of such inhibitors. The data of Reckhow and co-workers (Reckhow et al., 1986), are shown on Fig. 13-18c to illustrate the action of fulvic acids as initiators and promoters and carbonate and bicarbonate ions as HO· traps or inhibitors. The factors that influence the stability of ozone residuals are summarized in Table 13-7.

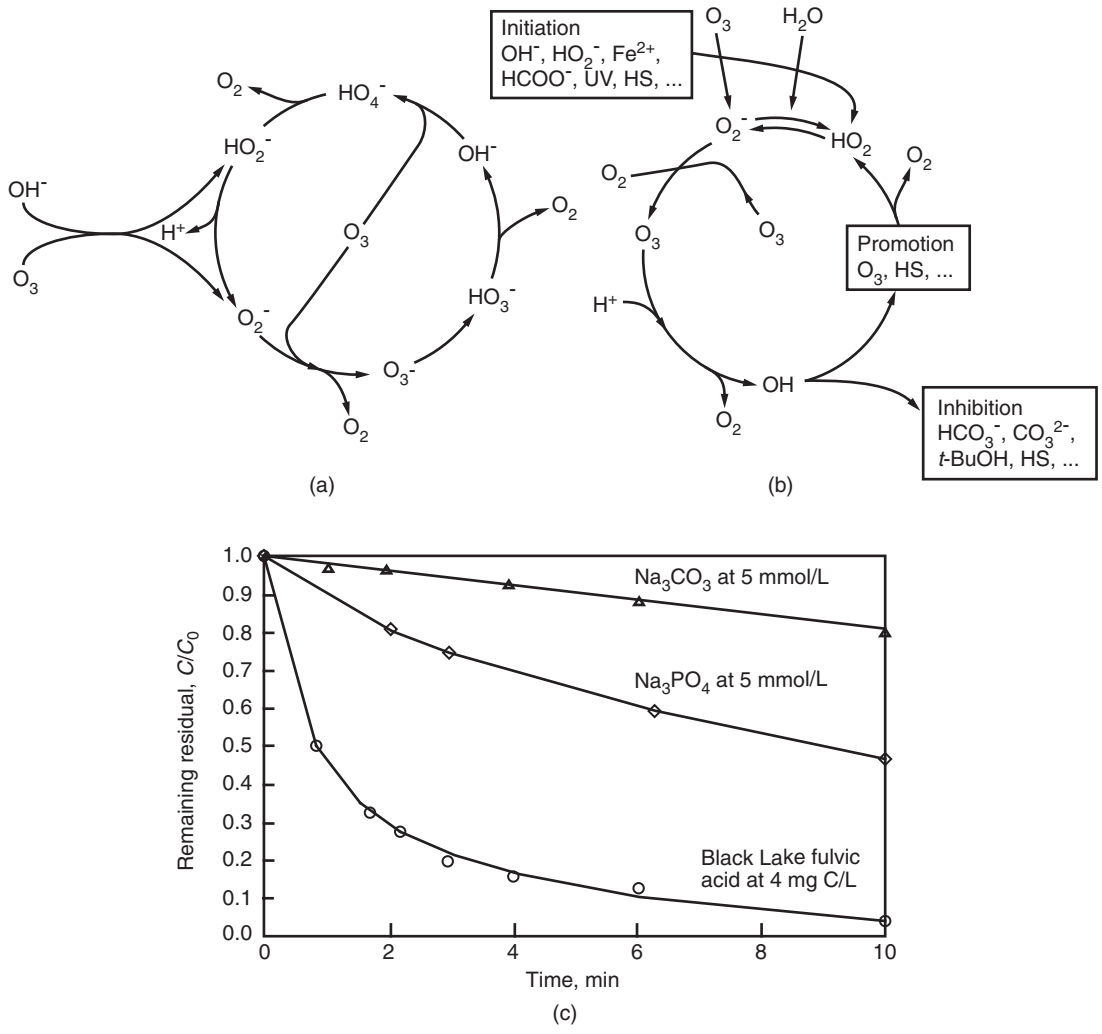

Figure 13-18
Understanding ozone reaction pathways and decay of residual ozone in natural waters: (a) influence of initiators, promotors, and inhibitors (adapted from Hoigné and Bader, 1976); (b) the ozone decay wheel—reaction pathways in pure water (adapted from Hoigné and Bader, 1976); (c) effect of fulvic acid and carbonate on ozone decay—all tests conducted at 20°C with GAC filtered, deionized tap water adjusted to pH 7, and $C_0 \sim 8$ mg/L. (Adapted from Reckhow et al., 1986).

Bench Testing for Determining Ozone Disinfection Kinetics

The conceptual design of any ozonation system requires a means for estimating mass transfer of ozone into the water, an understanding of the kinetics of ozone decay, and an understanding of the disinfection kinetics. These components are often investigated using bench and pilot testing. Both batch and flow-through reactors have been used for bench testing, as described in the following sections.

Table 13-7
Factors that influence stability of aqueous ozone residuals

Increases Stability	Reduces Stability
Low pH	High pH
High alkalinity	Low alkalinity
Low TOC	High TOC
Low temperature	High temperature

ANALYSIS USING BATCH REACTORS

Batch testing is often conducted by bubbling ozone directly into a gas wash bottle containing the sample of interest. The ozone concentration is measured in the gas entering and exiting the bottle, and the difference constitutes the ozone added to or consumed by the sample. For a number of reasons, the preferred technique is to prepare the ozonated water first and then add that to the sample of interest. In this case, the batch reactor might be a 1- or 2-L jar or a 0.5- to 1-L Teflon bag containing the water of interest. The concentrated ozone solution is prepared in a separate container by continuously bubbling ozone gas into a small volume of distilled–deionized (DI) water. At ambient temperature, the maximum ozone solution concentration may be about 15 mg/L. To prepare a more concentrated solution, the DI water can be chilled in an ice bath. At temperatures close to 1°C, the concentration of ozone in the stock solution can be as high as 40 mg/L. Aliquots of the ozone stock solution are then drawn and injected into the test water sample. The volume of each aliquot is calculated to deliver a predetermined ozone dose to the test water sample. Water samples are then drawn from the test water at various times after the ozone is added and analyzed for ozone residual concentration. This test is repeated using various ozone doses.

The profile of ozone residual concentration versus time can then be plotted. Two example ozone decay profiles in two waters dosed with 1.0 mg/L ozone are shown on Fig. 13-19a. Both waters have relatively high ozone demand, particularly water B. The profile of ozone decay in water A is typical of most moderate TOC, well-oxygenated surface waters. The curve fit through the data points is that of a pseudo-first-order decay equation with a decay coefficient of 0.3 min^{-1}. The decay of ozone in some waters does not always follow this uniform first-order decay model. Water B is an example of common ozone decay profiles where the ozone experiences an initial period of a high decay rate followed by a second period of slower decay. The curve fit through the data points for water B was accomplished using Eq. 13-9: Although this equation is based on the progress of two parallel first-order reactions, it should be viewed as a phenomenological model, not a mechanistic one. Based on experimental evidence, ozone, and

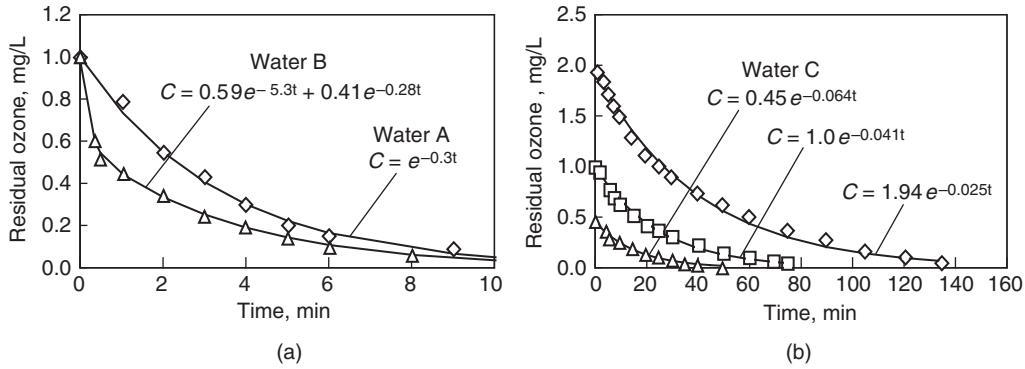

Figure 13-19
Typical batch ozone decay curves for three different waters: (a) waters A and B and (b) water C.

particularly the hydroxyl radical that is produced when it decays, participate simultaneously in many reactions of different orders at the same time.

Another result of this complexity is that with ozone, as with chlorine, the rate of decay observed in a batch test is also influenced by the ozone residual at the beginning of the decay period, as illustrated on Fig. 13-19b using the data from a pure mountain water supply. In general, these curves exhibit a low rate of decay; nevertheless they also show a rate of decay that decreases as the residual at the beginning of the decay process (C_0) increases. As with chlorine, the change in decay rate is approximately inversely proportional to C_0. As a result of these complexities, if only batch testing is conducted to determine the basis of design, a wide variety of test conditions must be evaluated to get an adequate database for design. Even with such data, a number of assumptions and approximations must be made during the process of design.

ANALYSIS USING FLOW-THROUGH REACTORS

Continuous-flow reactors (see Fig. 13-20) are better than batch reactors for gathering information for design of ozonation facilities, especially for an over–under ozone contactor with ozone addition via diffusers. In full-scale designs of this type, the ozone is generally added in the first few compartments of the design, and then the residual is allowed to decay as the water travels throughout the rest of the reactor. This approach to design and operation can be simulated by operating the small-scale continuous-flow unit so that it has the same detention time as the ozone addition compartments will have in the full-scale design. Once the reactor has reached steady-state operation, both the flow of water and the ozone dosing can be stopped and the decay of ozone residual can be observed as a function of time. The continuous operation simulates the ozone addition

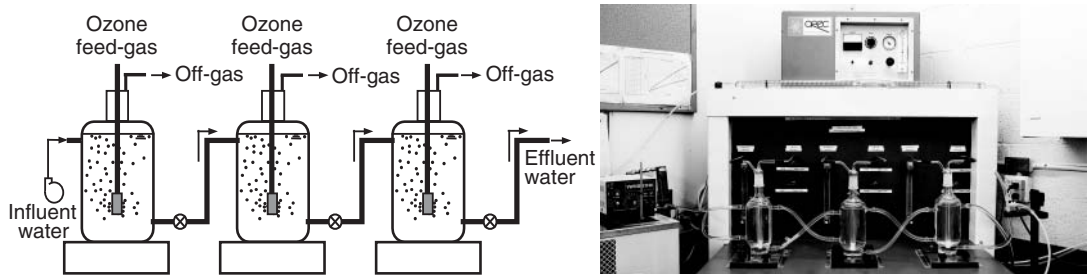

Figure 13-20
Bench-scale continuous-flow ozonation test system: (a) schematic and (b) photograph.

compartments and the decay curve can be used to estimate the residual in downstream compartments.

A continuous-flow setup requires measuring the ozone gas flow rate, water flow rate, ozone concentration in the feed gas, and ozone concentration in the off-gas. The ozone dose to the reactor is then calculated with a mass balance as

$$\text{Ozone dose, mg/L} = \frac{Q_g}{Q_l} \times (C_{g,\text{in}} - C_{g,\text{out}}) \qquad (13\text{-}39)$$

where Q_g = gas flow rate, L/min
Q_l = water flow rate, L/min
$C_{g,\text{in}}$ = concentration of ozone in feed gas, mg/L
$C_{g,\text{out}}$ = concentration of ozone in off-gas, mg/L

For each ozone dose, the operating conditions are kept constant until steady-state conditions are reached. This stabilization period can be between three and five times the hydraulic residence time of the reactor. It is essential that the continuous reactors be operated with approximately the same detention time as the ozone addition compartments in the full-scale design. An RTD curve similar to the full-scale reactor is also highly desirable. Unfortunately, tall, narrow pilot columns with long aspect ratios are often used because they achieve more efficient ozone transfer. The use of tall columns is not a particularly good choice because they much more closely approach plug flow than full-scale designs. This test must also be conducted at various doses because it is important to understand the relationship between the ozone dose and the ozone residual in the water exiting the ozone addition section of the reactor. The ozone decay rate downstream of these compartments will vary with this residual as well.

Example 13-8 Analysis of bench-scale ozone data

A municipality wishes to build a treatment plant incorporating an ozonation reactor and using water from a particular lake as a raw-water source. The lake water was studied using a bench-scale continuous-flow test unit (see Fig. 13-20), which included a three-compartment ozonation system, providing a total of 3.8 min of contact time (all three compartments). The system was operated at four different ozone doses. Samples were collected using two methods: (a) continuous-flow tests and (b) batch decay tests. In the continuous-flow test, the effluent from the third compartment was sampled for ozone residual after 15 min operation at each dose. For the batch test the system was shut down and the residual in the final compartment was sampled with time. The summary results of the testing program are given below. Using these data, estimate the ozone demand and the decay rate constant at each initial ozone residual.

For the sizing of the full-scale ozonation system, estimate the *Ct* product that can be achieved if the system is designed for an ozone dose of 3 mg/L at a temperature of 27°C. Assume the following conditions apply: (1) all ozone is added in the first compartment, which has a residence time of 3.8 min, (2) no *Ct* credit is allowed for the first compartment, and (3) the total residence time of the remaining compartments is 15 min.

Results from Continuous-Flow Tests		Results from Batch Decay Tests			
Ozone Dose, mg/L	O_3 Residual, mg/L	Time, min	O_3 Residual, mg/L	Time, min	O_3 Residual, mg/L
		0.0	1.23	0.0	0.60
2.10	0	1.0	0.98	1.0	0.42
2.72	0.36	2.0	0.85	2.0	0.29
3.00	0.60	3.0	0.71	3.0	0.23
3.80	1.05	4.0	0.59	4.0	0.17
4.01	1.23	5.0	0.53		
		7.0	0.42		
		9.0	0.31		
		11.0	0.23		
		13	0.16		
		15	0.14		

Solution

1. Analysis of continuous-flow data: The continuous-flow data for $\tau = 3.8$ min and $T = 27°C$ are plotted below. The best-fit line can be described using the equation

$$C_{Residual} = a(C_{dose} - C_{demand})$$

Using the form of the equation shown above, the best-fit line parameters from the plot are $a = 0.64$ and $C_{demand} = 2.1$ mg/L. The above equation can be used to estimate the dose required to achieve a specified residual exiting the ozone dosing compartment in the reactor.

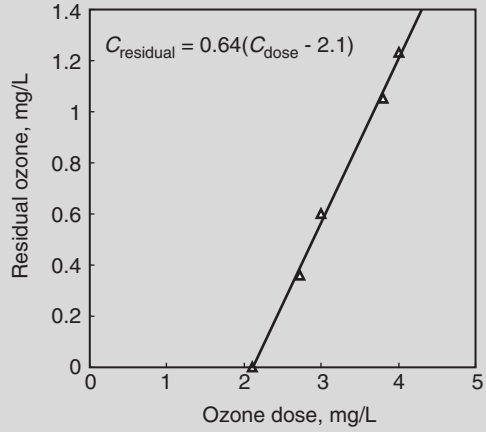

2. Analysis of the batch decay data: The batch decay data are plotted below. The best-fit parameters are obtained using an exponential curve fit. The corresponding equations are

For $C_o = 1.23$ mg/L(dose = 4 mg/L): $C_{residual} = 1.13e^{-1.14t}$

For $C_o = 0.60$ mg/L(dose = 3 mg/L): $C_{residual} = 0.58e^{-0.31t}$

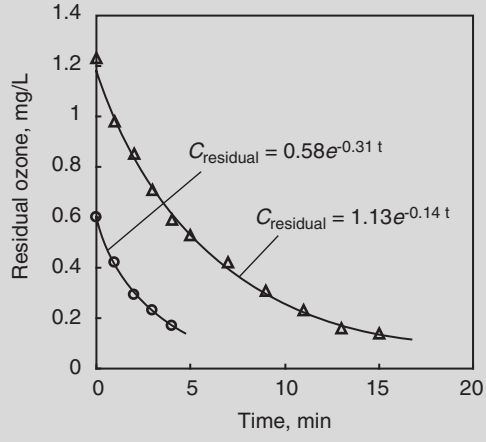

3. Determine the maximum *Ct* credit for the full-scale system assuming an ozone dose of 3 mg/L. Use the results from the batch decay data for the ozone dose of 3 mg/L.
   a. The maximum *Ct* credit can be estimated by numerical integration of the equation developed in step 2.

t, min	*C*, mg/L	$C\,\Delta t$, mg · min/L	$\Sigma\, C\,\Delta t$, mg · min/L	*t*, min	*C*, mg/L	$C\,\Delta t$, mg · min/L	$\Sigma\, C\,\Delta t$, mg · min/L
0.0	0.58	—	—	8.0	0.05	0.03	1.72
0.5	0.50	0.27	0.27	8.5	0.04	0.02	1.74
1.0	0.43	0.23	0.50	9.0	0.04	0.02	1.76
1.5	0.36	0.20	0.70	9.5	0.03	0.02	1.78
2.0	0.31	0.17	0.87	10.0	0.03	0.01	1.79
2.5	0.27	0.14	1.01	10.5	0.02	0.01	1.80
3.0	0.23	0.12	1.14	11.0	0.02	0.01	1.81
3.5	0.20	0.11	1.24	11.5	0.02	0.01	1.82
4.0	0.17	0.09	1.33	12.0	0.01	0.01	1.83
4.5	0.14	0.08	1.41	12.5	0.01	0.01	1.84
5.0	0.12	0.07	1.48	13.0	0.01	0.01	1.84
5.5	0.11	0.06	1.53	13.5	0.01	0.00	1.85
6.0	0.09	0.05	1.58	14.0	0.01	0.00	1.85
6.5	0.08	0.04	1.62	14.5	0.01	0.00	1.85
7.0	0.07	0.04	1.66	15.0	0.01	0.00	1.86
7.5	0.06	0.03	1.69				

   b. The maximum *Ct* credit is

$$\Sigma C dt = 1.86 \text{ mg} \cdot \text{min/L}$$

Comment

Dispersion and short circuiting are not considered in the above calculations.

Generation of Ozone

At high concentrations (>23 percent) ozone is unstable (explosive) and under ambient conditions it undergoes rapid decay. Therefore, unlike chlorine gas, it cannot be stored inside pressurized vessels and transported to the water treatment plant. It must be generated onsite. Ozone can be generated by photochemical, electrolytic, and radiochemical methods, but the corona discharge method is the most commonly used in water treatment. In this method, oxygen is passed through an electric field that is generated by applying a high-voltage potential across two electrodes separated by a dielectric material (see Fig. 13-21). The dielectric material

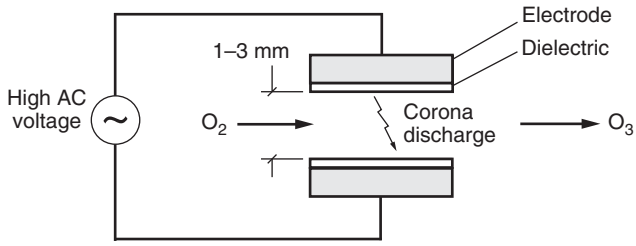

Figure 13-21
Ozone generation by corona discharge.

Table 13-8
Influence of increasing four key design factors on generator performance

Design Factor	Effect on Ozone Production
Frequency of applied current	Increases ozone production
Voltage of applied current	Increases ozone production
Gap between generator electrodes	Decreases ozone production
Dielectric constant of dielectric separating electrodes	Decreases ozone production

prevents arcing and spreads the electric field across the entire surface of the electrode. As the oxygen molecules pass through the electric field, they are broken down to highly reactive oxygen singlets (O·), which then react with other oxygen molecules to form ozone. The thickness of the gap through which the oxygen-rich gas stream passes is 1 to 3 mm wide. Because most of the energy used in ozone generation is lost as heat, cooling of the ozone generator is necessary to avoid overheating and subsequent decomposition of the ozone generated. Cooling is normally accomplished by passing a continuous stream of cooling water next to the ground electrode. Some of the key design factors that influence ozone generator performance are summarized in Table 13-8.

The equation below, while not intended to be quantitative, provides a general idea of the significance of a number of the variables of importance to the design of a corona discharge ozone generator:

$$Q_{O_3} \propto \left(f \frac{V^2 A}{d\varepsilon}\right) Q_{O_2} \tag{13-40}$$

where Q_{O_3} = ozone generation, kg/s
f = frequency of applied emf
V = emf across electrodes, V
A = surface area of electrodes, m^2
d = distance between electrodes, m
ε = dielectric constant
Q_{O_2} = oxygen flow rate, kg/s

Oxygen Source

Ozone can be generated directly from the oxygen in air or from pure oxygen. Pure oxygen is generated onsite from ambient air at larger plants or provided through the use of liquid oxygen (commonly referred to as LOX), which is generated offsite and transported to the plant. The most suitable method for providing oxygen for ozone generation in a particular plant depends on economic factors, the principal ones being the scale of the facility and the availability of industrial sources of liquid oxygen.

USE OF PREPARED, AMBIENT AIR

The most accessible oxygen source is ambient air, which contains about 21 percent oxygen by volume. Ambient air used to be the most common source of oxygen for ozone systems, but it has largely been replaced by liquid oxygen except for small, remote systems. Ambient air contains significant levels of particulates and water vapor, which must be removed. Water vapor is detrimental to corona discharge ozone generators for two reasons: (1) the presence of water vapor significantly reduces the ozone generation efficiency and (2) trace levels of water can react with the nitrogen present in the air and the generated ozone to form nitric acid, which attacks the ozone generator itself:

$$O_3 + N_2 + O_2 + H_2O \xrightarrow{h\nu} 2HNO_3 \qquad (13\text{-}41)$$

The moisture content of a gas is often defined by its dew point, which is the temperature to which the gas needs to be cooled to reach 100 percent saturation. The lower the dew point of a gas, the lower is its moisture content. For example, air with a dew point of 30°C contains about 28,000 ppm_v of water, whereas air with a dew point of 5°C contains about 5000 ppm_v of water. The dew point specified for many ozone generators is as low as −80°C, which corresponds to a moisture content of less than 1.5 ppm_v. Drying ambient air to this level is usually accomplished by a three-step process of compression, refrigeration, and desiccant drying. Compression and refrigeration help because the water vapor capacity of air decreases with increased pressure and decreased temperature, reducing the load on the desiccant system. Desiccant drying, however, is required to achieve the specifications for ozone generation. A schematic of all the components of such a system is shown on Fig. 13-22.

LIQUID OXYGEN DELIVERY

Liquid oxygen is widely available as a commercial, industrial-grade chemical and is the most common source of oxygen for ozone systems. Water treatment plants can purchase commercially available LOX, store it at the plant, and use it as the oxygen source for ozone generation. Liquid oxygen is delivered in trucks and stored in insulated pressurized tanks. Liquid oxygen is then drawn from the tank and piped to a vaporizer that warms and converts the oxygen to the gaseous form. Commercially available

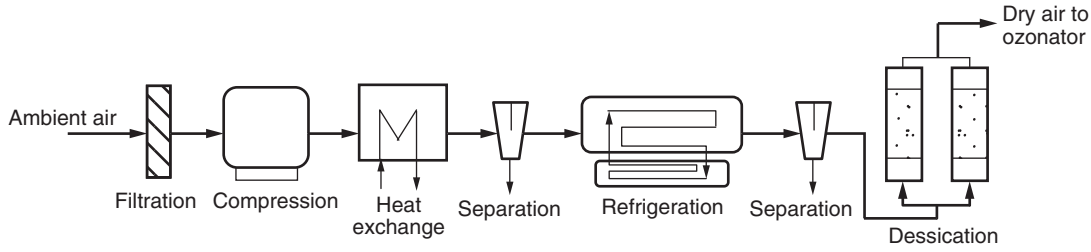

Figure 13-22
Preparation system for ozone generation from ambient air.

Figure 13-23
Liquid oxygen (LOX) storage container tanks at a large water treatment plant.

LOX is inherently low in contaminants and water vapor as a result of the manufacturing process. Therefore, minimal additional processing of the oxygen stream is required before it is introduced to the ozone generator. A LOX storage system at a large water treatment plant is shown on Fig. 13-23.

The use of LOX for ozone generation has several advantages over the use of ambient air, including (1) simpler operation and maintenance because fewer processes are required, (2) a smaller facility with lower capital cost, and (3) a smaller number of ozone generators. The disadvantages of LOX include (1) increased truck traffic caused by the need for regular LOX deliveries and (2) susceptibility to market pricing. Safety concerns associated with the storage of a large volume of concentrated oxygen must also be addressed. However, the advantages are significant and LOX has largely displaced the use of ambient air as the most common source of oxygen for ozone systems.

ONSITE OXYGEN GENERATION

Two types of onsite oxygen separation and concentration processes are used in water treatment plants that require oxygen: (1) pressure swing or vacuum swing adsorption (PSA or VSA) processes and (2) cryogenic oxygen generation processes. Generally, the economics of these processes improve as oxygen requirements increase. None are more economical than LOX feed systems in small applications. VSA systems are viable for systems requiring as much as 100 tonnes/d (110 tons/d) (Lotepro, 2002), and PSA systems can be used for smaller systems needing onsite oxygen generation. Cryogenic oxygen generation was installed at a few very large ozone systems in the past but are generally not economically competitive today for drinking water applications.

The PSA and VSA processes take advantage of the effect of gas pressure on the differences in the adsorption characteristics of the various constituents of ambient air on specialty adsorption resins. For the generation of oxygen, the affinity of the resin for nitrogen, water, and carbon dioxide is higher than that for oxygen and increases with increased pressure. Therefore, the PSA or VSA system cycles between ''high'' and ''low'' pressures. During the high-pressure period, water moisture, carbon dioxide, nitrogen, and any hydrocarbons present preferentially adsorb onto the resin while oxygen, now constituting about 90 to 95 percent of the remaining gas, passes through. Once the resin is saturated with the constituents removed, the system cycles to the low pressure, resulting in the desorption of the adsorbed material, which is then exhausted to the atmosphere before the cycle is repeated. For a PSA system, the high-pressure setting ranges from 200 to 400 kPa (30 to 60 psig), while the low setting is atmospheric pressure. In a VSA system, the high-pressure setting is at 20 to 70 kPa (3 to 10 psig), while the low setting is achieved using a vacuum pump. VSA systems are favored over PSA for large systems because they utilize less energy. However, a VSA system requires additional equipment compared to a PSA system in the form of a vacuum pump as well as a downstream compressor to boost the pressure of the oxygen stream to the level required by the ozone generator. The need for an extra pump translates into higher capital cost and higher maintenance cost. The schematic layout of a typical PSA system is illustrated on Fig. 13-24.

Regardless of whether air or pure oxygen is used for ozone generation, the efficiency of ozone generators is relatively low. When ambient air is used as the feed gas, ozone content in the generator outlet is typical between 1 and 4 percent by weight. With pure oxygen, typical generators produce about 6 to 16 percent ozone by weight.

Ozone Injection Systems

The addition of ozonation in a water treatment plant requires two components in the process treatment train: (1) a device for injecting the ozone

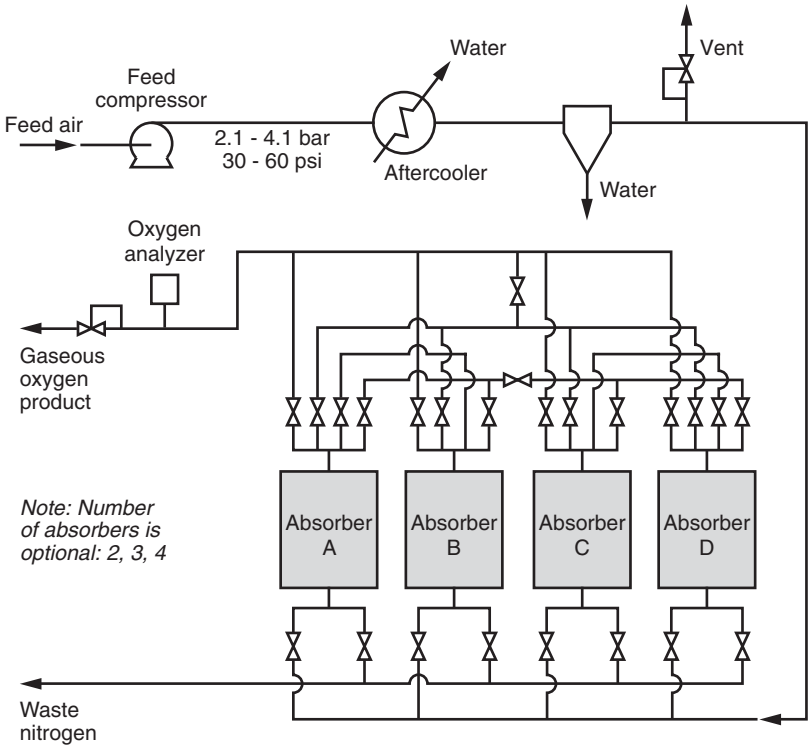

Figure 13-24
Schematic of pressure swing adsorption system for producing pure oxygen. (Adapted from Lotepro, Inc.)

into the water and (2) a contact chamber in which the disinfection reaction takes place. For several decades, the most common approach to ozonation has been to combine these components by introducing the ozone into the water in large, deep basins using porous diffusers. More recently, the injection and contact systems are designed separately. For injection systems, side-stream injection using venturi injectors with or without side-stream degassing has become more common than fine bubble diffusers. Ozone contactors can be pipeline contactors, serpentine basins, or over–under baffled contactors and are described in Sec. 13-8. Details of the design of side-stream ozone injection systems can be found in Rakness (2005) and are described briefly below.

In side-stream injection, a portion of the process flow is withdrawn from the main process line and pumped through a venturi injector. Low pressure in the throat of the injector draws ozone gas in from the ozone generator. After dissolution of the ozone gas, the side stream is injected back into the process stream through nozzles that provide good blending of the

ozonated side stream into the main flow. In some systems, the side stream passes through a degassing tower before being injected into the process stream. After the ozone is injected, the process water flows to a pipeline or serpentine basin contactor. Design of contactors is presented in the next section.

The purpose of the degasser in the side stream is to allow undissolved and supersaturated gases to separate from the water prior to injection to the main process flow and to minimize bubbles in the ozone contactor. Since the carrier gas for the ozone is typically pure oxygen, the process flow can become supersaturated with oxygen, which can lead to problems with downstream processes such as air binding in rapid granular filters. If the side stream does not contain a degas vessel, a mechanism for stripping supersaturated oxygen, such as by diffusing air after the ozone contactor, should be provided.

An advantage of side-stream injection coupled with pipeline or serpentine basin contactors is that these contactors can be designed with less dispersion and short-circuiting than over–under baffled contactors. The importance of dispersion in disinfection was presented in Sec. 13-4. In the case of ozonation, dispersion not only reduces the effectiveness of the disinfection reaction but also increases the formation of bromate.

Off-Gas Treatment

Because ozone is a strong oxidant, extended exposure to ozone-containing air is harmful. Even with the most efficient ozone contactor designs, off-gas ozone concentrations substantially exceed acceptable levels and, as a result, off-gas treatment is required. In the United States, the Occupational Safety and Health Administration (OSHA) sets an 8-h workday ozone exposure limit of 0.1 ppm_v by volume at standard temperature and pressure (STP), which is equivalent to 0.0002 mg/L in air (*Federal Register*, 1993). In general, the concentration in the ozone gas entering the contactor can range anywhere from 5000 to 160,000 ppm_v; so ozone contactors would have to achieve removals in excess of 99.998 percent to meet these standards directly. The efficiencies actually achieved in these reactors range from 90 to 99 percent, rarely higher. Therefore, the off-gas cannot be vented to the atmosphere before the residual ozone is destroyed.

Ozone in the off-gas stream can be destroyed thermally with or without the use of solid catalysts. When a catalyst is not used, ozone destruction is accomplished by heating the off-gas to a temperature between 300 and 350°C. At this temperature, the required contact time through the destruction unit is less than 5 s. Newer destruction units combine the use of specialty metal catalysts with moderate heating to achieve ozone destruction. Depending on the type of catalyst used, the off-gas temperature need only be raised to somewhere between 30 and 70°C (AWWARF, 1991).

Example 13-9 Estimating ozone concentration in contactor off-gas

An ozonation system produces ozone from air at a concentration of approximately 12 percent by volume. Assume the ozone contactor achieves a transfer efficiency of 99.5 percent. Estimate the concentration of ozone in the contactor off-gas from the contact chamber and compare it to OSHA standards.

Solution

1. Determine the downstream ozone concentration.
   a. Convert 12 percent by volume to ppm as follows:

$$12\% = \frac{12}{100}\left(\frac{10{,}000}{10{,}000}\right) = \frac{120{,}000}{1{,}000{,}000} = 120{,}000\ \text{ppm}_\text{v}$$

   b. Downstream of the contactor, the concentration is

$$C_{\text{off - gas}} = 120{,}000\ \text{ppm}_\text{v} \times (1 - 0.995) = 600\ \text{ppm}_\text{v}$$

2. How does the off-gas concentration compare to OSHA standards? To reduce the ozone concentration from 600 to 0.1 ppm, greater than 99.9 percent additional removal is required.

13-8 Design of Disinfection Contactors with Low Dispersion

Throughout much of the twentieth century, the design of specialized disinfectant contactors was not a particular concern. Chlorine was added early in the treatment process and the chlorine residual carried throughout the plant. Following the THM rule in 1980, many utilities moved the point of chlorine addition to the end of the treatment process. Later, when the first Surface Water Treatment Rule came about, many utilities struggled to find a way to get more credit for contact time in their existing facilities, often by baffling them to increase t_{10}. Because dispersion is so important in disinfection effectiveness (see Sec. 13-4), disinfectant contactors are now typically designed as a separate unit process. Engineered disinfectant contactors are typically of three types: (1) pipelines, (2) serpentine basins, and (3) over–under baffled contactors. Chlorine, combined chlorine, and chlorine dioxide contactors are typically pipelines or serpentine basins. Ozone contactors can be any of the three common types, and additionally deep U-tube contactors have also been used. Additional detail on dispersion and the design of reactors is presented in Chap. 6.

Design of Pipeline Contactors

A long channel or pipeline with plug flow characteristics can be an ideal disinfectant contactor. Occasionally, a long pipeline leaving the plant has sufficient contact time to make it an attractive alternative for chlorine or chloramines disinfection. Axial (longitudinal) dispersion in pipeline flow is the most straightforward case that will be considered. Taylor (1954) demonstrated that the longitudinal dispersion coefficient (D_L) can be described as

$$D_L = 5.05 D v^* \tag{13-42}$$

where D_L = longitudinal dispersion coefficient, m^2/s
D = diameter of conduit, m
v^* = shear velocity, m/s

In the above formula the shear velocity or friction velocity (v^*) may be defined in terms of the velocity of flow and the friction factor:

$$v^* = \sqrt{\frac{f v^2}{8}} \tag{13-43}$$

where f = Darcy–Weisbach friction factor, unitless
v = velocity of flow in pipe, m/s

The dispersion number is defined in terms of the longitudinal dispersion coefficient, the velocity of flow, and a characteristic length, in this case, the length of the pipe:

$$d = \frac{D_L}{vL} \tag{13-44}$$

where d = dispersion number, dimensionless

Combining Eqs. 13-42 through 13-44 results in a formula that can be used to describe the dispersion of flow in a pipe:

$$d = 5.05 \left(\frac{D}{L}\right) \sqrt{\frac{f}{8}} \tag{13-45}$$

Available data from laboratory experiments confirm Taylor's theory within a factor of 2. Generally, more dispersion is found in field-scale measurements than is predicted from the theory. For this reason, Sjenitzer (1958) gathered a great number of measurements, both in the laboratory and in the field, and correlated them to produce the empirical expression

$$d = 89{,}500 f^{3.6} \left(\frac{D}{L}\right)^{0.859} \tag{13-46}$$

Using Sjenitzer's data, Trussell and Chao (1977) demonstrated that Eq. 13-46 provides a significantly better fit of the data than Eq. 13-45. Even Sjenitzer's equation, however, is only accurate for a long pipeline without

bends, restrictions, or other disturbances to flow. Generally, the flow in a pipeline with 30 min of contact time, a flow rate greater than 3785 m^3/d (1 mgd), and a velocity greater than 0.6 m/s (2 ft/s) will be nearly ideal plug flow in behavior.

Example 13-10 Dispersion in pipelines

A treatment plant with a capacity of 25,000 m^3/d (6.6 mgd) is planning to use a 1-km treated-water pipeline as a chlorine contactor. Determine the diameter of the pipeline needed for a hydraulic residence time (τ) of 30 min and the resulting dispersion number of the flow in the pipeline. Using Fig. 13-7, determine whether dispersion will have a significant impact on achieving 4 log of inactivation with this pipeline. The Darcy–Weisbach friction factor is 0.018.

Solution

1. Determine the diameter D of the pipeline.

$$\tau = \frac{V}{Q} = \frac{AL}{Q} = \frac{\left[\pi/4D^2\right]L}{Q}$$

Rearranging and solving for D yields

$$D = \sqrt{\frac{4Q\tau}{\pi L}} = \sqrt{\frac{(4)(25{,}000\ \text{m}^3/\ \text{d})(30\ \text{min})}{(\pi)(1000\ \text{m})(1440\ \text{min/d})}} = 0.81\ \text{m}$$

2. Estimate the dispersion factor using Eq. 13-46:

$$d = 89{,}500(0.018)^{3.6}\left(\frac{0.81\ \text{m}}{1000\ \text{m}}\right)^{0.859} = 0.000104$$

3. Assess whether dispersion will have a significant impact on achieving 4 log of inactivation in the pipeline.

Comment

To acheive 4 log of inactivation with less than 5 percent deviation from the inactivation goal, the dispersion number must be less than 0.006 (see Fig. 13-7). Since the calculated dispersion number is less than that, the impact of dispersion on this contactor will be minimal. It should also be noted that pipe must be purchased in standard sizes, and the actual inside diameter of the pipeline would likely be larger than the calculated value, leading to an increase in τ, which would provide additional inactivation.

Design of Serpentine Basin Contactors

A pipeline is convenient if it is already necessary for some other purpose, but long, baffled, serpentine basins are generally more cost-effective means of achieving low dispersion. Serpentine basins are capable of achieving dispersion numbers less than 0.01 (Markse and Boyle 1973; Sepp, 1981; Trussell and Chao, 1977) and t_{10}/τ of 0.8 (Crozes et al., 1999). An optimal basin would be long and narrow, similar to the contactor discussed in the previous section. In the following discussion, the design of serpentine basins to achieve a specified level of dispersion is addressed first and then, because of U.S. regulatory requirements, designing these same facilities to meet a specified t_{10} will also be discussed. Computational fluid dynamics can be used to optimize the design of any large disinfection contactor (DuCoste, 2001; Hannoun et al., 1999).

DESIGNING FOR A SPECIFIED DISPERSION NUMBER

To develop a better understanding of design criteria, it is useful to start with a more general form of Eq. 13-42 (the Taylor equation):

$$D_L = CR_h v^* \tag{13-47}$$

where D_L = longitudinal dispersion coefficient, m^2/s
C = coefficient, unitless
R_h = hydraulic radius of channel, m
v^* = shear velocity, m/s

The coefficient C is a function of channel geometry and the Reynolds number. Elder (1959) applied Taylor's concept of dispersion to a logarithmic velocity profile and suggested that the coefficient C should have a value of approximately 5.9 for the circumstances in most chlorine contact chambers. For uniform flow in an open channel, the shear velocity can be defined as follows:

$$v^* = \frac{3.82\ nv}{R_h^{1/6}} \tag{13-48}$$

where v = velocity of flow in channel, m/s
n = Manning coefficient, unitless

Combining Eqs. 13-48, 13-47, and 13-44, the following approximate formula for dispersion coefficient in a long open channel is obtained:

$$d = \frac{22.7\ nR_h^{5/6}}{L} \tag{13-49}$$

Equation 13-49 may be rewritten to describe dispersion using the channel volume and height and length aspect ratios (Trussell and Chao, 1977):

$$d = 22.7\frac{n}{\beta_L}\left(\frac{\beta_H}{2\beta_H + 1}\right)^{5/6}\left(\frac{\beta_H\beta_L}{V_{\text{ch}}}\right)^{1/18} \tag{13-50}$$

where β_H = height aspect ratio or H/W (channel height/channel width)
β_L = length aspect ratio or L/W (channel length/channel width)
V_{ch} = channel volume, m^3

The dispersion values computed using Eq. 13-50 are not sensitive to the range of β_H values typical for concrete contact chambers (1 to 3). As a result, the following abbreviated form of Eq. 13-50 can be used satisfactorily (Trussell and Chao, 1977):

$$d = \frac{0.14}{\beta_L} \tag{13-51}$$

A plot of dispersion coefficients from field-scale tracer studies conducted on 17 different field-scale basins is illustrated on Fig. 13-25. Because the field tests were conducted in baffled, serpentine contactors, not long straight channels, none of the studies resulted in the performance predicted using Eq. 13-51. These basins include entrance effects, exit effects, 180° turns, and other nonidealities that would be expected to increase dispersion. Nevertheless, the results shown on Fig. 13-25 are encouraging for two reasons: (1) confirmation of the implication of Eq. 13-51 that dispersion is inversely proportional to the length aspect ratio and (2) the basins fall short of ideal performance, as expected. Recognizing this situation, a coefficient of ideality C_i was proposed (Trussell and Chao, 1977) such that

$$d = \frac{0.14 C_i}{\beta_L} \tag{13-52}$$

where C_i = coefficient of ideality

Lines corresponding to C_i values between 3 and 15 are also displayed on Fig. 13-25 and all the data lie on or between them. Based on the data

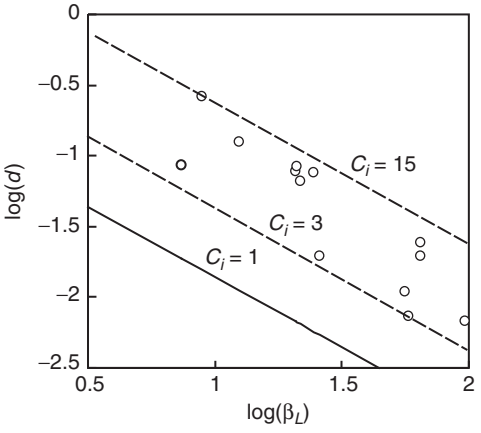

Figure 13-25
Impact of contactor aspect ratio on dispersion. (Adapted from Trussell and Pollock, 1983).

presented on Fig. 13-25, it appears that a good design should be able to equal or exceed the performance estimated by Eq. 13-52 with a C_i value of 3. A best-fit line corresponding to a C_i of 7.1 approximates the performance of a typical older reactor design.

DESIGNING FOR A SPECIFIED t_{10}/τ

Although the dispersion number is probably the most suitable means of assuring disinfection performance, a means of estimating t_{10}/τ must be used to be sure that the design will meet regulations (U.S. EPA, 1989). The impact of baffling rectangular contact tanks to improve hydraulic performance was evaluated by Crozes et al. (1999). A pilot contactor was baffled with nine different configurations having length aspect ratios ranging from 4.8 to 98. In addition, tracer tests were conducted on a full-scale, 34 ML/d (9-mgd) contactor before ($\beta_L = 6.1$) and after ($\beta_L = 52$) modifications. Finally, an empirical correlation between t_{10}/τ and β_L was developed and confirmed (Ducoste et al., 2001):

$$\left(\frac{t_{10}}{\tau}\right) = 0.198 \ln(\beta_L) - 0.002 \tag{13-53}$$

The data and correlation from the study are shown on Fig. 13-26. Note the results from full-scale tests lie close to model predictions.

Although the design of an effective disinfection contact basin requires attention to the length aspect ratio, other design details are also important. Any design detail that causes disturbances in flow is undesirable. Unnecessary gates, ports, or objects that constrict the flow lines are examples. In addition to minimizing the presence of these features, however, special attention should be given to three elements of design in every contactor:

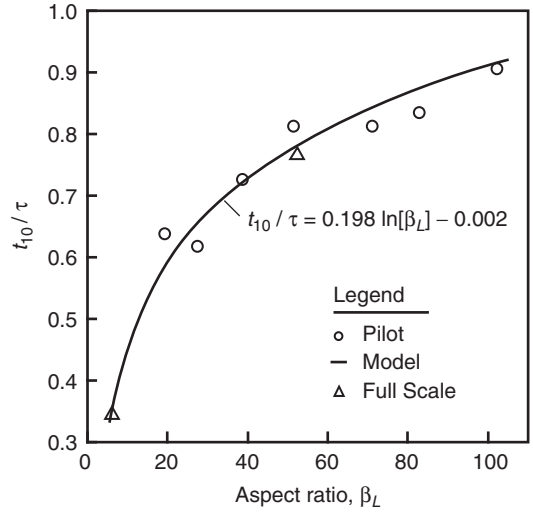

Figure 13-26
Impact of contactor aspect ratio on t_{10}. (Data from Crozes et al., 1999, and DuCoste et al., 2001.)

(1) inlet configuration, (2) outlet configuration, and (3) turns. Without proper attention, each of these is a likely cause of poor basin performance.

BASIN INLETS AND OUTLETS

Basin inlets are designed ordinarily as flow over a weir, through a pipe, or through a gate or gate valve into the basin. The momentum of the incoming water can cause significant dispersion in the first pass. When the entrance is a pipe, it is best for the water to exit through a tee so that the flow is not directed down the basin. With any of these inlet configurations (including a pipe with a tee) it is desirable to install a diffuser wall between the inlet of the basin and the first pass. Basin outlets are similar to inlets and have similar problems, although outlet effects are not quite as significant because outlets do not impart momentum to the basin flow. Often a diffuser wall is the best way to manage flow to outlets.

180° TURNS

To build a compact basin with the best possible length aspect ratio, rectangular basins are baffled in a serpentine fashion. However, the impact of baffling is not entirely benign. While increasing the tank's length–width ratio, the baffles also introduce flow separations at the 180° turns (Graber, 1972). Computational fluid dynamics (CFD) can be used to evaluate the flow in a chlorine contactor design and produce an estimate of the resulting tracer curve as illustrated on Fig. 13-27. A more complete discussion of CFD modeling may be found in Hannoun et al. (1999). Note that although the overall t_{10}/τ of the design shown on Fig. 13-27 is quite good, the CFD images illustrate the adverse impact of 180° turns on basin flow patterns. Flow separations can be observed at each turn, and these impact the character of the flow for some distance down each pass. Based on some estimates, as much as 40 percent of the volume in a baffled tank behaves as a dead zone (Louie and Fohrman, 1968). The increased dispersion decreases the effective contact time (early tracer appearance and a great deal of tailing in the tracer curve). Most of the nonideality in the tracer curve on Fig. 13-27 results from the 180° turns.

The primary way to minimize this dispersion is to keep the width of the flow path constant around a turn. A number of methods have been devised for controlling the problem, and some of them, illustrated on Fig. 13-28, are hammerheads and fillets (Louie and Fohrman, 1968; White, 1999), turning vanes (Crozes et al., 1999; Graber, 1972; Louie and Fohrman, 1968), and diffuser walls (Crozes et al., 1999; Hart, 1979). Turning vanes, hammerheads, and fillets are used to reduce or eliminate the flow separation. Diffuser walls, in contrast, redistribute the flow across the channel after the turn is complete. As a result, turning vanes, hammerheads, and fillets have the potential to actually *reduce* the head loss due to the turn as well as to reduce the flow nonideality introduced by the turn.

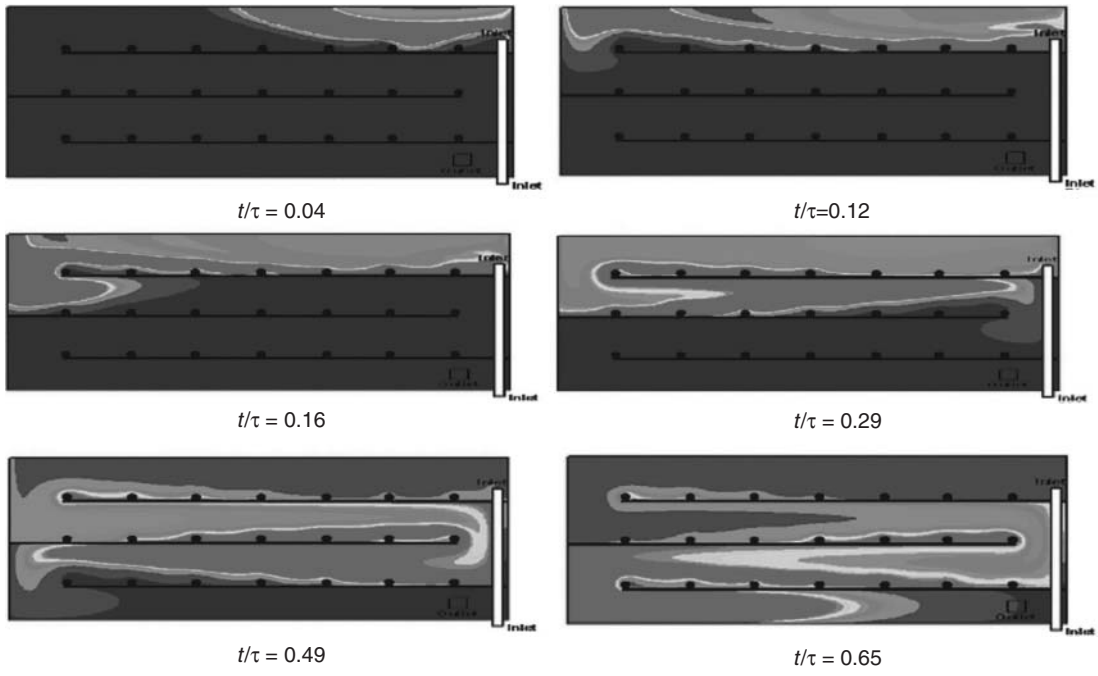

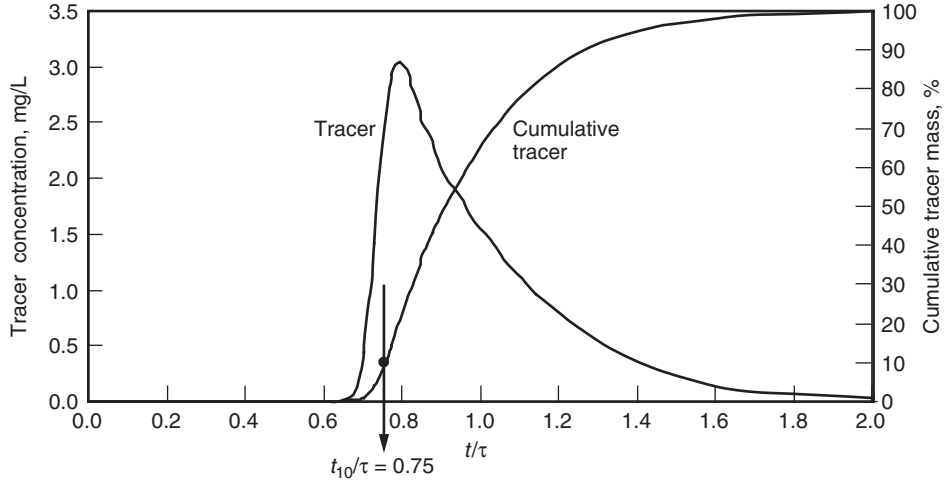

Figure 13-27
Using computational fluid dynamics (CFD) to evaluate RTD of disinfection contactor (CFD by Flow Science for an optimized design for the Weber Basin Water Conservancy District in Utah; $\tau = 110$ min, $t_{10} = 83$ min).

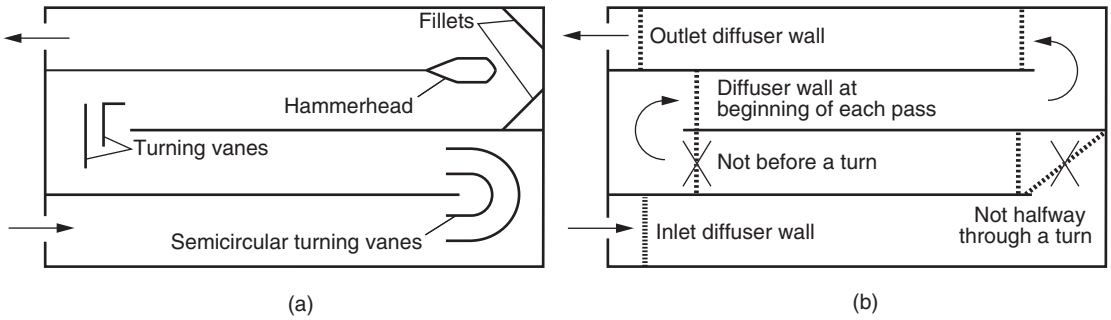

Figure 13-28
Controlling flow separation in serpentine basins using various devices: (a) fillets, hammerhead, and turning vanes (adapted from Louie and Fohrman, 1968) and semicircular turning vanes (adapted from Graber, 1972) and (b) diffusion walls (adapted from Trussell and Chao, 1977; Kawamura, 2000).

Diffuser walls always increase head loss because they depend on head loss to redistribute the flow.

Kawamura (2000) presented some useful criteria for designing diffuser walls between flocculation basins and sedimentation basins. These criteria are also useful for disinfection contact basins:

- Port openings should be uniformly distributed across the baffle wall.
- A maximum number of ports should be provided so that flow is evenly distributed.
- The size of the ports should be uniform in diameter.
- Ports should be 75 mm or larger to avoid clogging.
- Ports should be spaced with consideration to the structural integrity of the baffle. For wood baffles, this leads to 250- to 500-mm spacing.
- Ports should be designed to cause a head loss of 0.3 to 0.9 mm.

While diffuser walls have the advantage that some design criteria are available and they improve flow, they have the disadvantage that they increase the head loss. In fact, head loss and construction are the two major limitations on designing baffled, serpentine basins. Many baffle and channel designs become so narrow that construction is difficult. Moreover the head loss from the 180° turn can become significant. Nevertheless, baffled contactors with length aspect ratios as high as 100 and dispersion numbers below 0.01 are common.

Design of Over–Under Baffled Contactors

As noted in Sec. 13-7, over–under baffled contactors were the most common type of ozone contactor for many years but are less common now because of increased use of pipe contactors or serpentine basins for ozone contact systems. Pipeline and serpentine basins have better hydraulic characteristics that improve disinfection and minimize bromate formation.

Multichamber over–under baffled contactors often have several chambers where the water alternately flow up over a baffle and down under the next baffle (Rakness, 2005). Schematics of such a contactor are shown on Fig. 13-29. Ozone is typically added to the first one or two chambers via porous stone diffusers situated at the bottom of the chambers. Water enters the first chamber from the top and exists from the bottom. This countercurrent flow configuration (between the water and the air) helps increase the overall ozone transfer efficiency. The water depth in the contactor is typically between 4.6 and 6 m (15 and 20 ft) to achieve high transfer efficiency of the added ozone.

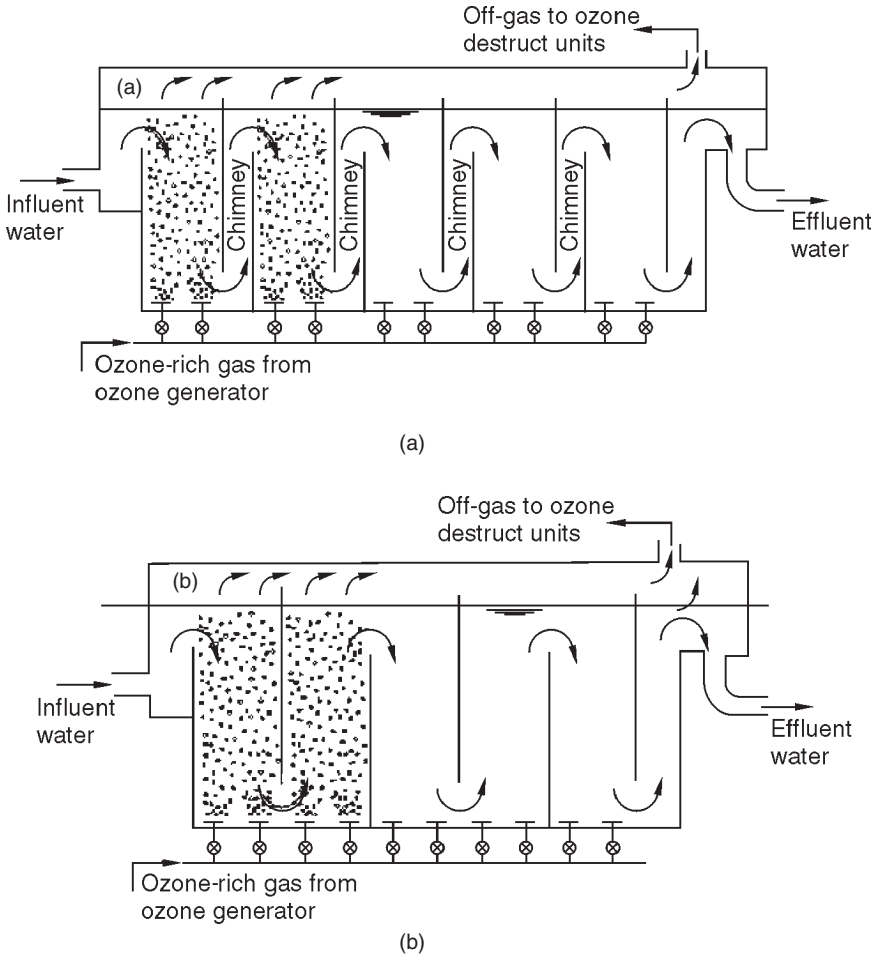

Figure 13-29
Schematics cross-sectional views of two alternate designs for five-chamber, over–under ozone contact chamber: (a) with chimneys and (b) without chimneys.

To achieve countercurrent flow in subsequent chambers, the contactor is also designed with segments that return the flow back to the top. A design is shown on Fig. 13-29a, where the water exiting the bottom of the first chamber rises to the surface through a narrow chamber, commonly called a *chimney*, before it enters the top of the second chamber. The chimney design achieves countercurrent flow in all chambers where ozone is added. A design with no chimneys is shown on Fig. 13-29b. In this design, the flow configuration alternates from countercurrent to co-current as the water moves from one chamber to the next. While lower transfer efficiency may take place in the co-current chambers, experience has shown that the impact is minimal. The passage of the water through the narrow chimneys of the alternate design causes a significant flow separation as the water enters and exits each down-flow contact chamber, resulting in high dispersion. On Fig. 13-30, schematic renderings of possible hydraulic flow patterns are shown in a multichamber contactor where the water is forced through a narrow pathway. Chimneys between chambers are indicated on Fig. 13-30a. The design shown on Fig. 13-30b no longer has chimneys but still exhibits significant flow separation at the turns.

The problem with the contactor design on Fig. 13-30b is that the openings through which the water flows between chambers are too narrow. The same principle that applies in the design of the serpentine basin contactors discussed previously applies here: the width of the flow path must be

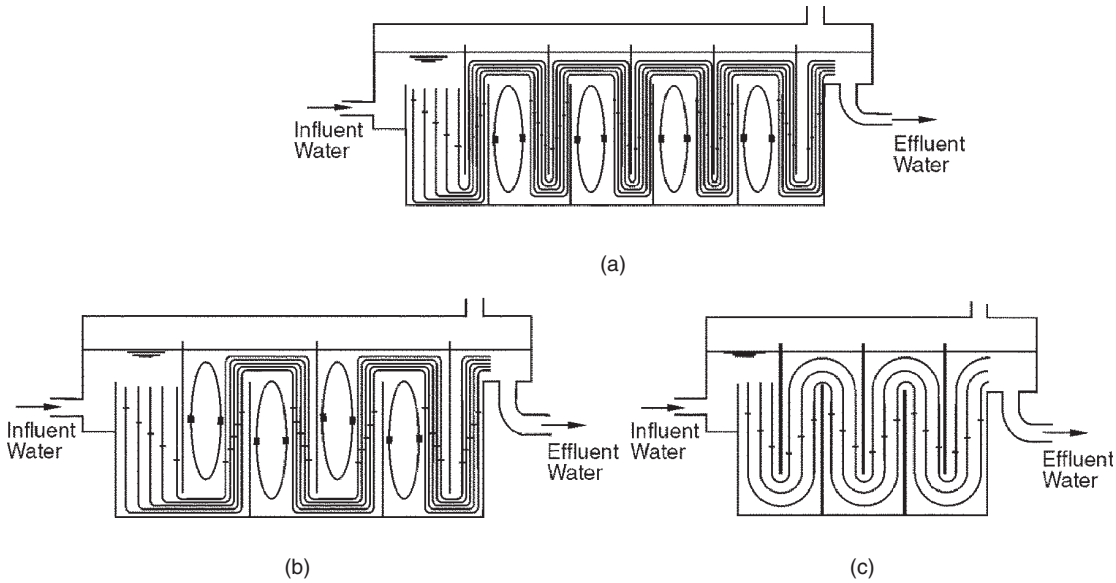

Figure 13-30
Conceptual impact of ozone contactor design flow hydrodynamics: (a) with chimneys, (b) without chimneys, and (c) with uniform flow path. (Adapted From Henry and Freeman, 1996.)

maintained. The flow path can be maintained by ensuring that the opening between two consecutive chambers is approximately the same width as the downstream chamber. The hydraulic flow pattern in a contactor designed with these considerations in mind is illustrated on Fig. 13-30c. It is noted that the hydraulic flow lines shown on Fig. 13-30 are only conceptual. A more accurate determination of the true hydraulic behavior can be determined using computational fluid dynamic (CFD) modeling of the contactor. Henry and Freeman (1996) conducted such modeling on various ozone contactor designs and determined that the contactor-baffling ratio (defined as the ratio of t_{10}/τ) is greatly impacted by the internal geometry of the contactor. The impact of the H/L ratio on the baffling ratio, where H is the water depth and L is the longitudinal width of the chamber, is shown on Fig. 13-31a (Henry and Freeman, 1996). Increasing the H/L ratio from 2 to 4 increases the t_{10}/τ ratio from 0.55 to 0.65. The impact of the G/L ratio, where G is the depth of the flow path under the baffle, on the baffling ratio is illustrated on Fig. 13-31b. Increasing the G/L ratio from 0.2 to 1.0 increases the t_{10}/τ ratio from 0.45 to 0.65. Based on this work, a maximum t_{10}/τ ratio can be achieved with an H/L ratio of 4 : 1 and a G/L ratio of 1:1.

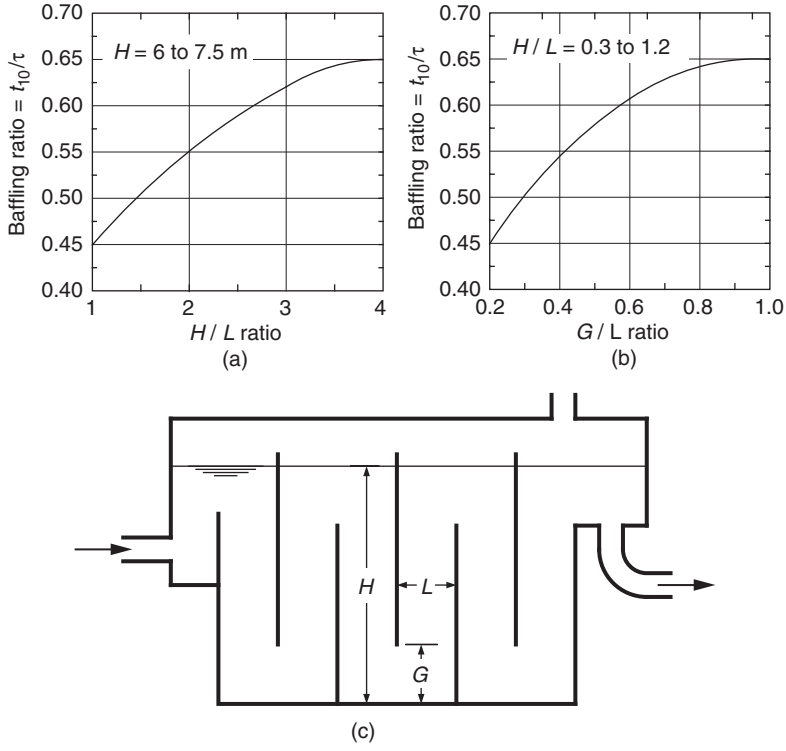

Figure 13-31
Impact of internal contactor design on its baffling ratio: (a) impact of *H/L* ratio; (b) impact of *G/L* ratio; and (c) contactor schematic. Dimensions *H*, *G*, and *L* are defined in contactor schematic. (Adapted from Henry and Freeman, 1996.)

Porous stone diffusers are used in ozone contactors to produce fine bubbles, which greatly increases the overall ozone transfer efficiency from the gas phase to the water, especially when compared to the use of a perforated-pipe diffuser. While both types of diffusers are used, experience has shown that perforated-pipe diffusers produce an excessively large bubble size. The cause of this problem is attributed to the way air exits the diffuser. When the diffuser is positioned horizontally, the air that exits on the underside of the diffuser seems to creep along the circumference of the diffuser before it rises into the water. As this creep occurs, the initial fine bubbles pick up more air and grow to large bubbles by the time they rise into the water column. Dome diffusers do not have this problem as the bubbles rise into the water column immediately after they exit the diffuser. Due to head loss limitations, a commercially available diffuser typically has a maximum gas flow rating that should not be exceeded.

13-9 Disinfection with Ultraviolet Light

All of the disinfectants discussed previously in this chapter are oxidizing chemicals. Disinfection can also be accomplished by other means, heat and electromagnetic radiation among them. Heat is used to disinfect, or ''pasteurize,'' beverages and even to disinfect water through boiling. Electromagnetic radiation, specifically gamma radiation and UV radiation, is also used for disinfection: gamma radiation in the case of food products and UV radiation in the case of air, water, and some medical surfaces. Of these, only UV radiation has so far found a place in the routine disinfection of drinking water.

Ultraviolet disinfection is not common for drinking water disinfection in the United States, as was shown in Fig. 13-1. It is used more commonly in other countries, however, and its use is growing in the United States. The purpose of this section is to provide a basis for understanding the use of UV radiation for the inactivation of microorganisms. In practice, the design and implementation of UV radiation for water treatment is governed by U.S. EPA (2006) and state guidelines, also discussed in this section.

What Is Ultraviolet Light?

Ultraviolet light is the name used to describe electromagnetic radiation having a wavelength between 100 and 400 nm. As illustrated on Fig. 13-32, electromagnetic radiation of slightly shorter wavelength has been named ''x-rays'' and electromagnetic radiation of slightly longer wavelength, visible to the human eye, is referred to as ''visible light.'' Radiation just long enough to be outside the visible range is referred to as infrared radiation. Light in the UV spectrum is often further subdivided into four segments, vacuum UV, short-wave UV (UV-C), middle-wave UV (UV-B), and long-wave UV (UV-A). These classifications can also be described as follows:

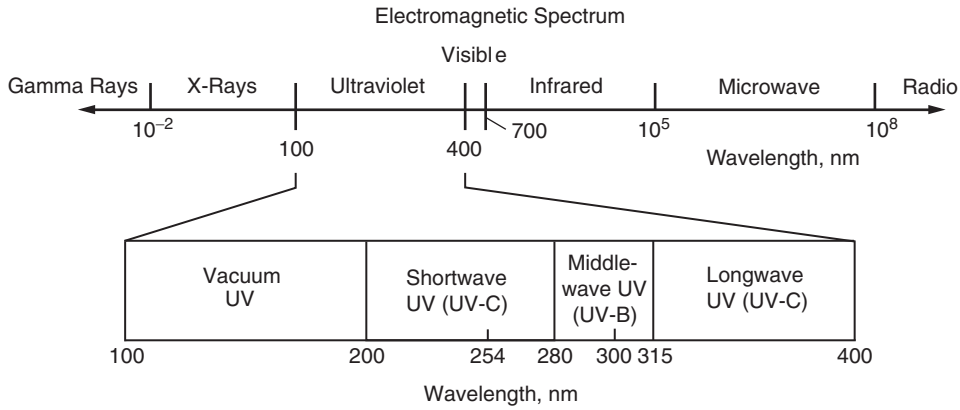

Figure 13-32
Location of the ultraviolet light region within the electromagnetic spectrum.

1. Both UV-A and UV-B activate the melanocytes in the skin to produce melanin (''a tan'').
2. UV-B radiation also causes ''sunburn.''
3. UV-C radiation is absorbed by the DNA and is the most likely of the three to cause skin cancer.

If electromagnetic radiation is thought of as photons, then the energy associated with each photon is related to the wavelength of the radiation (Einstein, 1905):

$$E = \frac{hc}{\lambda} \tag{13-54}$$

where E = energy in each photon, J
h = Planck's constant (6.6×10^{-34} J · s)
c = speed of light, m/s
λ = wavelength of radiation, m

As a general rule, the more energy associated with each photon in electromagnetic radiation, the more dangerous it is for living organisms. Thus, visible and infrared light have relatively little affect on organisms, whereas both x-rays and gamma rays can be quite dangerous. Beyond these broad considerations, there are other factors that determine the fraction of the UV spectrum that is effective in disinfection. The portion of the UV spectrum that is more effective in disinfection is called the ''germicidal range.'' On the lower end, the germicidal range is limited by the absorption of UV radiation by water. As wavelengths decrease, water becomes an increasingly efficient barrier for UV. For practical purposes, vacuum UV, the fraction of UV with a wavelength below 200 nm, cannot penetrate water. So radiation having a wavelength of 200 nm or less is not considered germicidal. It is also

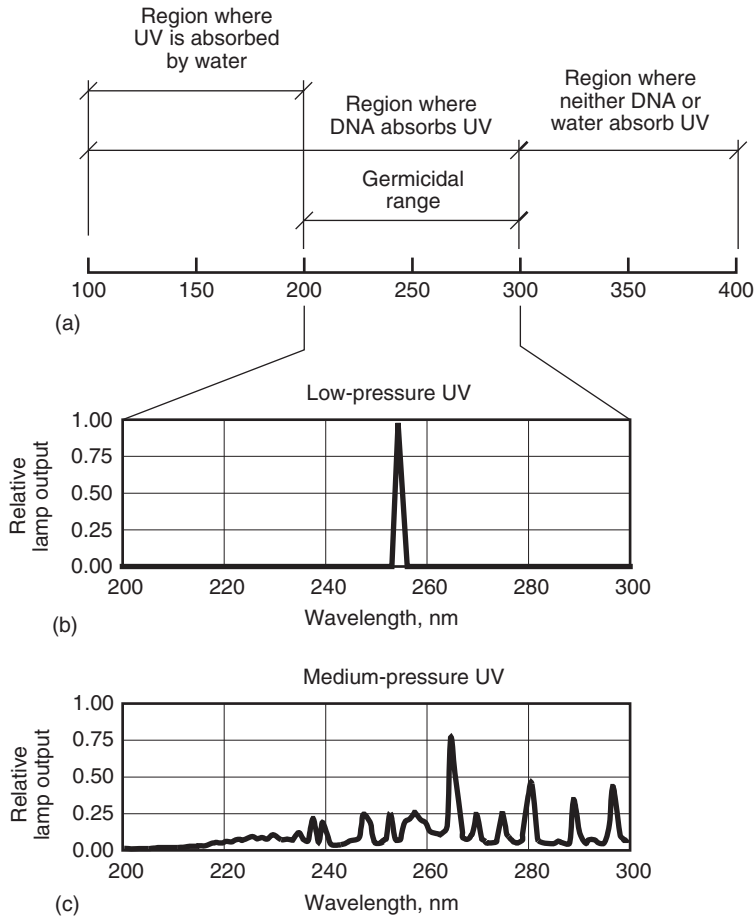

Figure 13-33
Ultraviolet sources and germicidal range: (a) ultraviolet portion of electromagnetic spectrum, (b) output from low-pressure UV lamp, and (c) output from medium-pressure UV lamp.

well established that UV inactivates microorganisms by transforming their DNA. This transformation cannot happen unless the UV is at a wavelength at which DNA will absorb it, and this absorption does not occur above wavelengths of approximately 300 nm. Therefore the germicidal range for UV is between approximately 200 and 300 nm (Fig. 13-33a).

Sources of Ultraviolet Light

The UV disinfection units used most commonly in the water industry employ three different types of UV lamps: (1) low-pressure low-intensity lamps, (2) low-pressure high-intensity lamps (also called low-pressure high-output lamps), and (3) medium-pressure high-intensity lamps. The design of these lamps closely approximates that of the common fluorescent light bulb. Low- and medium-pressure, high-intensity lamps are able to achieve a higher UV output in an equivalent space. Of the three technologies,

medium-pressure UV has the greatest output. The spectrum of the UV light output by both types of low-pressure lamps is essentially the same, a very small amount of the light energy emanating at a wavelength of 188 nm and the vast majority of it emanating at a wavelength of 254 nm. The spectrum of the UV light output by medium-pressure lamps includes a number of wavelengths. These spectra are illustrated and compared with the germicidal range on Fig. 13-33b and 13-33c.

Several important characteristics of each of these UV lamps are compared in Table 13-9; however, it must be noted that UV lamp technology is evolving continuously. One of the design engineer's more important challenges is to evaluate the technologies available at the time a design is prepared and to write specifications that will enable new technologies while protecting the owner against innovative, but unproven, alternatives where the prospect for failure can be significant. New UV technologies under development and testing include pulsed UV, narrowband excimer UV (Naunovic et al., 2008), and deep UV (DUV) semiconductor light-emitting diodes (LEDs). The pulsed UV lamp produces polychromatic light at very high intensity, the narrowband excimer lamp produces nearly monochromatic light at

Table 13-9
Characteristics of three types of UV lamps

Item	Unit	Type of lamp		
		Low pressure Low intensity	Low pressure High Intensity	Medium Pressure
Power consumption	W	40–100	200–500[a]	1,000–10,000
Lamp current	mA	350–550	Variable	Variable
Lamp voltage	V	220	Variable	Variable
Germicidal output/input	%	30–40	25–35	10–15[b]
Lamp output at 254 nm	W	25–27	60–400	Variable
Lamp operating temperature	°C	35–45	60–100	600–900
Partial pressure of Hg vapor	kPa	0.00093	0.0018–0.10	40–4000
Lamp length	m	0.75–1.5	Variable	Variable
Lamp diameter	mm	15–20	Variable	Variable
Sleeve life	yr	4–6	4–6	1–3
Ballast life	yr	10–15	10–15	1–3
Estimated lamp life	h	8,000–10,000	8,000–12,000	4,000–8,000
Decrease in lamp output at estimated lamp life	%	20–25	25–30	20–25

[a]Up to 1200 W in very high output lamp.
[b]Output in the most effective germicidal range (~255–265 μm).

wavelengths of 172, 222, and 308 nm, and UV LED lamps emit light at 280 to 285 nm.

Equipment Configurations

Before discussing the fundamentals of UV disinfection, it will be useful to consider the types of reactors used for UV disinfection, as many of the factors that affect the effectiveness of UV disinfection are related to the reactor configuration. The components of a UV disinfection system consists of (1) the UV lamps; (2) transparent quartz sleeves that surround the UV lamps, protecting them from the water to be disinfected; (3) the structure that supports the lamps and sleeves and holds them in place; (4) the power supply for the UV lamps and cleaning system; (5) online UV dose monitoring sensors and associated equipment, and (6) the cleaning system used to maintain the transparency of the quartz sleeves. By themselves, UV lamps, which use an electrical arc, are not electrically stable because their electrical resistance decreases as their current increases. As a consequence, the electrical system must be ballasted to limit the current to the lamp. Cleaning systems are necessary for low-pressure high-intensity and medium-pressure UV lamps because they operate at such high temperatures (see Table 13-9) that salts with inverse solubility can precipitate, fouling the outer surface of the quartz sleeve and reducing the net UV output. These UV system components are installed in closed-vessel pressurized systems or as open-channel gravity flow systems, as shown on Fig. 13-34. Closed-vessel systems are used most commonly for the disinfection of drinking water, whereas open-channel systems are more common in wastewater disinfection.

CLOSED-VESSEL SYSTEMS

Whereas most low-pressure systems are designed with open-channel flow, most low-pressure high-intensity and medium-pressure systems for drinking water are designed using closed vessels. These closed-vessel systems have the advantage that they can (and usually do) operate under pressure, and this feature makes them particularly attractive in upgrades and retrofits because it is not necessary to ''break head'' to use them. The placement of UV lamps in closed systems can be either perpendicular to the flow (see Fig. 13-34a) or parallel to the flow (see Fig. 13-34b). Because low-pressure high-intensity and the medium-pressure systems, operate with a limited number of lamps, more care is required to ensure that short circuiting does not occur. Biodosimetry methods, as discussed subsequently, have evolved that can be used to assess whether a UV reactor will perform as specified.

Of critical importance in the application of UV radiation for the inactivation of microorganisms is the ability to monitor the UV reactor online to be assured that the required UV dose is being delivered. The method used to monitor the UV dose is of importance both in the validation of the of

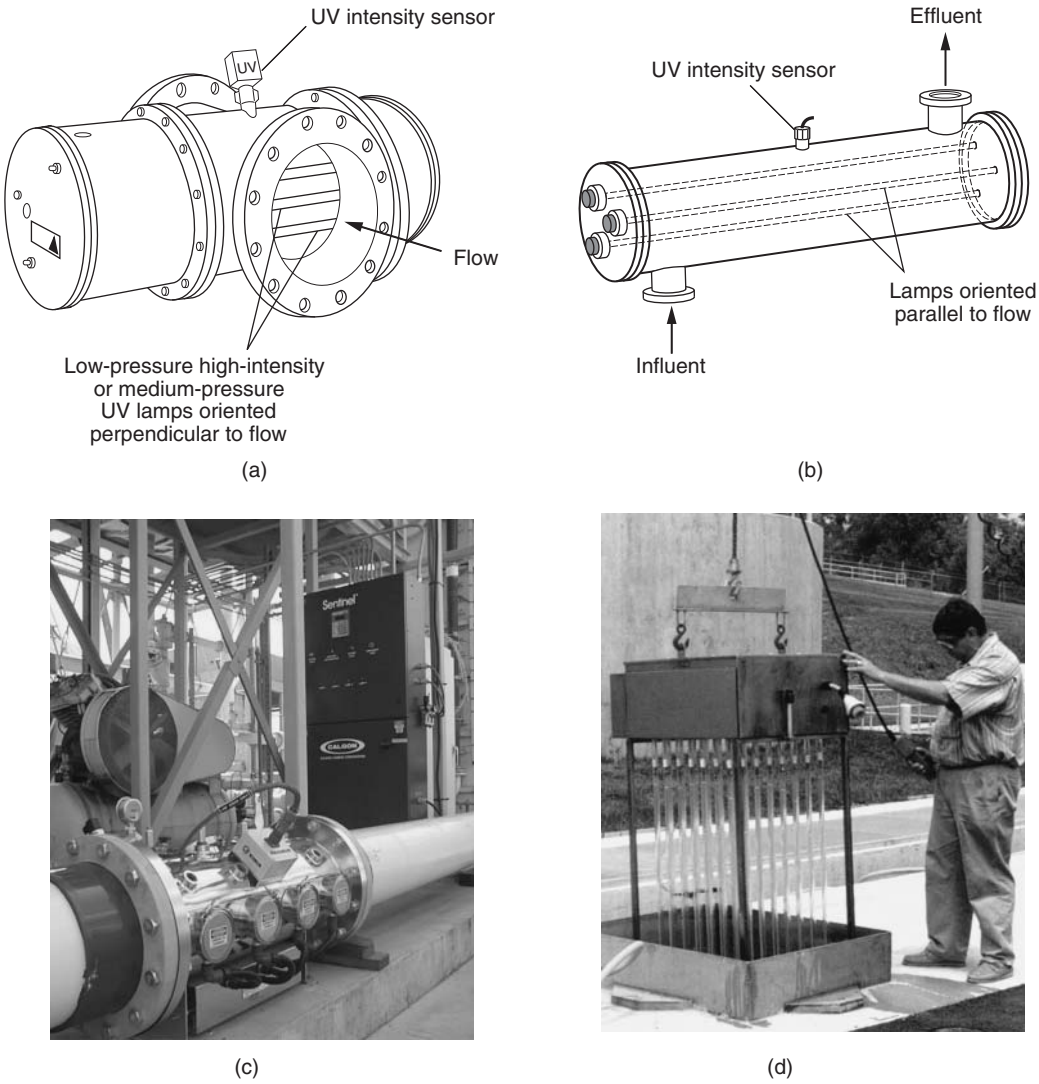

Figure 13-34
Common UV configurations: (a) medium pressure lamps placed perpendicular to the flow in a closed reactor, (b) low-pressure high-intensity lamps placed parallel to flow, (c) view of medium-pressure closed reactor, and (d) view of vertical low-pressure lamp arrangement in open reactor.

UV reactors as well as for monitoring the long-term performance of the UV reactor. The most common methods are:

1. ***UV Intensity Set Point*:** The reactor UV dose is monitored based on UV intensity, flow rate, and lamp status.

2. ***UV Transmittance and UV Intensity Set Point***: The reactor UV dose is monitored based on UV intensity, UV transmittance, flow rate, and lamp status.
3. ***Calculated Dose*:** The UV dose received by a microorganism is calculated continuously, using a predetermined algorithm, based on the UV transmittance, flow rate, and lamp status including the effects of aging and lamp fouling.

OPEN-CHANNEL SYSTEMS

Open-channel designs are available for all types of UV systems. Typically, the UV lamps are retained in modules or racks that are placed in the flow channel (see Fig. 13-34d). Designs are available with lamps placed horizontally parallel to the flow and with lamps placed vertically perpendicular to the flow. Conventional low-pressure low-intensity systems are typically designed so that they can be removed and cleaned easily. Most low-pressure high-intensity and all medium-pressure systems are provided with mechanical or mechanical/chemical self-cleaning systems.

Mechanism of Inactivation

More is known about the specific mechanisms of disinfection by UV than for any other disinfectant used in water treatment. The photons in UV light react directly with the nucleic acids in the target organism, damaging them. The genetic code that guides the development of every living organism is made up of nucleic acids. These nucleic acids are either in the form of deoxyribonucleic acid (DNA) or ribonucleic acid (RNA). The DNA serves as the databank of life while the RNA directs the metabolic processes in the cell. Ordinarily DNA is a double-stranded helical structure that includes the nucleotides adenine, guanine, thymine, and cytosine. Ordinarily RNA is a single-stranded structure with the nucleotides adenine, guanine, uracil, and cytosine (refer to Chap. 3).

Ultraviolet light damages DNA by dimerizing adjacent thymine molecules, inhibiting further transcription of the cell's genetic code (see Fig. 13-35). While not usually fatal to the organism, such dimerization will

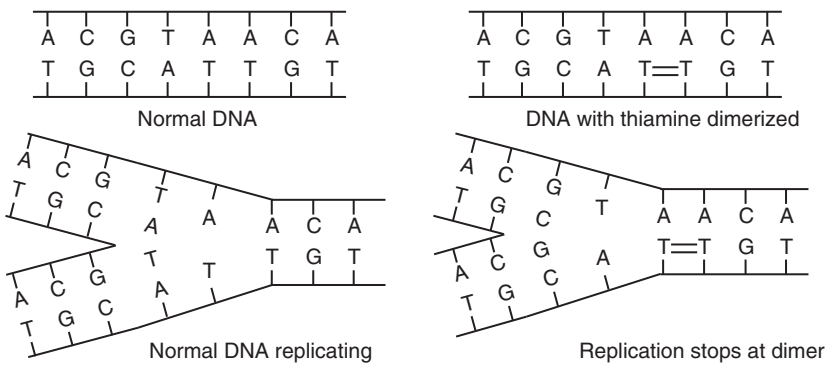

Figure 13-35
Formation of thiamine dimers by UV light interferes with normal replication of microorganisms.

prevent its successful reproduction (Setlow, 1967). Ultraviolet light also forms cytosine–cytosine and cytosine–thymine dimers, but these reactions have a lower quantum yield (they occur less frequently). As a result, organisms rich in thymine tend to be more sensitive to UV irradiation. For example, *C. parvum* and *G. lamblia* both contain DNA and both are inactivated by UV at relatively low doses (see Table 13-3). Most viruses of significance in drinking water have only RNA (which contains uracil instead of thymine) and, thus, are less sensitive to UV radiation. Among the most resistant organisms are viruses such as rotavirus and adenovirus, which incorporate a special double-stranded RNA. Other factors also influence the rate of inactivation, and some are not as well understood. Ultraviolet radiation can also cause damage of a more severe kind, breaking chains, crosslinking DNA with itself, crosslinking DNA with other proteins, and forming other by-products. These effects have an even lower quantum yield, and they are usually observed only at high doses of irradiation.

Reactivation

Reactivation is a more important consideration in UV disinfection than it is with disinfection by other methods. It is important to note that most forms of life evolved with some exposure to the sun and that sunlight includes significant amounts of UV irradiation. As a result, the process of evolution has addressed UV-induced damage by generating mechanisms for repairing the damage it causes. These mechanisms fall into two basic classes: (1) photoreactivation and (2) dark repair. Photoreactivation only takes place in the presence of light, whereas dark repair has no such requirement. Organisms capable of dark repair generally show much greater UV resistance; however, understanding the importance of photoreactivation requires that special tests be conducted, evaluating samples with and without light exposure to understand its effects.

Certainly when water is being disinfected for discharge into the environment, only the net inactivation after photoreactivation is important. Even in the case of drinking water systems, where light exposure is often more limited, the most conservative approach is to consider photoreactivation as well. Eventually, it may be possible to determine if an organism is capable of photorepair by using its genetic fingerprint to map its position on the evolutionary tree. In general, it is not safe to assume that any organism is incapable of photorepair, unless through testing it has been demonstrated to be the case. Even some viruses have been shown to be capable of photorepair, apparently taking advantage of enzymes in the host organism following infection.

Concept of Action Spectrum

Until recent years, low-pressure low-intensity lamps were the only source of ultraviolet light available for disinfection of drinking water. The principal light output of these lamps is at only one wavelength, 254 nm. Medium-pressure lamps, on the other hand, emit light at a variety of wavelengths (see Fig. 13-33c). There is no reason to expect that light will have the

same disinfecting power at each wavelength. Earlier, the boundaries of the *germicidal range* of wavelengths were broadly established, the lower boundary (200 nm) being defined by the absorption of light by water and the upper boundary (300 nm) being defined by the lack of absorption of light by DNA. To compare the effectiveness of medium- and low-pressure low- and high-intensity lamps for disinfection, a better understanding is required of possible significance of UV radiation at different wavelengths. A number of researchers have looked at this issue and the results of their research are generally expressed in the form of an action spectrum. To generate the action spectrum, a modification of Eq. 13-3 for UV light of a particular wavelength λ can be used:

$$r_{N_\lambda} = -N\Lambda_\lambda I_\lambda \tag{13-55}$$

where r_{N_λ} = rate of change in number of organisms exposed to light of wavelength λ
N = number of organisms exposed to light, organisms/100 mL
Λ_λ = coefficient of specific lethality for light of wavelength λ, m^2/J
I_λ = intensity of light at wavelength λ, W/m^2

The action spectrum is a representation of Λ_λ over a range of wavelengths.

Often it is displayed as a plot of the ratio $\Lambda_\lambda/\Lambda_{254\,nm}$ versus wavelength. The action spectrums for *C. parvum* (Linden et al., 2001) and MS2 (Rauth, 1965) are compared with the absorption spectrum for DNA on Fig. 13-36. A close correlation between Λ_λ and DNA absorption is observed. The action spectra of a number of organisms have been determined and are similar to the results shown on Fig. 13-36. As a result, many scientists believe that the germicidal efficiency determined for one species of microorganism to medium-pressure UV may be used to represent the relative response of other microorganisms as well (Giese and Darby, 2000).

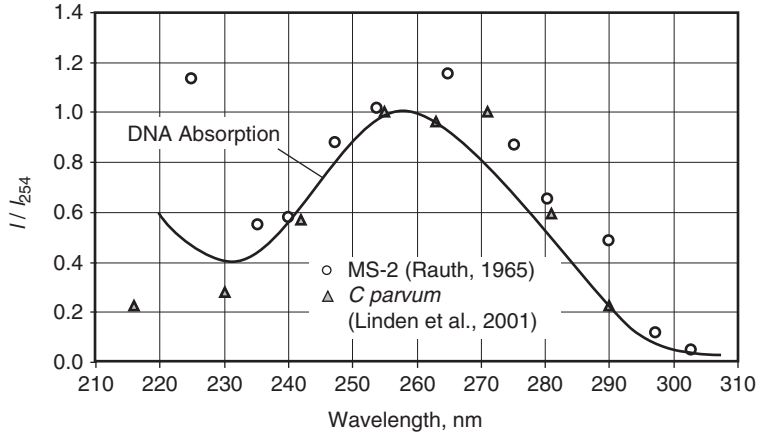

Figure 13-36
Comparing action spectra for *C. parvum* and MS-2 coliphage with absorption spectrum for DNA.

Ultraviolet Light Dose

The effectiveness of UV disinfection is based on the UV dose to which the microorganisms are exposed. The UV dose D is defined as

$$D = I_{avg} t \tag{13-56}$$

where $D = UV$ dose, mJ/cm^2 (note mJ/cm^2 = mW· s/cm^2)
I_{avg} = average UV intensity, mW/cm^2
t = exposure time, s

Note that the UV dose term is analogous to the dose term used for chemical disinfectants (i.e., Ct). As given by Eq. 13-56, the UV dose can be varied by changing either the average UV intensity or the exposure time. Determination of the average UV intensity, as a function of the distance from the light source, was illustrated previously in Example 2-2 in Chap. 2. The impact of dissolved and suspended substances on average UV intensity, and ultimately dose, are discussed below (Linder and Rosen Feldt, 2011; U.S. EPA, 2006).

Influence of Water Quality

The quality of the water being treated can have an important influence on the performance of UV disinfection systems. The two most important impacts stem from the action of dissolved and suspended substances.

DISSOLVED SUBSTANCES

Pure water absorbs light in the lower UV wavelengths. A number of dissolved substances also have important influence on the absorption of UV radiation as it passes through the water on its way to the target organism. Among the more significant are iron, nitrate, and natural organic matter. Chlorine, hydrogen peroxide, and ozone can also have important effects.

The absorption of light in aqueous solution by dissolved substances is described by the Beer–Lambert law. This relationship, discussed in Chaps. 2 and 8, takes the form

$$\log\left(\frac{I}{I_0}\right) = -\varepsilon(\lambda)\, Cx \tag{13-57}$$

where I = light intensity at distance x from light source, mW/cm^2
I_0 = light intensity at light source, mW/cm^2
C = concentration of light-absorbing solute, mol/L
x = light path length, cm
$\varepsilon(\lambda)$ = molar absorptivity of light-absorbing solute at wavelength λ, L/mol · cm

The term on the right-hand side of Eq. 13-57 is defined as the absorbance A, which is unitless. As discussed in Chap. 2, the absorptivity is the absorbance

corresponding to a path length of 1 cm, or

$$k(\lambda) = \varepsilon(\lambda)\, C = \frac{A}{x} \tag{13-58}$$

where $k(\lambda)$ = absorptivity, cm^{-1}

The absorptivity of the water is an important aspect of UV reactor design. Waters with higher absorptivity absorb more UV light and need a higher energy input for an equivalent level of disinfection. Absorbance is measured using a spectrophotometer typically using a fixed sample path length of 1.0 cm. The absorbance of water is typically measured at a wavelength of 254 nm.

In the application of UV radiation for microorganism inactivation, transmittance, which reflects the amount of UV radiation that can pass through a specified length at a particular wavelength, is the water quality parameter used in the design and monitoring of UV systems. The transmittance of a solution is defined as

$$\text{Transmittance, } T, \% = \left(\frac{I}{I_0}\right) \times 100 \tag{13-59}$$

The transmittance at a given wavelength can also be derived from absorbance measurements using the following relationship:

$$T = 10^{-A(\lambda)} \tag{13-60}$$

Thus, for a perfectly transparent solution $A(\lambda) = 0$, $T = 1$ and for a perfectly opaque solution $A(\lambda) \rightarrow \infty$, $T = 0$. At a UV radiation wavelength of 254 nm, Eq. 13-60 is written as follows:

$$\text{UVT}_{254} = 10^{-A_{254}} \tag{13-61}$$

The term percent transmittance, commonly used in the literature is

$$\text{UVT}_{254,}\% = 10^{-A_{254}} \times 100 \tag{13-62}$$

Typical absorbance and transmittance values for various waters are presented in Table 13-10.

PARTICULATE MATTER

Particulate matter can also interfere with the transmission of UV light. Particulates are an aspect of water quality that can be particularly important where UV disinfection is concerned. Two mechanisms of particular importance are shading and encasement, as shown on Fig. 13-37. Interference of this kind has been studied at great depth for the case of coliform organisms in secondary wastewater effluents, and models have been developed that do an excellent job of characterizing the situation (Loge et al., 2001). The effect of shading can be integrated into models for the absorption of

Table 13-10
Typical absorbance and transmittance values for various waters

Type of Water	UV_{254} Absorbance, AU/CM	Transmittance UVT_{254}, %
Groundwater	0.0706–0.0088	85–98
Surface water, untreated	0.3010–0.0269	50–94
Surface water, after coagulation, flocculation, and sedimentation	0.0969–0.0132	80–97
Surface water, after coagulation, flocculation, sedimentation, and filtration	0.0706–0.0088	85–98
Surface water after microfiltration	0.0706–0.0088	85–98
Surface water after reverse osmosis	0.0458–0.0044	90–99

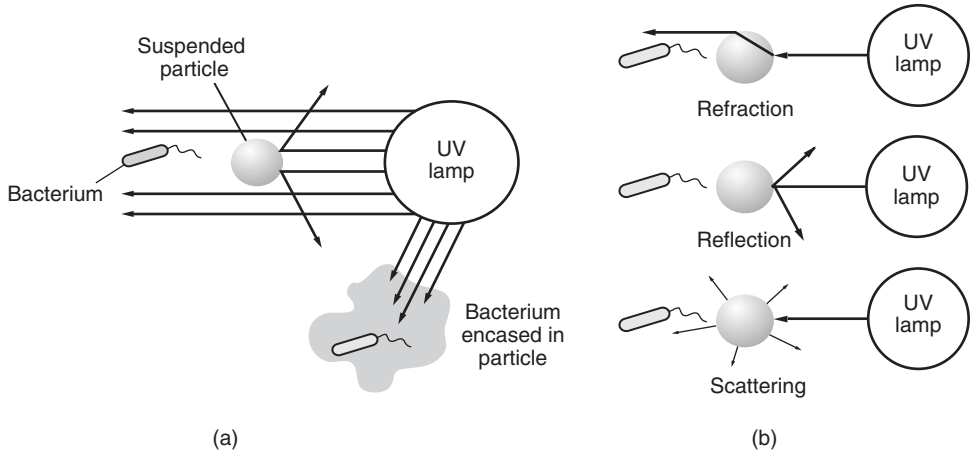

Figure 13-37
Illustration of mechanisms for interference in disinfection by particles: (a) overview of mechanisms for interference and (b) mechanisms of "shading."

light. Beyond that, the number of organisms is dominated by the effect of organisms associated with particles. Particles can ''shade'' target organisms from UV light via three mechanisms: refraction, reflection, and scattering. Where filtration is used, these effects are not very important, but in the treatment of unfiltered water supplies and unfiltered wastewater effluents, these effects can be quite significant.

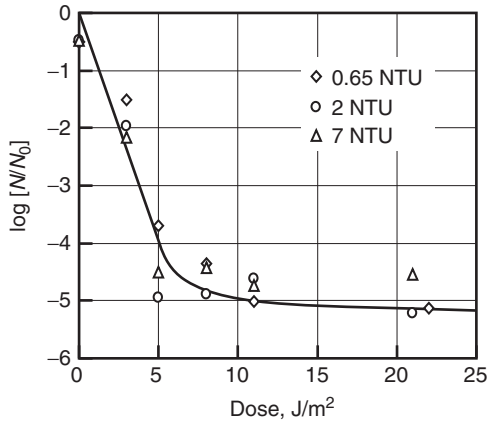

Figure 13-38
Impact of low levels of turbidity on inactivation of *G. muris* with UV radiation. (Adapted from Oppenheimer et al., 2001).

The effects of particle shading are not particularly significant at low turbidities, as illustrated by the work of Oppenheimer et al. (2002), who examined the inactivation of *G. muris* added to waters with turbidities ranging from 0.65 to 7 NTU (see Fig. 13-38). A collimated beam apparatus (see Fig. 13-41) was used to study the inactivation of *G. muris* with waters at three different turbidity levels ranging from 0.65 to 7 NTU. After the UV dose was corrected for apparent absorbance (absorbance including the effects of particle shading), turbidities at these levels seemed to have little significance.

Influence of UV Reactor Hydraulics

Ultraviolet disinfection systems, particularly medium-pressure systems, are characterized by overall residence times that are much shorter than other kinds of disinfection systems. In these systems short circuiting and dispersion are difficult design issues. Designing these systems to achieve good performance requires a greater appreciation of the factors that influence dispersion and short circuiting than is required for the design of most other disinfection systems. The issues are the same as those discussed earlier with contactors for disinfection with chlorine, chloramines, chlorine dioxide, and ozone; however, with UV disinfection contactors, the time spent in transition zones becomes much more important.

In chlorine contactors, for example, inlet conditions can have a big influence on performance. If the contactor is designed with a sufficiently long aspect ratio, good performance can be achieved in spite of nonideal inlet conditions. In many UV reactors, the zones of flow transition can dominate most of the contact time. Also because for the short contact time it is extremely difficult to conduct a meaningful tracer study. The outcome of a tracer study often depends on the UV reactor configuration and precisely where the tracer is introduced. A further complication in UV reactors is that the UV light intensity varies throughout the reactor. As a

result, the UV dose that an organism receives is not only a function of the length of time the organism spends in the reactor and the amount of light being emitted by the UV lamps but also of the specific path the organism takes as it makes its way through the reactor. Thus, the issue is not just the contact time the organism receives, but its cumulative exposure to UV.

Because there are so many complications in determining the performance of a given full-scale UV reactor, it is increasingly common for regulators to require full-scale tests of each reactor design to establish, by actual disinfection measurements, how much of a UV dose a given reactor design will be credited with delivering. The use of a test microorganism to determine the performance of a UV reactor is known as *biodosimetry*. The principal limitation with biodosimetry, in light of the above discussion, is that it cannot be used to measure the dose distribution. Computational fluid dynamics (CFD) modeling and chemical actinometry, employing dyed microspheres, are also being used in conjunction with biodosimetry to assess the performance of UV reactors including the UV dose distribution. CFD modeling and chemical actinometry and are discussed briefly below. Biodosimetry is considered subsequently in greater detail because it is the method now used most commonly for the assessment of UV reactor performance.

COMPUTATIONAL FLUID DYNAMICS

Because of the expense of conducting biodosimetry testing, CFD modeling is now used routinely to simulate mathematically the movement of particles (e.g., microorganisms) through a UV reactor. One of the earliest simulations of the movement of microorganisms through a hypothetical UV reactor was conducted be Chiu et al. 1999. Examples of their model simulation results are illustrated on Fig. 13-39. As shown on Fig. 13-39b, the dose a microorganism depends not only on the intensity of the lamps and the time the organism spends in the reactor but also on the specific path the organism takes through the reactor. The early CFD modeling studies have been extended by a number of researchers, including Lyn and Blatchley (2005) and Ducoste et al. (2005). Because so many different operating conditions can be modeled quickly, CFD modeling is now used essentially by all UV reactor manufacturers to develop new UV reactor configurations. When CFD modeling is coupled with chemical actinometry, and biodosimetry, the performance of UV reactors can be predicted with a greater degree of reliability as compared to the use of a single method.

CHEMICAL ACTINOMETRY

Determination of UV intensity from the measurement of the quantum yield of a chemical reaction induced by UV radiation is known as *chemical actinometry*. The quantum yield of a reaction, as given by Eq. 8-100, is a measure of the number of photolysis reactions (e.g., fluorescence) divided

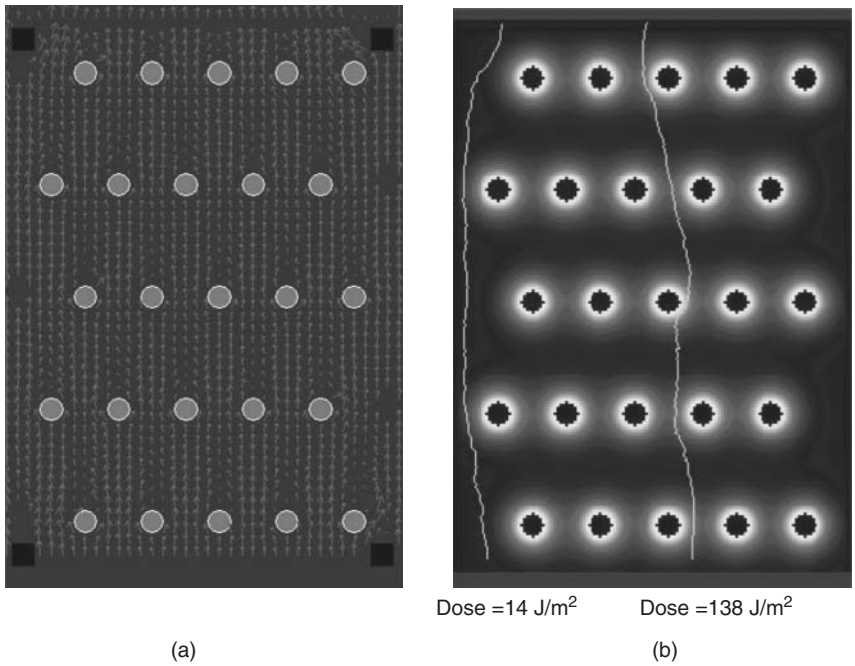

Figure 13-39
Performance of UV reactor: (a) flow pattern and (b) UV dose based on two alternative microorganism travel tracks. The microorganism on the left was exposed to a UV dose of 14 J/m^2 whereas the microorganism on the right was exposed to a UV dose of 138 J/m^2. (Adapted from Chiu et al., 1999.)

by the number of photons adsorbed. Ideally, chemical actinometry involves the use of a chemical that is easy to measure and has a known quantum yield. Microsphere chemical actinometry involves coating, imbedding, or attaching a chemical to polystyrene microspheres (specific gravity 1.05, mean diameter 5.6 μm) that will fluoresce when exposed to UV light (Bohrerova et al., 2005; Blatchley et al., 2008; Shen et al., 2009). If the fluorescence of the individual microsphere particles is measured, the increase in fluoresce intensity can be related to the UV dose received by an individual microsphere. If a sufficient number of microspheres are measured, the UV dose distribution can be assessed. This method has been demonstrated at full scale and the results have been compared with CFD modeling and biodosimetry results (Blatchley et al., 2008; Shen et al., 2009). When all three techniques are used together to evaluate the performance of new UV reactor designs, a high degree of predictability can be achieved.

BIODOSIMETRY

Biodosimetry, as illustrated on Fig. 13-40, involves conducting both bench-scale laboratory and field-scale tests with the same biological test organism. The laboratory study is conducted to establish the relationship between UV dose and the inactivation of a test organism. The field-scale test is conducted at design flow and under conditions designed to represent a conservative

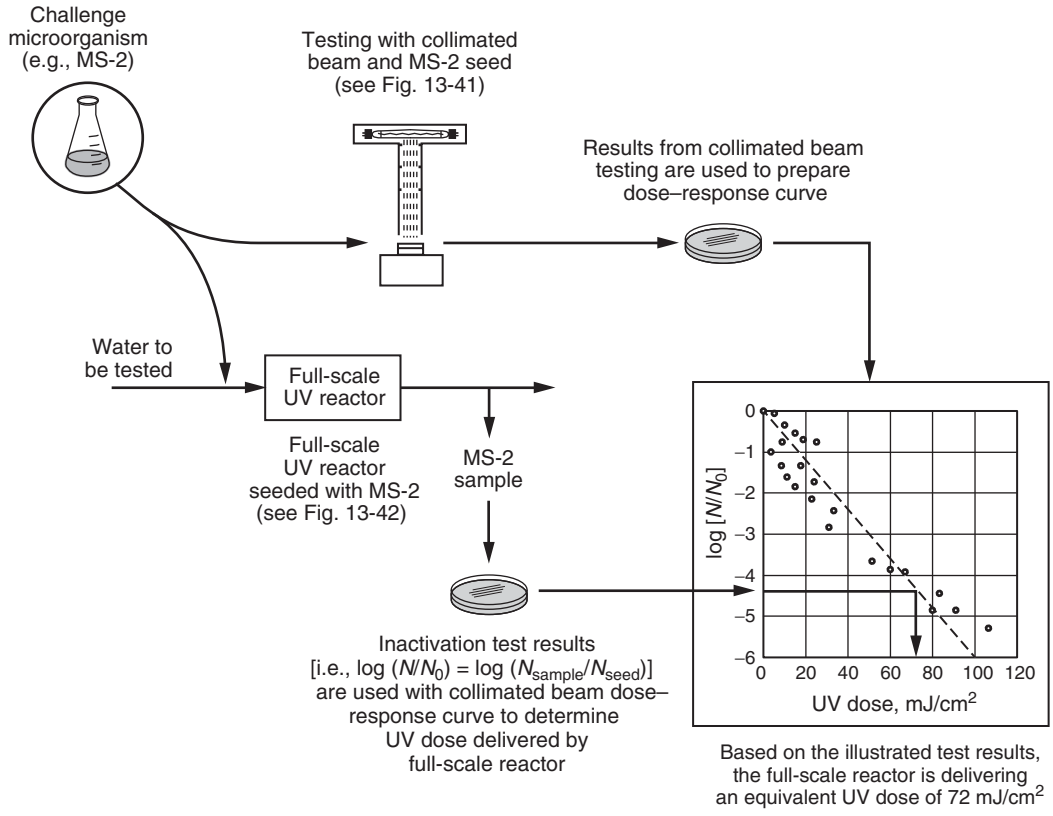

Figure 13-40
Schematic illustration of the application of biodosimetry as used to determine the performance of a full-scale UV reactor.

simulation of full-scale operation. The specifics of the conduct of this test are outlined in the appropriate guidelines (see subsequent section). The disinfection dose that a UV reactor is credited with is determined by the dose that accomplishes the same level of inactivation under laboratory conditions. Biodosimetry is most effective when it is conducted with an organism that shows approximately the same resistance to UV radiation as the target organism. The principal limitation of biodosimetry, as discussed previously is that the test cannot be used to assess the UV dose distribution within the reactor. The elements of biodosimetry are examined in what follows.

Determination of UV Dose Using Collimated Beam

The most common procedure for determining the required UV dose for the inactivation of challenge microorganism involves the exposure of well-mixed water sample in a small batch reactor (i.e., a Petri dish) to collimated beam of UV light of known UV intensity for a specified period of time, as

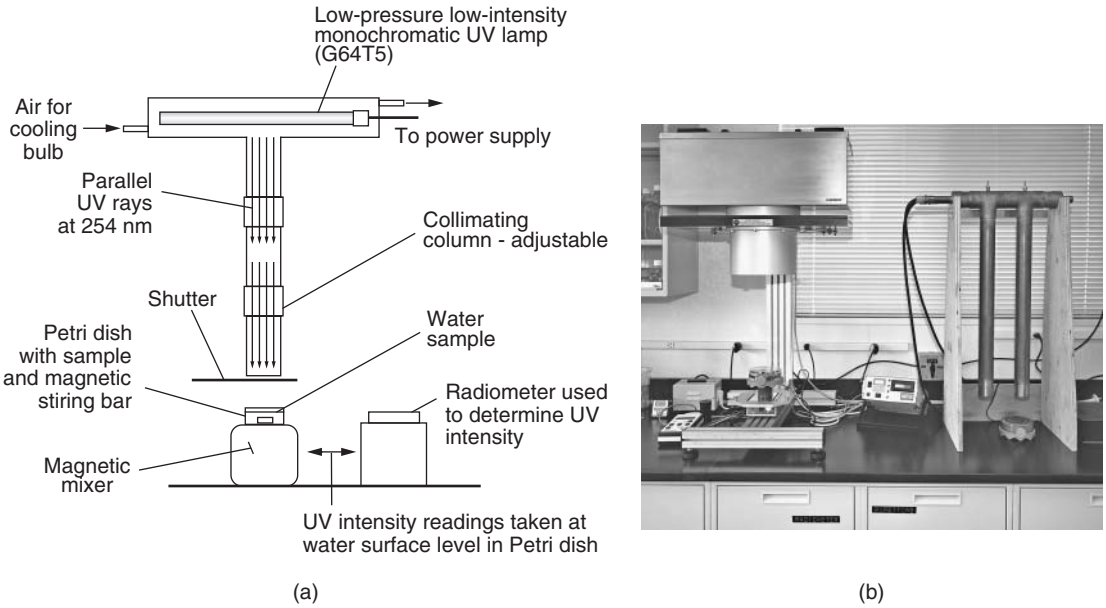

Figure 13-41
Collimated beam devices used to develop dose–response curves for UV disinfection: (a) schematic of the key elements of a collimated beam setup and (b) view of two different types of collimated beam devices. The collimated beam on the left is of European design; the collimated beam on the right is of the type shown in the schematic on the left.

illustrated on Fig. 13-41. Use of a monochromatic low-pressure low-intensity lamp in the collimated beam apparatus allows for accurate characterization of the applied UV intensity. Use of a batch reactor allows for accurate determination of exposure time. The applied UV dose, as defined by Eq. 13-56, can be controlled either by varying the UV intensity or the exposure time. Because the geometry is fixed, the depth-average UV intensity within the Petri dish sample (i.e., the batch reactor) can be computed using the following relationship, which also takes into account other operational variables that may affect the UV dose:

$$D_{CB} = E_s t(1-R)P_f\left[\frac{1-10^{-k_{254}d}}{2.303(k_{254}d)}\right]\left(\frac{L}{L+d}\right) \tag{13-63}$$

$$D_{CB} = E_s t(1-R)P_f\left[\frac{1-e^{-2.303k_{254}d}}{2.303(k_{254}d)}\right]\left(\frac{L}{L+d}\right) \tag{13-64}$$

where D_{CB} = average collimated beam UV dose, mW/cm^2
E_S = incident UV intensity at the center of the surface of the sample, before and after sample exposure, mW/cm^2

t = exposure time, s
R = reflectance at the air–water interface at 254 nm
P_f = Petri dish factor
K_{254} = absorptivity, a.u./cm (base 10)
d = depth of sample, cm
L = distance from lamp centerline to liquid surface, cm

Without the other correction factors, the basic form of Eqs. 13-63 and 13-64 is the same as that derived in Example 2-2 in Chap. 2. The term (1 – R) on the right-hand side accounts for the reflectance at the air–water interface. The value of R is typically about 2.5 percent. The term P_f accounts for the fact that the UV intensity may not be uniform over the entire area of the Petri dish. The value of P_f is typically greater than 0.9. The term within the brackets is the depth averaged UV intensity within the Petri dish and is based on the Beer–Lambert law. The final term is a correction factor for the height of the UV light source above the sample. The application of Eqs. 13-63 illustrated in Example 13-11. The uncertainty of the computed UV dose at a given UV intensity can be estimated using the sum of the variances as given by either of the following expressions:

Maximum uncertainty:

$$U_D = \sum_{n=1}^{N} \left| U_{V_n} \frac{\partial D}{\partial V_n} \right| \tag{13-65}$$

Best estimate of uncertainty

$$U_D = \left[\sum_{n=1}^{N} \left(U_{V_n} \frac{\partial D}{\partial V_n} \right)^2 \right]^{1/2} \tag{13-66}$$

where U_D = uncertainty of UV dose value, %
U_{Vn} = uncertainty or error in variable n
V_n = variable n
$\partial D/\partial V_n$ = partial derivative of the expression with respect to the variable V_n
N = number of variables

The maximum estimate of uncertainty as given by Eq. 13-65 represents the condition where every error will be a maximum value. The best estimate of uncertainty, as given by Eq. 13-66, is used most commonly because it is unlikely that every error will be a maximum at the same time and the fact that some errors may cancel each other. The application of Eq. 13-66 is illustrated in Example 13-11.

Example 13-11 Estimation of UV dose using collimated beam

A collimated beam, with the following characteristics, is to be used for biodosimetry testing. Using these data estimate the average UV dose delivered to the sample and best estimate of the uncertainty associated with the measurement.

$E_S = 15 \pm 0.75$ mW/cm^2 (accuracy of meter ±5%), $t = 10 \pm 0.2$ s, $R = 0.025$ (assumed to be the correct value), $P_f = 0.94 \pm 0.02$, $kA_{254} = 0.065 \pm 0.005$ cm^{-1}, d $= 1 \pm 0.05$ cm, L $= 40 \pm 0.5$ cm.

Solution

1. Using Eq. 13-63 estimate the delivered dose:

$$D_{CB} = E_s t(1 - R)P_f \left[\frac{1 - 10^{-k_{254}d}}{2.303(k_{254}d)}\right]\left(\frac{L}{L + d}\right)$$

$$D_{CB} = (15) \times (10)(1 - 0.025)(0.94)\left[\frac{1 - 10^{-(0.065\times 1)}}{(2.303)(0.065) \times (1)}\right]\left(\frac{40}{40 + 1}\right)$$

$$D_{CB} = (150)(0.975)(0.94)(0.928)(0.976) = 124.6 \text{ mJ/cm}^2$$

2. Determine the best estimate of uncertainty for the computed UV dose. The uncertainty of the computed dose can be estimated using Eq. 13-66. The procedure is illustrated for one of the variables and summarized for the remaining variables.
   a. Consider the variability in the measured time, t. The partial derivative of the expression used in step 1 with respect to t is

$$U_t = U_{t_e}\frac{\partial D}{\partial t_n} = t_e E_S(1 - R)P_f \left[\frac{1 - 10^{-k_{254}d}}{2.303(k_{254}d)}\right]\left(\frac{L}{L + d}\right)$$

   where t_e is the uncertainity of the measured value of (0.25). Substituting known values and solving for u_t the uncertainity with respect to t, yields

$$U_t = (0.2)(15)(1 - 0.025)(0.94)\left[\frac{1 - 10^{-(0.065)\times 1}}{(2.303)(0.065) \times (1)}\right]\left(\frac{40}{40 + 1}\right)$$

$$U_t = 2.49 \text{ mJ/cm}^2$$

   Percent $= 100\ U_t/D = (100) \times (2.49)/124.6 = 2.0\%$

b. Similarly for the remaining variables, the corresponding uncertainty values are given below:

$$U_{ES} = 6.23 \text{ mJ/cm}^2 \text{ and } 5.0\%$$
$$U_{Pf} = 2.65 \text{ mJ/cm}^2 \text{ and } 2.13\%$$
$$U_a = -0.7 \text{ mJ/cm}^2 \text{ and } -0.56\%$$
$$U_d = -0.61 \text{ mJ/cm}^2 \text{ and } -0.49\%$$
$$U_L = 0.038 \text{ mJ/cm}^2 \text{ and } 0.03\%$$

c. The best estimate of uncertainty using Eq. 13-66 is

$$U_D = \left[(2.49)^2 + (6.23)^2 + (2.65)^2 + (-0.7)^2 + (-0.61)^2 + (0.038)^2\right]^{1/2}$$
$$U_D = 7.27 \text{ mJ/cm}^2$$
$$\text{Percent} = (100) \times (7.27)/124.6 = 5.84\%$$

3. Based on the above uncertainty computation the most likely UV dose is 124.6 ± 7.27 mJ/cm^2

Comment

Thus, the most conservative estimate of the UV dose that can be delivered consistently is 117.3 mJ/cm^2 (124.6 – 7.27). If a similar analysis is carried for each of the UV doses evaluated, a curve of the most likely UV dose can be drawn as a function of the microorganism inactivation achieved with each UV dose, as discussed below.

DEVELOPMENT OF UV DOSE RESPONSE CURVE USING COLLIMATED BEAM

To assess the degree of inactivation that can be achieved at a given UV dose, the concentration of microorganism is determined before and after exposure in a collimate beam apparatus (see Fig. 13-41). Microorganism inactivation is measured using an most probable number (MPN) procedure for bacteria, a plaque count procedure for viruses, or an animal infectivity procedure for protozoa. To verify the accuracy of the laboratory collimated beam dose–response test data, the collimated beam test must be repeated to obtain statistical significance. To be assured that stock solution of the challenge microorganisms is monodispersed, the laboratory inactivation test data must fall within an accepted set of quality control limits. Quality control limits proposed by the National Water Research Institute (NWRI, 2003) and the U.S. EPA (2000) for bacteriophage MS2 spores are as follows:

NWRI:

$$\text{Upper bound: } -\log_{10}(N/N_0) = 0.040 \times D + 0.64 \quad (13\text{-}67)$$
$$\text{Lower bound: } -\log_{10}(N/N_0) = 0.033 \times D + 0.20 \quad (13\text{-}68)$$

U.S. EPA:

$$\text{Upper bound: } -\log_{10}(N/N_0) = -9.6 \times 10^{-5} \times D^2 + 4.5 \times 10^{-2} \times D \quad (13\text{-}69)$$

$$\text{Lower bound: } -\log_{10}(N/N_0) = -1.4 \times 10^{-4} \times D^2 + 7.6 \times 10^{-2} \times D \quad (13\text{-}70)$$

where $D = \text{UV dose, mJ/cm}^2$

As illustrated in Example 13-12, the bounds proposed by the U.S. EPA are more lenient as compared to those used by NWRI. Similar bounding curves have been proposed for *B. subtilus* (U.S. EPA, 2006; AWWARF and NYSERDA, 2007). The NWRI guidelines are used for water reuse applications in California.

Example 13-12 Develop dose response curve for bacteriophage MS2 using a collimated beam.

Bacteriophage MS2 (ATCC 15597) is to be used to validate the performance of a full-scale UV reactor. The following collimated beam test results were obtained for MS2 in a phosphate buffer solution with a UVT_{254} in the range from 95 to 99 percent (Data courtesy B. Cooper, BioVir Labs). Verify that the laboratory test results are acceptable and develop the dose–response curve for use in the full-scale validation. Also, estimate the UV dose required to achieve 2 log of inactivation.

Dose, mJ/cm^2	Surviving Concentration, phage/mL	Log Survival, Log (phage/mL)	Log Inactivation
0.	5.00×10^6	6.70	
20	4.00×10^5	5.60	1.10[a]
40	4.30×10^4	4.63	2.07
60	6.31×10^3	3.80	2.9
80	8.70×10^2	2.94	3.76
100	1.20×10^2	2.08	4.62

[a]Sample calculation: log inactivation = 6.70 – 5.60 = 1.10.

Solution

1. Plot the collimated beam test results and compare to the quality control range expressions provided in the NWRI (Eqs. 13-67 and 13-68) and (Eqs. 13-69 and 13-70) U.S. EPA UV Guidelines. The results are plotted in the figure given below.

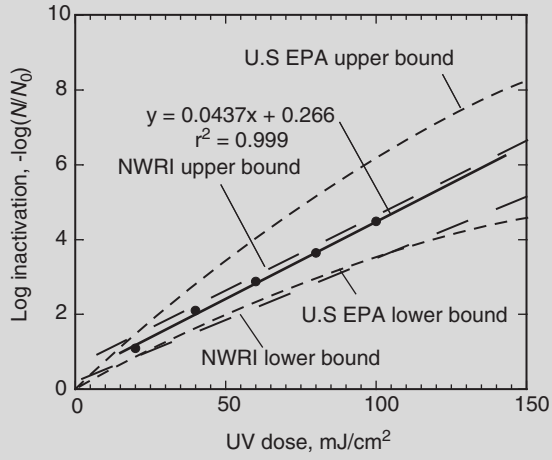

2. As shown in the above plot, all of the data points fall within the acceptable range.
3. Dose–response curve for bacteriophage MS2. The slope of the line, based on a linear fit, is

$$y = 0.0437 \times +0.266$$

which corresponds to

$$-\log(N/N_0) = 0.266 + (0.0437\ \text{cm}^2/\text{mJ})(\text{UV dose, mJ/cm}^2)$$

4. UV dose required for 2 log of inactivation of MS2. Using the equation from step 3, the required UV dose is

$$\text{UVdose} = \frac{-\log(N/N_0) - 0.266}{0.0437\ \text{cm}^2/\text{mJ}} = \frac{2 - 0.266}{0.0437\ \text{cm}^2/\text{mJ}}$$

$$= 39.7\ \text{mJ/cm}^2$$

Comment

As shown in the above plot, there is a considerable difference in the upper quality control limit between the NWRI and the U.S. EPA UV guidelines (U.S. EPA, 2006). Also note that the U.S. EPA guidelines are curvilinear, whereas the NWRI guidelines are linear. Clearly, the NWRI guidelines are more restrictive.

UV DOSE REQUIRED FOR INACTIVATION OF *CRYPTOSPORIDIUM*, *GIARDIA*, AND VIRUSES

Using the biodosimetry approach, outlined above, the U.S. EPA has developed minimum UV dose requirements for various levels of inactivation for *Cryptosporidium*, *Giardia*, and virus (U.S. EPA, 2006). Adenovirus was utilized as the test virus because it is considered the most difficult to inactivate by UV radiation. It is important to note that the UV values reported in Table 13-11 are based on tests conducted using the specific organisms and take into account the uncertainty associated with dose–response relationships. Other sources of uncertainty associated with the full-scale installation such as the design of the UV reactors, the system hydraulics, the measured UV intensity, and monitoring approach are not included but are considered during the validation testing of UV reactors.

When a surrogate microorganism, such as MS2, is used, the values reported in Table 13-11 must be adjusted to reflect the differences in resistance between the target organism and the surrogate (see discussion under Validation of UV Reactors). The ideal surrogate should be

- ❑ Nonpathogenic
- ❑ Easy to culture at high titers (on the order of 10^{11} to 10^{12} org./mL)
- ❑ Stable over long periods
- ❑ Easy to enumerate

In the United States, the organism of choice is MS2 bacteriophage, whereas in Europe *B. subtilis* is the microorganism of choice. Other organisms such as the T1 and Q beta phage that more closely mirror the response of *Cryptosporidium* are also under investigation. Also, it is important to note that the host organism used for the culture of MS2 or other phage organisms must be specified if comparable results are to be obtained. Additional information on the types of microorganisms that have been examined may

Table 13-11
UV dose required for inactivation of *Cryptosporidium, Giardia*, and virus

Log Inactivationxe Credit	UV Dose (mj/cm^2)		
	Cryptosporidium	Giardia	Virus[a]
0.5	1.6	1.5	39
1.00	2.5	2.1	58
1.5	3.9	3.0	79
2.0	5.8	5.2	100
2.5	8.5	7.7	121
3.0	12	11	143
3.5	15	15	163
4.0	22	22	186

[a]UV dose for virus based on adenovirus.
Source: Adapted from *Fed. Reg.*, Vol. 68, No. 154, August 11, 2003.

be found in an extensive report prepared by AWWARF and NYSERDA (2007).

Validation Testing of UV Reactors

At the present time there are a number of UV manufacturers that produce UV reactors suitable for the inactivation of microorganisms. Unfortunately, the performance of the various UV reactors varies from unit to unit and manufacturer to manufacturer. Because of the interest in utilizing UV by the water industry to obtain partial inactivation credit for *Cryptosporidium, Giardia,* and viruses (in some cases) and the need to protect public health, the United States and many other countries have established regulations and guidelines for the use of UV radiation for water and wastewater treatment. The regulations typically involve validation testing of the UV reactors to verify minimum levels of performance (i.e., specifically the delivered UV dose) under varying the conditions of operation including:

1. High and low water transmittance
2. Varying flow rate
3. Varying power levels
4. Simulated lamp aging

Testing is also used to determine a set of operating conditions that can be monitored on a continuing basis to be assured that the UV dose needed for the inactivation credit is delivered at all times. Operationally, the method of controlling the UV dose, as discussed previously, is of critical importance. A number of prevalidated UV reactors, varying in size from 40 L/min (10 gal/min) to 225 ML/d (60 Mgal/d), are available from a number of manufacturers.

In general, validation testing must be done and certified by an independent third party. Typically, as illustrated in Fig. 13-40, validation testing involves:

1. Generation of a UV dose response curve for the challenge microorganism.
2. Determination of the inactivation achieved with the full-scale reactor, at the actual installation location or at an approved test site (see Fig. 13-42), using the challenge microorganism.
3. Determination of the UV dose corresponding to the measured inactivation achieved with the full-scale reactor using the dose–response curve developed with the collimated beam. The computed UV dose delivered by the reactor is known as the reduced equivalent dose (RED).
4. Determination of a validated UV dose by dividing the RED value by a validation factor VF. The VF is used to account for the fact that a challenge microorganism was used instead of the target organism and for the experimental uncertainty associated with the testing program.

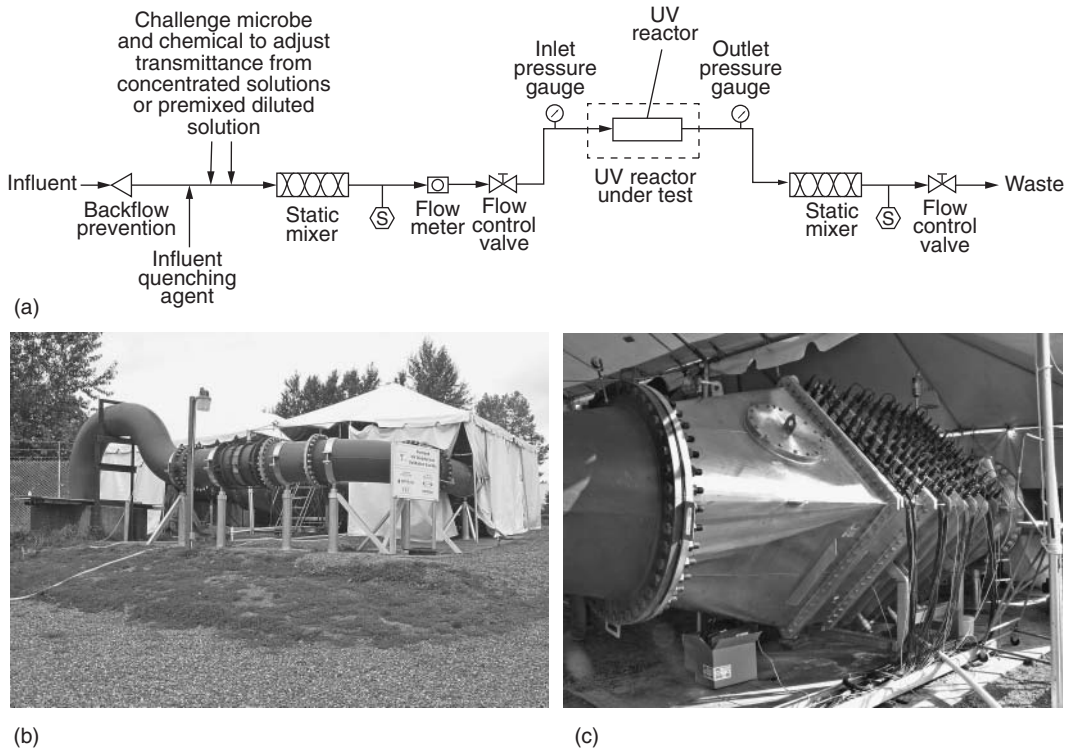

Figure 13-42
Experimental setup for validation of UV reactors under controlled conditions: (a) schematic of setup requirements for testing full-scale UV reactor, (b) view of test facility at Portland, OR, and (3) large UV reactor instrumented for UV dose validation by dosimetry.

For most drinking water applications the target RED value is 40 mJ/cm^2. The principal validation guidelines now used for the validation of various UV reactors are summarized in Table 13-12. Validation test centers in the United States are located in Johnstown, New Yark, and Portland, Oregen. While the approach of using a prevalidated UV reactor is favored by most Public Water Systems because of simplicity, it tends to be more conservative as compared to the onsite validation.

U.S. EPA UV Disinfection Guidance Manual Validation Process

As discussed previously in Chap. 4, the U.S. EPA developed the Long Term 2 Enhanced Surface Water Treatment Rule (LT2) to protect public health by further reducing the microbial contamination of drinking water. Based on the source water *Cryptosporidium* concentrations and current treatment practices, additional treatment may be required for some public water systems (PWS). Public water systems utilizing surface that must provide additional treatment under the LT2 rule can utilize UV radiation as one of the many different treatment options to meet the treatment requirements.

Table 13-12
UV reactor validation protocols used in the United Stated and Europe

Test Protocol	Discussion
German DVGW W294-3 (GAGW, 2003)	Use of reference sensor with multiple set points and a minimum number of monitoring ports. Although the protocol has a 10-year history, many feel the protocol is too prescriptive. UV validation based on a dose of 40 mJ/cm^2. Test results guarantee a UV dose of 40 mJ/cm^2 or more.
Austrian ONORM M5873-1 Low pressure, and M5873-2 Medium pressure (Onorm, 2001, 2003)	Use of reference sensor with multiple set points. UV validation based on a dose of 40 mJ/cm^2. Test results guarantee a UV dose of 40 mJ/cm^2 or more.
U.S. EPA UV Disinfection Guidance Manual (UVDGM) (U.S. EPA, 2006)	Greater flexibility as compared to German and Austrian guidelines, but more complex to understand. With proper testing, potential to reduce cost. Used for validation of community scale UV systems
ANSI/NSF Standard 55 (ANSI/NSF, 2004)	Unit must produce UV dose of 40 mJ/cm^2 at the alarm set point. A UV sensor to measure UV intensity continuously at 254 nm, a flow control device, and other related appurtenances are required. The challenge microorganism is MS2. Protocol is applied to residential point of use devices primarily.
National Water Research Institute (NWRI, 2003)	Developed primarily for wastewater reuse applications. Discussion of water applications is limited

Recognizing the desire of PWSs to use UV radiation to meet drinking water disinfection standards established under the Safe Drinking Water Act (SDWA), the U.S. EPA developed the UV Disinfection Guidance Manual (UVDGM) (U.S. EPA, 2006) to (1) delineate the design, operation, and maintenance needs for UV disinfection systems, which are quite different from those traditionally used in drinking water applications, (2) clarify the requirements for UV disinfection in the LT2 rule, and (3) familiarize states and PWSs with these distinctions, as well as associated regulatory requirements contained in the LT2 rules.

Two validation protocols are set forth in the UVDGM, the details of which are beyond the scope of this book. The two approaches are as follows:

1. PWS purchases a prevalidated UV reactor(s).

a. If the UV reactor(s) are installed in accordance with specified hydraulic constraints, onsite validation is not necessary.

b. Onsite validation may be necessary if the full UVT range was not tested in the offsite validation, if the hydraulic constraints cannot be met, and/or if more information is needed to match current operation conditions.

2. PWS purchases a UV reactor that has not been prevalidated.

a. In this case, the PWS can develop a plan for offsite validation and has the flexibility of using any hydraulic installation option.

b. PWS develops a validation plan and conducts an onsite validation, as outlined in the UVDGM.

Problems and Discussion Topics

13-1 Based on your reading of this chapter, provide brief responses to the following questions:

a. In waterworks practice, what two activities are described with the term disinfection?

b. What were the two principal means of controlling waterborne disease for the first five decades after John Snow did his work with cholera in the 1850s?

c. Why did chlorination encounter difficulties from the start?

d. What was the main discovery that caused concern about disinfection by-products?

e. What organism caused more stringent standards to be established for pathogen reduction?

f. What other organism was found to be so chlorine resistant that it began to raise questions about inactivation as a strategy for pathogen reduction?

13-2 Based on your reading of this chapter, discuss briefly two different ways in which the effect of concentration on the disinfection process can be handled. What are the advantages and disadvantages of each approach?

13-3 Describe how Watson proposed that the effect of concentration be handled in modeling disinfection.

13-4 Given below are some data from Wattie and Butterfield (1944) on the inactivation of *E. coli* with free chlorine at 2°C and pH 8. Fit the data to the Chick–Watson, Rennecker–Mariñas, and Collins–Selleck models and comment on the results.

C, mg/L	T, min	$\log(N/N_0)$
0.05	1.0	−0.02
0.05	3.0	−0.09
0.05	4.9	−0.15
0.05	9.6	−0.68
0.05	18	−2.52
0.07	1.0	−0.06
0.07	3.0	−0.22
0.07	4.9	−0.58
0.07	9.7	−2.28
0.14	1.0	−0.24
0.14	2.8	−0.95
0.14	4.5	−2.15

13-5 Fit the Rennecker–Mariñas model to the following disinfection data and determine the coefficient of leathality and the lag coefficient b:

C, mg/L	T, min	$\log(N/N_0)$
1.0	5	0.0
1.1	10	0.0
1.05	25	−1.0
1.03	30	−1.5
1.05	35	−2.1
2.05	20	−2.55
2.0	23	−3.1
2.03	25	−3.45
5.02	11	−4.1

13-6 Using data from Table 13-3, estimate the Ct required for a 3 log reduction of *C. parvum* and *B. subtilus* using combined chlorine and chlorine dioxide. Is either one practical? What about UV?

13-7 From an examination of Fig. 13-5, which organism varies the least in Ct or It between one disinfectant and the next? Which varies the most? Which disinfectant shows the smallest range of Ct or It values required for all organisms?

13-8 A treatment plant has been designed to achieve 99 percent inactivation of *C. parvum* using ozonation. The engineer used data on ozonation of *C. parvum* at 20°C for the design, but the plant operates in a northern climate and current estimates are that the low water temperature in some winters will be 0.5°C. Estimate how much inactivation the plant will actually achieve when the water is at that temperature. You may assume that the inactivation of *C.*

parvum follows the Chick–Watson relationship (Eq. 13-4). Use the E_a value of Rennecker et al. (1999) as reported in Table 13-4.

13-9 Use the Segragated Flow Model (SFM) to redo the dispersion estimate in Example 13-4 two times. In the first estimate, assume the contactor is operated so that the product $C\tau$ is adequate to accomplish an 8 log reduction in the target organism, and in the second estimate assume the contactor is operated so that the product $C\tau$ is adequate to accomplish a 0.5 log reduction in the target. Discuss the implications of the results.

13-10 A treatment plant with a design capacity of 80 ML/d has a pipeline between the plant and the clearwell that the operators would like to use as a contactor for disinfection. The pipeline was built with future expansions in mind and is 4 m in diameter and 80 m in length. What would be the dispersion in this pipeline when the plant is operating at design flow? Assume the Darcy–Weisbach friction factor is 0.02.

13-11 A water treatment plant with a capacity of 80 ML/d is being constructed. The plant includes a baffled chlorine contact chamber that has a length-to-width ratio of 40 : 1. Estimate both the dispersion and the t_{10}/τ ratio for the chamber. Assume the coefficient of nonideality for the design, C_i, is 5. Other than baffling, what sort of provisions might have been made to improve the basin's performance? What might the design engineer have done to confirm this performance before going to construction?

13-12 Given below are data on the decay of ozone gathered by Gurol and Singer (1982). Fit the data to the first-order decay model and to the parallel first-order decay model and discuss.

T, min	*C*, mg/L
0.0	8.15
0.3	6.95
0.6	5.80
1.0	5.05
1.4	4.95
1.6	4.07
2.0	3.95
2.4	3.60

13-13 A treatment plant doing color removal by coagulation is using combined chlorine as a means of residual control. There have been complaints about chlorinous odors. The plant is operating with a chlorine-to-ammonia molar ratio of 5 : 1 and at a pH of 7. What precautions might be taken to reduce the odor complaints?

13-14 A water plant has influent ammonia levels of about 0.5 mg/L as N. The utility plans on installing a basin to remove the ammonia by breakpoint chlorination prior to using free chlorine for disinfection. What should the hydraulic detention time of that basin be to ensure that the ammonia is completely removed? The water is highly buffered at a pH of approximately 7.

13-15 What can the second plant in Example 13-7 do to improve performance of its residual control system?

13-16 A utility in south Florida has converted its plant to sodium hypochlorite because of community complaints about the safety of using chlorine gas. The hypochlorite is delivered at a concentration of 7 percent by weight and stored in a new fiberglass tank that was installed behind the maintenance building. The plant delivers an average of 8 ML/d of water with a chlorine dose of 4 mg/L. The storage tank is just large enough for one delivery, about 40,000 L. Recently, the local health department sampled the system and found high levels of chlorate ion. Also, periodically, especially during the summer, the utility finds that the strength of its bleach has dropped substantially. What precautions might be considered to improve the situation?

13-17 A gas chlorine system is being designed for residual control in the discharge line of a water treatment plant. The maximum and minimum design flows are 19 and 1.90 ML/d, respectively. The treated water discharge pipe is 2600 mm in diameter. The velocity of the chlorine gas in the vacuum line from the chlorinator to the injectors is 2 m/s, and the line is 20 m (66 ft) in length. The pipe from the injector to the application point is 152 m long, and the design velocity in the pipe is 1.5 m/s. The chlorine application point and the residual sampling point on the discharge line are 150 m apart. The sample runs for 100 m in a 6.35-mm sample line. The sample pump is designed for a flow of 200 mL/min. Sample analysis takes 20 s, and signal response times are assumed to be instantaneous. Prepare a sketch of the control loop similar to Fig. 13-13. Prepare a table analyzing the loop time and comment on the strengths and weaknesses of this design.

13-18 A continuous-flow pilot ozonation system was used to ozonate surface water at several different doses. The results are tabulated below. Assuming the pilot system successfully emulated the ozone dosing stage of the full-scale design, plot a curve of the ozone residual versus ozone dose and estimate the ozone demand and the ozone dose required to achieve a residual of 1 mg/L entering the disinfection section downstream.

Ozone Applied, mg/L	Residual, mg/L
1.30	0.04
2.45	0.28
2.74	0.43
3.05	0.56
3.39	0.56
4.01	0.90
4.49	1.12
6.01	1.50
6.05	1.74

13-19 The data below by Hermanowicz et al. (1999) show the decay of ozone residual in treated water from the upper Hackensack River. Estimate the *Ct* that can be achieved after 20 min of contact time.

T, min	*C*, mg/L	*T*, min	*C*, mg/L
0	0.97	12	0.155
1	1.02	13	0.135
2	0.85	14	0.12
3	0.71	15	0.115
4	0.58	16	0.11
5	0.49	17	0.105
6	0.41	18	0.1
7	0.35	19	0.1
8	0.295	20	0.095
9	0.25	21	0.09
10	0.22	22	0.09
11	0.185		

13-20 A full-scale UV reactor was tested with MS 2 bacteriophage and was rated to have an effective UV dose of 25 mJ/cm^2. Using an analogy to the thought experiment shown on Fig. 13-1, how much flow could have been bypassed around the reactor during the test without changing $\log(N/N_0)$ for MS 2 by more than 10 percent? Assuming no short circuiting, how many logs of reduction should the reactor achieve with *C. parvum*? How many logs reduction in *C. parvum* would the reactor achieve if the bypass discussed earlier were to occur? Discuss the significance of these results.

13-21 Given the following UV disinfection data (courtesy B. Cooper, BoiVir Labs) determine for water sample number (to be selected by instructor) whether the results are consistent with the NWRI and U.S. EPA quality control limits and the expected log inactivation as a UV dose of 50 mJ/cm^2.

UV dose, mJ/cm^2	Titer, Pfu/mL Water sample number 1	2	3	4	5
0.00	5.30E+05	1.60E+05	2.80E+05	5.00E+06	2.60E+06
20.00	3.10E+04	1.30E+04	2.30E+04	4.00E+05	1.50E+05
40.00	5.30E+03	1.70E+03	1.90E+03	4.30E+04	1.70E+04
80.00	1.20E+02	6.00E+01	6.70E+01	8.70E+02	3.60E+02
100.00	2.20E+01	1.40E+01	1.30E+01	1.20E+02	7.00E+01

13-22 In Example 13-12, a linear relationship was used to define the UV dose response for MS2. What difference will it make with respect to the required UV dose if the linear relationship is replaced with a polynomial of the following form.

$$\log(N/N_0) = a + b(\text{UV dose}) + \text{c}(\text{UV dose})^2$$

where a, b, and c are empirical constants.

13-23 Verify the results given in Example 13-11 for the error of the following variables are correct.

$$U_{\text{ES}} = 6.23 \text{ mJ/cm}^2 \text{ and } 5.0\%$$

$$U_{\text{Pf}} = 2.65 \text{ mJ/cm}^2 \text{ and } 2.13\%$$

$$U_a = -0.7 \text{ mJ/cm}^2 \text{ and } -0.56\%$$

$$U_d = -0.61 \text{ mJ/cm}^2 \text{ and } -0.49\%$$

$$U_L = 0.038 \text{ mJ/cm}^2 \text{ and } 0.03\%$$

13-24 Review the current literature on the use of light emitting diode (LED) UV lamps for disinfection and prepare a brief assessment of their feasibility. A minimum of three articles, dating no further back than the year 2000, should be cited in your assessment.

References

ANSI/NSF 2004. Standard Number 55, *Ultraviolet Microbiological Water Treatment Systems* American National Standards Institute/National Sanitation Foundation, Ann Arbor, MI.

AWWA Disinfection Systems Committee (2008) ''Committee Report: Disinfection Survey, Part 1—Recent Changes, Current Practices, and Water Quality,'' *J. AWWA*, **100**, 10, 76–90.

AwwaRF (1991) *Ozone in Water Treatment: Application and Engineering*, Cooperative Research Report, B. Langlais, D. Reckhow, and D. Brink (eds.), American Water Works Association, Research Foundation, Denver, CO, and Lewis Publishers, Chelsea, MI.

AwwaRF and NYSERDA (2007) *Optimizing UV Disinfection*, American Water Works Association. Research Foundation and New York State Energy Research and Development Authority, Denver, CO,

Baker, M. (1948) *The Quest for Pure Water, Vol. I*, 2nd ed., American Water Works Association, Denver, CO.

Bellamy, W., Haas, C., and Finch, G. (1998) *Integrated Disinfection Design Framework*, American Waterworks Research Foundation, Denver, CO.

Bellar, T. A., and Lichtenberg, J. J. (1974) ''Determining Volatile Organics at Microgram-per-Litre Levels by Gas Chromatography,'' *J. AWWA*, **66**, 12, 739–744.

Blatchley, E. R., Shen, C., Scheible, O.K., Robinson, J.P., Ragheb, K., Bergstrom, D.E., and Rokjer, D. (2008) ''Validation of Large-Scale, Monochromatic UV Disinfection Systems for Drinking Water using Dyed Microspheres,'' *Water Res.*, **42**, 3, 677–688.

Bohrerova, Z., Bohrer, G., Mohanraj, S., Ducoste, J., and Linden, K.G. (2005) ''Experimental Measurements of Fluence Distribution in a UV Reactor Using Fluorescent Dyed Microspheres,'' *Environ. Sci. Technol.*, **29**, 22, 8925–8930.

Bolyard, M., Fair, P., and Hautman, D. (1992) ''Occurrence of Chlorate in Hypochlorite Solutions Used for Drinking Water Disinfection,'' *Environ. Sci. Tech.*, **26**, 8, 1663–1665.

Bolyard, M., Fair, P., and Hautman, P. (1993) ''Sources of Chlorate Ion in US Drinking Water,'' *J. AWWA*, **85**, 9, 81–88.

Brazis, A., Leslie, J., Kabler, P., and Woodward, R. (1958) ''The Inactivation of Spores of *Bacillus globiglii* and *Bacillus anthracis* by Free Available Chlorine'', *Public Health Reports*, **6**, 338–342.

Bull, R., Gerba, R., and Trussell, R. (1990) ''Evaluation of Health Risks Associated with Disinfection,'' *Crit. Rev. Environ. Control*, **20**, 2, 77–114.

Butterfield, C., and Wattie, E. (1946) ''Influence of pH and Temperature on the Survival of Coliforms and Enteric Pathogens When Exposed to Chloramine,'' *Public Health Reports*, **61**, 6, 157–193.

Butterfield, C., Wattie, E., Megregian, S., and Chambers, C. (1943). ''Influence of pH and Temperature on the Survival of Coliforms and Enteric Pathogens When Exposed to Free Chlorine,'' *Public Health Reports*, **58**, 51, 1837–1866.

Buxton, G., and Subhani, M. (1971) ''Radiation Chemistry and Photochemistry of Oxychlorine Ions,'' *Faraday Trans.*, **68**, 5, 958–971.

Cal DHS (1999) *Proposed Regulations: Water Recycling Criteria*, California Department of Health Services, Drinking Water Technical Programs Branch, Sacramento, CA.

Cal DHS (2002) *Drinking Water Action Levels: Contaminants of Current Interest*, California Department of Health Services, Sacramento, CA; also available at http://www.dhs.ca.gov/ps/ddwem/chemicals/AL/actionlevels.htm.

Chick, H. (1908) ''An Investigation of the Laws of Disinfection,'' *J. Hygiene*, **8**, 92–158.

Chiu, K., Lyn, D., Savoye, P., and Blatchley, E. (1999) ''Integrated UV Disinfection Model Based on Particle Tracking,'' *J. Environ. Engr., ASCE*, **125**, 1, 7–15.

Collins, H., and Selleck, R. (1971) ''Problems in Obtaining Adequate Sewage Disinfection,'' *JSAE, ASCE*, SA5, **97**, 10, 549–562.

Cooper, R., Salveson, A., Sakaji, R., Tchobanoglous, G., Requa, D., and Whitley, R. (2001) Comparison of the Resistance of MS-2 and Poliovirus to UV and Chlorine Disinfection, paper presented at the Proceedings WateReuse 2000, Napa Valley, CA, Fountain Valley, CA.

Corona-Vasquez, B., Rennecker, J., Driedger, A., and Mariñas, B. (2002) ''Sequential Inactivation of *Cryptosporidium parvum* Oocysts with Chlorine Dioxide Followed by Free Chlorine or Monochloramine,'' *Water Res.*, **36**, 1, 178–188.

Craik, S., Weldon, D., Finch, G., Bolton, J., and Belosevic, M. (2001) ''Inactivation of *Cryptosporidium parvum* Oocysts Using Medium Pressure and Low Pressure Ultraviolet Light,'' *Water Res.*, **35**, 6, 1387–1398.

Crozes, G., Hagstrom, J., Clark, M., Ducoste, J., and Burns, C. (1999) *Improving Clearwell Design for Ct Compliance*, American Water Works Association Research Foundation, Denver, CO.

Driedger, A., Rennecker, J., and Mariñas, B. (2000) ''Sequential Inactivation of *Cryptosporidium parvum* Oocysts with Ozone and Free Chlorine,'' *Water Res.*, **34**, 14, 3591–3597.

Driedger, A., Rennecker, J., and Mariñas, B. (2001) ''Inactivation of *Cryptosporidium parvum* Oocysts with Ozone and Monochloramine at Low Temperature,'' *Water Res.*, **35**, 1, 41–48.

Drown, T. (1893/1894) ''Electrical Purification of Water,'' *J. NEWWA*, **8**, 183–186.

Ducoste, J., Carlson, K., and Bellamy, W. (2001) ''The Integrated Disinfection Design Framework Approach to Reactor Hydraulics Characterization,'' *J. Water Supply Res. Technol.-Aqua*, **50**, 44, 245–261.

Ducoste, J., Liu, D., and Linden, K.G. (2005) ''Alternative Approaches To Modeling Dose Distributionand Microbial Inactivation in Ultraviolet Reactors: Lagrangian vs Eulerian,'' *J. of Environ. Engr., ASCE*, **131**, 10, 1393–1403.

DVGW (1997) *DVGW-W294 UV Disinfection Devices for Drinking Water Supply—Requirements and Testing*, German Gas and Water Management Union, Bonn, Germany.

Einstein, A. (1905) ''Über einen die Erzeugung und Verwandlung des Lichtes betreffenden heuristischen Gesichtspunkt,'' *Ann. Physik*, **17**, 3, 131–148.

Elder, J. (1959) ''The Dispersion of Marked Fluid in Turbulent Shear Flow,'' *J. Fluid Mech.*, **5**, 544–560.

Federal Register (1993) *Code of Federal Regulations* (29 CFR), Part 1915, ***58***, FR 35514.

Finch, G., Haas, C., Openheimer, J., Gordon, G., and Trussell, R. (2001) ''Design Criteria for Inactivation of *Cryptospordium* by Ozone in Drinking Water,'' *Ozone: Sci Eng.*, **23**, 4, 259–284.

Floyd, R., and Sharp, D. (1979) ''Inactivation by Chlorine of Single Poliovirus Particles in Water,'' *Environ. Sci. Tech.*, **13**, 4, 138–442.

Floyd, R., Sharp, D., and Johnson, J. (1978) ''Inactivation of Single Poliovirus Particulates in Water by Hypobromite Ion, Molecular Bromine, Dibromamine and Tribromamide,'' *Environ. Sci. Technol.*, **16**, 7, 377–383.

Fuller, G. W. (1897) *Report on the Investigations into the Purification of Ohio River Water at Louisville, KY*, Van Nostrand, New York.

Galasso, G., and Sharp, D. (1965) ''Effect of Particle Aggregation on Survival of Irradiated Viruses,'' *J. Bacteriol.*, **90**, 4, 1138–1142.

Gard, S. (1957) ''Chemical Inactivation of Viruses,'' pp. 123–146 in *CIBA Foundation Symposium on the Nature of Viruses*, Little Brown, Boston, MA.

GAGW (2003) *Technical Standard DVGW 294, UV Systems for German Association on Gas and Water*, 2nd ed., German Association on Gas and Water, Bonn, *Germany*.

Giese, N., and Darby, J. (2000) ''Sensitivity of Microorganisms to Different Wavelengths of UV Light—Implications on Modeling of Medium Pressure UV Systems,'' *Water Res.*, **34**, 16, 4007–4013.

Gordon, G., Adam, L., and Bubnis, B. (1995a) *Minimizing Chlorate Formation in Drinking Water When Hypochlorite Ion Is the Chlorinating Agent*, AWWA American Water Works Assocation Research Foundation, Denver, CO.

Gordon, G., Adam, L., and Bubnis, B. (1995b) ''Minimizing Chlorate Ion Formation,'' *J. AWWA*, **87**, 6, 97–106.

Gordon, G., Adam, L., Bubnis, B., Hoyt, B., Gillette, S., and Wilczek, A. (1993) ''Controlling the Formation of Chlorate Ion in Hypochlorite Feedstocks,'' *J. AWWA*, **85**, 9BI, 89–97.

Gordon, G., Adam, L., Bubnis, B., Kuo, C., Cushing, R., and Sakaji, R. (1997) ''Predicting Liquid Bleach Decomposition,'' *J. AWWA*, **89**, 4, 142–149.

Graber, D. (1972) ''Discussion/Communication on: 'Hydraulic Model Studies of Chlorine Contact Tanks,''' *J. WPCF*, **44**, 10, 2029–2035.

Grasso, D., and Weber, W. (1989) ''Mathematical Interpretation of Aqueous-Phase Ozone Decomposition Rates,'' *J. Environ. Engr. ASCE*, **115**, 541–559.

Griese, M., Hauser, K., Berkemeier, M., and Gordon, G. (1991) ''Using Reducing Agents to Eliminate Chlorine Dioxide and Chlorite Ion Residuals in Drinking Water,'' *J. AWWA*, **85**, 5, 56–61.

Gurol, M., and Singer, P. (1982) ''Kinetics of Ozone Decomposition: A Dynamic Approach,'' *Environ. Sci. Technol.*, **16**, 7, 377–383.

Haas, C. (1979) ''Discussion of Kinetics of Bacterial Deactivation with Chlorine,'' *J. Environ. Eng. ASCE*, **105**, 1198–1199.

Haas, C., and Heller, B. (1990) ''Kinetics of Inactivation of *Giardia lamblia* by Free Chlorine,'' *Water Res.*, **24**, 2, 233–238.

Haas, C., and Joffe, J. (1994) ''Disinfection under Dynamic Conditions: Modification of Hom's Model for Decay,'' *Environ. Sci. Technol.*, **28**, 7, 1367–1369.

Haas, C., Joffe, J., Anmangandla, U., Hornberger, J., Heath, M., Jacangelo, J., and Glicker, J. (1995) *Development and Validation of Rational Design Methods of Disinfection*, American Water Works Association Research Foundation, Denver, CO.

Haas, C., Joffe, J., Anmangandla, U., Jacangelo, J., and Heath, M. (1996) ''The Effect of Water Quality on Disinfection Kinetics,'' *J. AWWA*, **88**, 95–103.

Haas, C., and Karra, S. (1984) ''Kinetics of Microbial Inactivation by Chlorine—I. Review of Result in Demand-Free Systems,'' *Water Res.*, **18**, 11, 1443–1449.

Haas, C., and Karra, S. (1984) ''Kinetics of Wastewater Chlorine Demand Exertion,'' *J. WPCF*, **56**, 170–182.

Hannoun, I., Boulos, P., and List, J. (1999) ''Using Hydraulic Modeling for CT Compliance,'' *J. AWWA*, **90**, 8, 77–87.

Harris, G., Adam, V., Sorenson, D. L., and Curtis, M. S. (1987) ''Ultraviolet Inactivation of Selected Bacteria and Viruses,'' *Water Res.*, **6**, 687–692.

Hart, F. (1979) ''Improved Hydraulic Performance of Chlorine Contact Chambers,'' *J. WPCF*, **51**, 12, 2868–2875.

Henry, D. J., and Freeman E. M. (1996) ''Finite Element Analysis and T10 Optimization of Ozone Contactors,'' *Ozone Sci. Eng.*, **17**, 587–606.

Hermanowicz, S., Bellamy, W., and Fung, L. (1999) ''Variability of Ozone Reaction Kinetics in Batch and Continuous Flow Reactors,'' *Water Res.*, **33**, 2130–2138.

Hess, S., Diachishin, A., and De Falco, Jr., P. (1953) ''Bactericidal Effects of Sewage Chlorination, Theoretical Aspects,'' *Sewage Ind. Wastes*, **25**, 909–917.

Hoehn, R. C., Dietrich, A. M., Farmer, W. S., Orr, M. P., Lee, R. G., Aieta, M., Wood, D. W. III, and Gordon, G. (1990) ''Household Odors Associated with the Use of Chlorine Dioxide,'' *J. AWWA*, **81**, 4, 166–172.

Hoigné, J., and Bader, H. (1976) ''Role of Hydroxyl Radical Reactions in Ozonation Processes in Aqueous Solutions,'' *Water Res.*, **10**, 377–386.

Hunt, N., and Mariñas, B. (1997) '' *Escherichia coli* Inactivation with Ozone'' *Water Res.*, **31**, 1355–1267.

Hunt, N., and Mariñas, B. (1999) ''Inactivation of *Escherischia coli* with Ozone: Chemical and Inactivation Kinetics,'' *Water Res.*, **33**, 11, 2633–2641.

Iatrou, A., and Knocke, W. (1992) ''Removing Chlorite by the Addition of Ferrous Iron,'' *J. AWWA*, **86**, 11, 63–68.

Jacangelo, J. G., Laîné, J. M., Carns, K. E., Cummings, E. W., and Mallevialle, J. (1989) ''Low-Pressure Membrane Filtration for Removing *Giardia* and Microbial Indicators,'' *J. AWWA*, **83**, 9, 97–106.

Jacangelo, J., Patania, N., Haas, C., Gerba, C., and Trussell, R. (1997) *Inactivation of Waterborne Emerging Pathogens by Selected Disinfectants*, Report No. 442, American Water Works Research Foundation, Denver, CO.

JMM (1991) *Disinfection Report for the Water Treatment Pilot Study*, The City of Portland Bureau of Water Works, Portland, OR.

Johnson, G. A. (1911) ''Hypochlorite Treatment of Public Water Supplies,'' *Am. J. Public Health*, 562–565.

Katzenelson, E., Kletter, B., Schechter, H., and Shuval, H. (1974) Inactivation of Viruses and Bacteria by Ozone, in A. Rubin (ed.), *Chemistry of Water Supply, Treatment, and Distribution*, Ann Arbor Science, Ann Arbor, MI.

Kawamura, S. (2000) *Integrated Design and Operation of Water Treatment Facilities*, 2nd ed., Wiley-Interscience, New York.

Kimball, A. (1953) ''The Fitting of Mulit-Hit Survivial Curves,'' *Biometrics*, **9**, 6, 201–211.

Kim, J., Tomiak, R., and Mariñas, B. (2002a) ''Inactivation of *Cryptosporidium* Oocysts in a Pilot-Scale Ozone Bubble-Diffuser Contactor. I: Model Development,'' *J. Environ. Eng. ASCE*, **128**, 6, 514–521.

Kim, J., Tomiak, R., Rennecker, J., Mariñas, B., Miltner, R., and Owens, J. (2002b) ''Inactivation of *Cryptosporidium* in a Pilot-Scale Ozone Bubble-Diffuser Contactor. Part II: Model Verification and Application.'' *J. Environ. Eng.*, **128**, 6, 522–532.

Kim, J., Urban, M., Echigo, S., Minear, R., and Mariñas, B. (1999) Integrated Optimization of Bromate Formation and *Cryptosporidum parvum* Oocyst Control in Batch and Flow-Through Ozone Contactors, Proc. 1999 American Water Works Association Water Quality Technology Conference, on CD, Tampa, FL.

Knudson, G. (1986) ''Photoreactivation of Ultraviolet-Irradiated, Plasmid-Bearing and Plasmid-Free Strains of *Bacillus anthracis*,'' *Appl. Environ. Microbiol.*, **52**, 3, 444–449.

Krasner, S., and Barrett, S. (1984) Aroma and Flavor Characteristics of Free Chlorine and Chloramines, pp. 381–389. *Proc. AWWA WQTC*, American Water Works Association, Denver, CO.

Larson, M., and Mariñas, B. (2003) ''Inactivation of *Bacillus subtilis* Spores with Ozone and Monochloramine,'' *Water Res.*, **37**, 4, 833–844.

Lawler, D., and Singer, P. (1993) ''Analyzing Disinfection Kinetics and Reactor Design: A Conceptual Approach versus the SWTR,'' *J. AWWA*, **97**, 11, 67–76.

Le Chevallier, M., Cawthon, C., and Lee, R. (1988) ''Factors Promoting Survival of Bacteria in Chlorinated Water Supplies,'' *Appl. Environ. Microbiol.*, **54**, 2492–2499.

Lev, O., and Regli, S. (1992) ''Evaluation of Ozone Disinfection Systems: Characteristic Time *T*,'' *J. Environ. Eng. ASCE*, **118**, 268.

Linden, K., Shin, G., and Sobsey, M. (2001) ''Comparative Effectiveness of UV Wavelengths for the Inactivation of *Cryptosporidium parvum* oocysts in water,'' *Water Sci. Technol.*, **43**, 12, 171–174.

Linden, K.G. and Rosenfeldt, E.J. (2011) ''Ultraviolet Light Processes,'' Chap. 18, in J.K. Edzwald (ed) *Water Quality And Treatment: A Handbook Drinking Water*, 6th ed., American Water Works Association, Denver CO.

Lister, M. (1952) ''Decomposition of Sodium Hypochlorite,'' *Can. J. Chem*, **30**, 879.

Lister, M. (1956) ''Uncatalyzed and Catalyzed Decomposition of Sodium Hypochlorite,'' *Can. J. Chem.*, **34**, 6, 465–478.

Loge, F., Bourgeous, K., Emerick, R., and Darby, J. (2001) ''Variations in Wastewater Quality Parameters Influencing UV Disinfection Performance: Relative Impact of Filtration,'' *J. Environ. Eng. ASCE*, **127**, 9, 832–837.

Lotepro (2002) Technical Bulletin. Available at: www.loteproesg.com/DownLoads/OXGEN3.pdf.

Louie, D., and Fohrman, M. (1968) ''Hydraulic Model Studies of Chlorine Mixing and Contact Chambers,'' *J. WPCF*, **40**, 174.

Lyn, D.A. and Blatchley, E.R. (2005) ''Numerical Computational Fluid Dynamics-Based Models of Ultraviolet Disinfection Channels,'' *Journal of Environmental Engineering, ASCE*, **131**, 6, 838–849.

Marske, D., and Boyle, J. (1973) ''Chlorine Contact Chamber Design—a Field Evaluation,'' *Water Sewage Works*, **120**, 1, 70–76.

Masschelein, W. J. (1992) *Unit Processes in Drinking Water Treatment*, Marcel Decker, New York.

Morris, C. (1975) Aspects of the Quantitative Assessment of Germicidal Efficiency, pp. 1–10, in D. Johnson (ed.), *Disinfection: Water and Wastewater*, Ann Arbor Science, Ann Arbor, MI.

Morris, J. C. (1966) ''The Acid Ionization Constant of HOCl from 5 to 35°,'' *J. Phys. Chem.*, **70**, 12, 3798–3806.

Najm, I., and Trussell, R. (2000) NDMA Formation in Water and Wastewater, in Proceedings American Water Works Association Water Quality Technology Conference, on CD, Denver, CO.

Najm, I., and Trussell, R. (2001) ''NDMA Formation in Water and Wastewater,'' *J. AWWA*, **93**, 2, 92–99.

Naunovic, Z., Lim, S., and Blatchley, E.R. (2008) ''Investigation of Microbial Inactivation Efficiency of a UV Disinfection System Employing an Excimer Lamp,'' *Water Res.*, **42**, 4838–4846.

Nowell, L., and Hoigné, J. (1992a) ''Photolysis of Aqueous Chlorine at Sunlight and Ultraviolet Wavelengths—I. Degradation Rates,'' *Water Res.*, **26**, 5, 593–598.

Nowell, L., and Hoigné, J. (1992b) ''Photolysis of Aqueous Chlorine at Sunlight and Ultraviolet Wavelengths—II. Hydroxyl Radical Production,'' *Water Res.*, **26**, 5, 599–605.

NWRI (2003) *Ultraviolet Disinfection Guidelines for Drinking Water and Water Reuse*, 2nd ed., National Water Research Institute, Fountain Valley, CA.

NWRI (2003) *Ultraviolet Disinfection Guidelines for Drinking Water and Water Reuse*, 2nd ed., National Water Research Institute, Fountain Valley, CA, in collaboration with American Water Works Association Research Foundation.

ÖNORM. 2001. Plants for the Disinfection of Water Using Ultraviolet Radiation—Requirements and Testing—Part 1: Low Pressure Mercury Lamp Plants. ÖNORM M 5873-1. Osterreichisches Normungsinstitut, Vienna, Austria.

ÖNORM. 2003. Plants for the Disinfection of Water Using Ultraviolet Radiation—Requirements and Testing—Part 2: Medium Pressure Mercury Lamp Plants. ÖNORM M 5873-2. Osterreichisches Normungsinstitut, Vienna, Austria.

Oppenheimer, J. A., Aieta, E. M., Trussell, R. R., Jacangelo, J. G., and Najm, I. N. (2000) Evaluation of *Cryptosporidium* Inactivation in Natural Waters, American Water Works Association Research Foundation, Denver, CO.

Oppenheimer, J., Gillogly, T., and Trussell, R. (2001) Technical Memorandum to the Los Angeles Department of Water and Power, Los Angeles, CA.

Oppenheimer, J., Gillogly, T., Stolarik, G., and Ward, G. (2002) Comparing the Efficiency of Low and Medium Pressure UV Light for Inactivating *Giardia muris* and *Cryptosporidium parvum* in Waters with Low and High Levels of Turbidity, in *Proc. 2002 Annual AWWA Conference and Exhibition*, New Orleans, LA. American Water Works Association, Denver, CO.

Palin, A. (1975) Water Disinfection—Chemical Aspects and Analytical Control, pp. 71–93 in J. Johnson (ed.) *Disinfection—Water and Wastewater*, Ann Arbor Science, Ann Arbor, MI.

Parker, J. A., and Darby, J. L. (1995) ''Particle-Associated Coliform in Secondary Effluents: Shielding from Ultraviolet Light Disinfection,'' *Water Environ. Res.*, **67**, 1065.

Powell, J., Hallam, N., West, J., Forster, C., and Simms, J. (2000) ''Factors Which Affect Bulk Chlorine Decay Rates,'' *Water Res.*, **34**, 1, 117–126.

Qualls, R., Flynn, M., and Johnson, J. (1983) ''The Role of Suspended Particles in Ultraviolet Disinfection,'' *J. WPCF*, **55**, 1280–1285.

Radziminski, C., Ballantyne, L., Hodson, J., Creason, R., Andrews, R., and Chauret, C. (2002) ''Disinfection of *Bacillus subtilis* Spores with Chlorine Dioxide: A Bench-Scale and Pilot Scale Study,'' *Water Res.*, **36**, 1629–1639.

Rahn, O. (1973) *Physiology of Bacteria*, Blankston's and Son, Philadelphia, PA.

Rakness, K. L. (2005) *Ozone in Drinking Water Treatment: Process Design, Operation, and Optimization*, American Water Works Association, Denver, CO.

Rauth, A. (1965) The Physical State of Viral Nucleic Acid and the Sensitivity of Viruses to Ultraviolet Light, *Biophys. J.*, **5**, 257–273.

Reckhow, D., Legube, B., and Singer, P. (1986) ''The Ozonation of Organic Halide Precursors: Effect of Bicarbonate,'' *Water Res.*, **20**, 8, 987–998.

Rennecker, J., Kim, J., Corona-Vasquez, B., and Mariñas, B. (2001) ''Role of Disinfectant Concentration and pH in the Inactivation Kinetics of *Cryptosporidium parvum* Oocysts with Ozone and Monochloramine,'' *Environ. Sci. Tech.*, **35**, 13, 2752–2757.

Rennecker, J., Mariñas, B., Owens, J., and Rice, E. (1999) ''Inactivation of *Cryptosporidium parvum* oocysts with ozone,'' *Water Res.*, **33**, 11, 2481–2488.

Rennecker, J., Mariñas, B., Rice, E., and Owns, J. (1997) Kinetics of *Cryptosporidium parvum* Oocyst Inactivation with Ozone, pp. 299–316, in *Proc. 1997 Annual AWWA Conference, Water Research, Vol. C*.

Roberts, P., Aieta, E., Berg, J., and Chow, B. (1980) *Chlorine Dioxide for Wastewater Disinfection: A Feasibility Evaluation*, Tech. Rep., No. 251, Stanford University, Palto Alto, CA.

Rook, J. J. (1974) Formation of Haloforms During the Chlorination of Natural Water, *Water Treatment Exam.*, **23**, 234–243.

Ruffell, K., Rennecker, J., and Mariñas, B. (2000) ''Inactivation of *Cryptosporidium parvum* Oocysts with Chlorine Dioxide,'' *Water Res.*, **34**, 3, 868–876.

Saunier, B., and Selleck, R. (1979) ''The Kinetics of Breakpoint Chlorination in Continuous Flow Systems,'' *J. AWWA*, **71**, 3, 164–172.

Scarpino, P., Cronier, S., Zink, M., and Brigano, F. (1977) ''Effect of Particulates on Disinfection of Enteroviruses and Coliform Bacteria in Water by Chlorine Dioxide,'' paper 2B-3 Proceedings of AWWA Water Quality Technology Conference, Denver, CO.

Schieble, O. (1987) ''Development of a Rationally Based Design Protocol for the Ultraviolet Light Disinfection Process,'' *J. WPCF*, **59**, 1, 25–31.

Selleck, R., Collins, H., and White, G. (1970) Kinetics of Wastewater Chlorination in a Continuous Flow Process, paper presented at the International Water Pollution Research Conference, San Francisco, CA.

Selleck, R., and Saunier, B. (1978) ''Kinetics of Bacterial Deactivation with Chlorine,'' *J. Environ. Eng. ASCE*, **104**, 1197–1212.

Selleck, R., Saunier, B., and Collins, H. (1980) ''Closure to Discussion of Kinetics of Bacterial Deactivation with Chlorine,'' *J. Environ. Eng. ASCE*, **106**, 1000–1002.

Sepp, E. (1981) ''Optimization of Chlorination Disinfection Efficiency,'' *ASCE JEED*, **107**, EE1, 139–153.

Setlow, J. (1967) ''The Effects of Ultraviolet Radiation and Photoreactivation,'' *Comprehensive Biochem.*, **27**, 157–209.

Severin, B. (1980) ''Disinfection of Municipal Wastewater Effluents with Ultraviolet Light,'' *J. WPCF*, **52**, 7, 2007–2018.

Shen, C., Scheible, O.K., Chan, P., Mofidi, A., Yun, T.I., Lee, C.C., and Blatchley, E.R. (2009) ''Validation of Medium-Pressure UV Disinfection Reactors by Lagrangian Actinometry using Dyed Microspheres,'' *Water Res.*, **43**, 1370–1380.

Sjenitzer, F. (1958) ''How Much Do Products Mix in a Pipeline?'' *Pipeline Eng.*, **12**, D-31–34.

Staehelin, J., and Hoigné, J. (1982) ''Decomposition of Ozone in Water: Rate of Initiation by Hydroxide Ions and Hydrogen Peroxide,'' *Environ. Sci. Tech.*, **16**, 10, 676–681.

Staehelin, J., and Hoigné, J. (1985) ''Decomposition of Ozone in Water in the Presence of Organic Solutes Acting as Promoters and Inhibitors of Radical Chain Reactions,'' *Environ. Sci. Tech.*, **19**, 12, 1206–1213.

Stevens, A. and Symons, J. (1977) ''Measurement of Trihalomethanes and Precursor Concentration Changes,'' *J. AWWA* **69**, 10, 546–554.

Stolarik, G. F., Christie, D., Prendergast, R., Gillogly, T. E. T., and Oppenheimer, J. A. (2001) Long-Term Performance and Reliability of a Demonstration-Scale UV Reactor, in *Proc. of the First International Congress on Ultraviolet Technologies*, Washington, DC. International Ultraviolet Association, Ontario, Canada.

Taylor, G. (1954) ''The Dispersion of Matter in Turbulent Flow through a Pipe,'' *Proc. Royal Soc.*, A223, 446–484.

Tchobanoglous, G., Burton, F., and Stensel, H. (2003) *Wastewater Engineering*, 4th ed., Metcalf and Eddy, McGraw-Hill, New York.

Tomiyasu, H., Fukutomi, H., and Gordon, G. (1985) ''Kinetics and Ozone Decomposition in Basic Aqueous Solution,'' *Inorg. Chem.* **24**, 2962.

Trussell, R. R. (1992) Control Strategy I: Alternate Oxidants and Disinfectants and Disinfectant Residuals, pp. 43–95, in *Seminar on Control of Disinfectant By-products*, Proceedings 1992 Annual AWWA Conference, Philadelphia, PA. American Water Works Association, Denver, CO.

Trussell, R. R. (1993) Treatment for the Control of Disinfectant Byproducts and Disinfectant Residuals, in G. F. Craun (ed.), *Safety of Water Disinfection: Balancing Chemical and Microbial Risks*, International Life Science Institute (ILSI), Washington, DC.

Trussell, R., and Chao, J. (1977) ''Rational Design of Chlorine Contact Tanks,'' *J. WPCF*, **49**, 4, 659–667.

Trussell, R. R., and Kreft, P. (1984) Engineering Considerations of Chloramine Application, pp. 47–73 in Chlorination for THM Control: Principles and Practices, AWWA Special Workshop, Dallas, TX.

Trussell, R. R., and Pollock, T. (1983) Design of Chlorination Facilities for Wastewater Disinfection, ''paper presented at Wastewater Disinfection Alternatives—Design, Operation, Effectiveness,'' Preconference Workshop for 56th WPCF Conference, Atlanta, GA.

U.K. Department of the Environment (1999a) Transport and the Regions. Water Supply (Water Quality) (Amendment) *Regulations 1999*. Statutory Instruments 1999 No. 1524. *Cryptosporidium* in Water Supplies.

U.K. Department of the Environment (1999b) Transport and the Regions. Standard Operating Protocols for the Monitoring of *Cryptosporidium* Oocysts in Treated Water Supplies to Satisfy Water Supply (Water Quality) Amendment Regulations 1999 Statutory Instruments No. 1524.

U.S. EPA (1979) ''Control of Trihalomethanes in Drinking Water. Final Rule,'' *Fed. Reg.*, **44**, 231, Nov. 29, 68624.

U.S. EPA (1986) *Design Manual: Municipal Wastewater Disinfection*, EPA/625/1-86/021, U.S. Environmental Protection Agency, Washington, DC.

U.S. EPA (1989) ''Filtration and Disinfection; Turbidity, *Giardia lamblia*, Viruses, *Legionella*, and Heterotrophic Plate Count Bacteria. Final Rule,'' *Fed. Reg.* **54**, 124, June 29, 27486–27541.

U.S. EPA (1991) Guidance Manual for Compliance with the Filtration and Disinfection Requirements for Public Water Systems Using Surface Water Sources, U.S. Environmental Protection Agency, Washington, D.C.

U.S. EPA (1998) ''Disinfectants and Disinfection By-Products Rule: Final Rule,'' *Fed. Reg.*, **63**, 241, Dec. 16, 69390.

U.S. EPA (1999) *Alternative Disinfectants and Oxidants Guidance Manual*, 815-R-99-014, U.S. Environmental Protection Agency, Washington, DC.

U.S. EPA (2006) *Ultraviolet Disinfection Guidance Manual*, for the Final Long Term 2 Enhanced Surfance Water Treatment Ru EPA 815-R-06-00, U.S. Environmental Protection Agency, Washington, DC.

U.S. EPA (2004) ''National Primary Drinking Water Regulations: Stage 2 Disinfectants and Disinfection Byproducts Rule; National Primary and Secondary Drinking Water Regulations; Approval of Analytical Methods for Chemical Contaminants; Proposed Rule'', *Fed. Reg.*, **68**, 159, 49548–49681.

U.S. PHS (1943) ''National Census of Water Treatment Plants of the United States,'' *Water Works Eng.*, **96**, 63–117.

Wallis, P., van Roodselaar, A., Neurwirth, M., Roach, P., Buchanan-Mappin, J., and Mack, H. (1989) Inactivation of *Giardia* Cysts in a Pilot Plant Using Chlorine Dioxide and Ozone, pp. 695–708, in *Proceedings AWWA WQTC*, Philadelphia, PA. American Water Works Association, Denver, CO.

Watson, H. (1908) ''A Note on the Variation of the Rate of Disinfection with Change in Concentration of the Disinfectant,'' *J. Hygiene*, **8**, 536.

Wattie, E., and Butterfield, C. (1944) ''Relative Resistance of *Escherichia coli and Eberthella typhosa* to Chlorine and Chloramines,'' *Public Health Reports*, **59**, 52, 1661–1671.

Whipple, G. C. (1906) Disinfection as a means of water purification, pp. 266–288, in *Proc. AWWA*. American Water Works Association, New York.

White, G. C. (1999) *Handbook of Chlorination and Alternative Disinfectants*, 4th ed., Wiley-Interscience, New York.

WHO (1994) *Guidelines for Drinking Water Quality*, World Health Organization, Geneva, Switzerland.

Wickramanyake, G., Rubin, A., and Sproul, O. (1984a) ''Inactivation of *Nagleria* and *Giardia* Cysts in Water by Ozonation,'' *J. WPCF*, **56**, 983–988.

Wickramanyake, G., Rubin, A., and Sproul, O. (1984b) ''Inactivation of *Giardia lamblia* Cysts with Ozone,'' *Appl. Environ. Microbiol.*, **48**, 3, 671–672.